



Title	Studies on Bandwidth Allocation Scheme in Time Sensitive Network for Mobile Fronthaul
Author(s)	久野, 大介
Citation	大阪大学, 2018, 博士論文
Version Type	VoR
URL	<a href="https://doi.org/10.18910/70763">https://doi.org/10.18910/70763</a>
rights	
Note	

*The University of Osaka Institutional Knowledge Archive : OUKA*

<https://ir.library.osaka-u.ac.jp/>

The University of Osaka

Doctoral Dissertation

Studies on Bandwidth Allocation Scheme in  
Time Sensitive Network for Mobile Fronthaul

Daisuke Hisano

July 2018

Graduate School of Engineering,  
Osaka University



# 内容梗概

本論文は、筆者が NTT アクセスサービスシステム研究所在職中、ならびに大阪大学 大学院工学研究科 電気電子情報工学専攻在学中に行った、モバイルフロントホールを収容する時間制約型ネットワークにおける帯域割当手法に関する研究成果をまとめたものであり、以下の 6 章で構成される。

第 1 章は序論であり、本研究の背景として低遅延性が求められる産業用ネットワークである時間制約型ネットワーク (Time sensitive network: TSN) の概要及び適用先について述べ、TSN が産業用ネットワークのみならず、無線アクセスネットワーク (Radio access network: RAN) への適用が検討されていることを示す。次に、RAN の構成要素であるアクセスネットワークにおける転送技術について、その歴史と最近の動向について述べる。また、将来モバイルアクセスシステムにおける小セル化及び無線基地局数の増加について述べる。その上で、無線基地局と他サービスを収容するための TSN を光アクセスネットワークで構築し、経済性を高める必要性を示す。そして、本論文の研究対象である無線基地局と他サービスを収容する TSN における帯域割当技術に関して概説し、本研究の技術課題と目的を述べる。

第 2 章では、無線基地局と他サービスを同一 TSN に収容する帯域割当方式を実現するためのシステム要件を述べる。初めに本論文で考察する TSN を定義し、次に、TSN に収容する無線基地局の特徴として、無線基地局における機能分割点の再定義と、TSN 収容の対象であるモバイルフロントホール (Mobile fronthaul: MFH) の遅延要求及びバースト特性について述べる。そして、MFH の TSN 収容時の課題として、MFH のみを収容する TSN では、収容可能な無線基地局数が制限されることを明確にする。その上で、MFH と他サービスを同一 TSN に収容し、経済性を高める必要性を示す。経済的な TSN を構築するための信号多重方式に関する先行研究の紹介と研究対象とする方式を述べ、技術課題が帯域利用効率 (Bandwidth usage efficiency: BUE) の低下と他サービスのスループットの低下にあることを明らかにする。この技術課題を解決するために、TSN における帯域割当技術の確立が必要であることを示し、MFH と他サービスを収容する TSN のシステム要件について述べる。

第 3 章では、時分割複信 (Time division duplex: TDD) 方式を適用した無線アクセスシステムと他システムを収容する時分割多重受動光ネットワーク (Time division multiplexing passive optical network: TDM-PON) システムにおける転送性能評価について述べる。TDD 方式は、単一の周波数帯で上下リンクの通信を行うことが出来るため、周波数利用効率が高い。一方、TDM-PON システムにおける上下リンクの転送には波長分割多重 (Wavelength division multiplexing: WDM) 方式が適用されるため、モバイル信号の未使用区間が常在する。また、TDD 方式は、隣接する無線基地局間で時刻の同期をとるため、MFH へは信号が同着するという特性を持つ。本章では、TDD 方式に対応した無線基地局を TDM-PON システムに収容した際に常在する未使用区間に他サービスを収容する方式及び未使用区間の推定方式を提案する。まず、提案方式の構成及び動作原理について述べた上で、その実現可能性を評

価するために、計算機シミュレーション、原理確認実験、及び理論評価を行った。これらにより、MFH と他サービスを同一 TDM-PON システムに收容した場合の、MFH への影響と他サービスのスループット及び遅延性能の改善について示す。

第 4 章では、第 3 章で述べた MFH と他サービスの同一 TDM-PON システム收容に関して、TDD 方式を適用した無線リンクの上下リンク比が変更された場合もしくは上下リンク比の推定を誤った場合に、無線基地局から情報を取得することなく、TDM-PON システムで無線リンクにおける上下リンク比の変更を検知する方法について述べる。本章では、無線基地局の未使用区間に推定誤り検出用の帯域を割当てする方式、及び標準で定められる 7 種類の上下リンク比と上り MFH 信号間の相関係数をそれぞれ計算し、TDD 方式を適用した無線リンクにおける上下リンク比を推定する方式を提案する。まず、提案方式の構成及び動作原理について述べた上で、その実現可能性を評価するために、計算機シミュレーション、原理確認実験を行った。これらにより、TDD の上下リンク比が変更された際の MFH への影響と提案手法による遅延量の改善、他サービスのスループットと遅延量の提案手法による改善について示す。

第 5 章では、MFH と他サービスの同一ブリッジネットワーク收容における転送性能評価について述べる。MFH を收容するブリッジネットワークにおいて、信号の遅延及びジッタを最小化することを目的として時間告知シェーパ (Time aware shaper: TAS) の適用が検討されている。しかしながら、TAS を適用した際に帯域利用効率が低下するという課題がある。本章では、MFH の信号転送時のバースト性に着目した TAS の動作方法を提案する。まず、提案方式の構成及び動作原理について述べた上で、その実現可能性を評価するために、計算機シミュレーションによる性能評価を行った。評価結果により、MFH の低遅延性を保ちつつ、他サービスのスループット及び遅延量を改善し、帯域利用効率を向上できることを示す。

第 6 章では、以上の研究によって得られた成果を総括し、本論文の結論を述べる。

# Preface

This dissertation treats a bandwidth allocation scheme in a time sensitive network (TSN) for mobile fronthaul (MFH) based on research carried out by the author during his Ph.D. studies at the Division of Electrical, Electronic, and Information Engineering, Graduate School of Engineering, Osaka University, and his tenure at NTT Access Network Service Systems Laboratories.

Chapter 1 is an introduction to the thesis, and it presents the background and purpose of the study. Firstly, a general overview and the applications of a TSN for an industrial network that requires a low latency are described. A TSN for a radio access network (RAN) as well as an industrial network is studied.

Next, the historical perspective and recent investigations into radio and optical access networks are summarized. The number of mobile base stations (MBSs) on RANs has been increasing; accordingly, the cell size has been decreasing. The necessity of a cost-effective optical access network based on a TSN that accommodates both MBSs and secondary services is discussed. An outline of the bandwidth allocation scheme in the TSN, which accommodates the MBSs and the secondary services, is expected. The purpose and technical issues of this research are described.

Chapter 2 describes the system requirements of a TSN in order to establish bandwidth allocation schemes for accommodating an MFH link and secondary services. Firstly, the TSN studied in this thesis is clearly defined. Next, a redefinition of a functional splitting point in an MBS and the latency requirement and burst characteristic in an MFH link, which are the technical preconditions of future RANs, are described. Furthermore, the issue that a TSN accommodating only MFH links has a limitation on the number of MBSs that can be accommodated is clarified. Thus, the necessity of realizing a cost-effective TSN that accommodates the MFH link and the secondary services is described. Signal multiplexing schemes are introduced, including the related work on constructing a cost-effective TSN. Then, We show that the technical issues in the conventional schemes are decreases in the bandwidth usage efficiency (BUE) and throughput of secondary systems. In order to overcome the above issues, we explain the necessity of novel bandwidth allocation schemes and the system requirements for the TSN accommodating the MFH link and the secondary systems.

Chapter 3 deals with a bandwidth allocation scheme for the uplink transmission in a TDM-PON with focusing on that the MBS was expected to adopt a time division duplex (TDD) scheme. The high frequency usage efficiency is high in the TDD scheme because the uplink and downlink signals are transmitted by using the same frequency

band. Meanwhile, the TDM-PON employs a wavelength division multiplexing (WDM) scheme in the optical transmission link. Thus, unallocated intervals appear periodically in the optical link. Moreover, the signals from the user equipment arrive at each MBS simultaneously since all of MBSs are synchronized in time. In this chapter, we propose a technique in which the optical line terminal (OLT) allocates the bandwidth to the optical network units (ONUs) connected to the secondary systems during the unallocated intervals for MBS. The mobile operator sends a pre-information for the timing of the unallocated interval to the OLT when the MBS is first deployed. Then the OLT estimates the timing of the periodical unallocated interval and a head of the burst signal. The details of the proposed scheme and the principle of the operation are described. The results of the numerical simulation, experiments, and theoretical evaluation are given. Finally, the performance of the throughput and the latency for the MFH link and secondary systems are discussed.

Chapter 4 describes a technique called automatic recovery scheme from the TDD estimation error in the TDM-PON system accommodating the MFH link and the secondary services. The OLT distinguishes the unallocated interval from the uplink interval of the MFH link. It assigns the unallocated interval to the secondary system. However, there is an issue that the OLT cannot obtain the information on the configuration of the uplink and downlink in the wireless link when the mobile system changes the configuration of the uplink and downlink during operation. In this chapter, we propose an automatic recovery scheme, in which the OLT changes the assignment of the bandwidth by detecting the variation of the configuration of the uplink and downlink, and an estimation scheme for detecting the configuration variation without preinformation. The details of the proposed schemes and principles of operation are described. The proposed estimation scheme is evaluated by numerical simulation and experiments, and the effectiveness of the proposed bandwidth allocation scheme is confirmed experimentally.

Chapter 5 deals with a bridged network employing a time-aware shaper (TAS) that accommodates the MFH link and the secondary services. The purpose of employing the TAS is to minimize the latency and the time jitter in the MFH link. However, employing the TAS causes a decrease in the BUE and the throughputs of the secondary services. In this chapter, a gate shrunk TAS (GS-TAS) is proposed to achieve a high BUE using the MFH characteristics. The details of the proposed scheme and its principle of operation are described. The performance of the proposed scheme is evaluated by numerical simulation to show improvements on the throughput and latency of the secondary services without suffering low-latency transmission in the MFH link.

Chapter 6 summarizes the above results.

# Acknowledgements

本論文は、筆者が NTT アクセスサービスシステム研究所在職中ならびに大阪大学 大学院工学研究科 電気電子情報工学専攻 博士後期課程在学中に行った研究を、大阪大学 大学院工学研究科 電気電子情報工学専攻、丸田 章博 教授の御指導のもとにまとめたものであり、本研究を遂行するにあたり、終始懇切丁寧なる御指導、御鞭撻を賜りました丸田 章博 教授に謹んで深謝の意を表します。

論文作成にあたり有益な御指導を頂きました、大阪大学 大学院工学研究科 電気電子情報工学専攻、三瓶 政一 教授、三科 健 准教授に深く感謝いたします。

筆者の大阪大学 大学院工学研究科 電気電子情報工学専攻 博士前期課程在学中において、光通信工学の基礎及び研究を遂行するための基礎的な御指導、御鞭撻を賜りました大阪大学 大学院工学研究科 電気電子情報工学専攻、北山 研一 教授 (現大阪大学名誉教授、光産業創成大学院大学 特任教授、及び国立研究開発法人情報通信研究機構 (NICT) R&D アドバイザー)、吉田 悠来 助教 (現大阪大学 招聘准教授及び国立研究開発法人情報通信研究機構 (NICT) 主任研究員) に謹んで深謝の意を表します。

さらに、大阪大学 大学院工学研究科に在学中、情報通信工学全般ならびに本研究に関して多大なるご指導、ご教示を賜った、滝根 哲哉 教授、馬場口 登 教授、宮地 充子 教授、井上 恭 教授をはじめとする大阪大学 大学院工学研究科 電気電子情報工学専攻情報通信工学コースの諸先生方、鷲尾 隆 教授、駒谷 和範 教授をはじめとする大阪大学 産業科学研究所の諸先生方に厚く感謝申し上げます。

また、筆者の奈良工業高等専門学校 電気工学科在学中において、本論文に関連する基礎分野にて御指導を頂きました奈良工業高等専門学校 電気工学科、小野 俊介 准教授に深く感謝いたします。

また、NTT アクセスサービスシステム研究所において、これらの研究を行う機会を与えていただき、熱心な励ましを賜った NTT アクセスサービスシステム研究所、大高 明浩 プロジェクトマネージャーに深く感謝いたします。

本研究の遂行にあたり、日頃より熱心な御指導、御討論を頂いた、NTT アクセスサービスシステム研究所、寺田 純 グループリーダー (現プロジェクトマネージャー)、桑野 茂 主任研究員 (現大同大学教授)、島田 達也 主幹研究員、中村 浩崇 主任研究員、深田 陽一 主任研究員、清水 達也 主任研究員、小林 孝行 主任研究員、久保 尊広 研究主任、鵜澤 寛之 研究主任、中山 悠 研究員、柴田 直剛 研究主任、王 寛 研究員 (現 NTT ドコモ)、千葉大学 大学院工学研究院 丸田 一輝 助教に心より感謝いたします。特に、NTT アクセスサービスシステム研究所 柴田 直剛 研究員には、研究テーマの立ち上げ、研究の進め方、並びに課題抽出の方法等、本論文を構成する大部分にわたって、筆者が入社 1 年目からご指導いただきました。また、NTT アクセスサービスシステム研究所の同期である椎名 亮太 研究員、鈴木 貴大 研究員、西本 恵太 研究員をはじめ、職場の皆様には研究を進めるにあたり多大なる御協力を頂き

ましたことを，深く感謝いたします。

本論文執筆にあたり，御協力頂いた大阪大学 大学院工学研究科 事務補佐員 西谷 由子 氏，博士前期課程 2 年 児玉 剛征 氏，日高 隆揮 氏をはじめとする大阪大学 大学院工学研究科 電気電子情報工学専攻 フォトニックネットワーク工学領域の皆様にご感謝申し上げます。特に，博士前期課程 2 年 児玉 剛征 氏には，NTT アクセスサービスシステム研究所のインターンシッププログラムにも御参加いただき，シミュレータや原理確認実験の立ち上げに御助力いただきました。

また，友人である大川 佳奈恵 氏並びに東 晨 氏には英文校正のサポートをいただいたことを深く感謝いたします。

最後に，日頃から援助，協力を頂いた両親，妻 桃華に心から感謝いたします。本論文の製本並びに英文校閲等のサポートもいただきました。

# Acronyms

3GPP	Third Generation Partnership Project
5G	Fifth Generation Mobile Communication System
ACK	Acknowledgment
ADC	Analog-to-Digital Converter
ADS	Active Double Star
BBU	Baseband Processing Unit
B-PON	Broadband PON
BUE	Bandwidth Usage Efficiency
CA	Carrier Aggregation
CAGR	Compound Average Growth Rate
CDF	Cumulative Distribution Function
CO	Central Office
CPRI	Common Public Radio Interface
CPU	Central Processing Unit
C-RAN	Centralized RAN
CU	Central Unit
DAC	Digital-to-Analog Converter
DBA	Dynamic Bandwidth Allocation
DPM-16QAM	Dual Polarization Multiplexed Sixteen Quadrature Amplitude Modulation
DPM-QPSK	Dual Polarization Multiplexed Quadrature Phase Shift Keying
D-RAN	Distributed RAN
D-RoF	Digital Radio over Fiber
DU	Distributed Unit
DwPTS	Downlink Pilot Time Slot
eNB	evolved Node B
FBA	Fixed Bandwidth Allocation
FDD	Frequency Division Duplex
FFT	Fast Fourier Transform
FPGA	Field Programmable Gate Array
FTTH	Fiber-To-The-Home
GEM	G-PON Encapsulation Method
GE-PON	Gigabit Ethernet PON
GP	Guard Time Period
G-PON	Gigabit PON
GS-frame	Gate Shrunk frame

---

GS-TAS	Gate Shrunk TAS
HARQ	Hybrid Automatic Repeat Request
HetNet	Heterogeneous Network
HLS	Higher Layer Split
IDFT	Inverse Discrete Fourier Transform
IEEE	The Institute of Electrical and Electronics Engineers
IoT	Internet of Things
IP	Internet Protocol
ITU-T	International Telecommunication Union Telecommunication Standardization Sector
L2-CRAN	Layer-2 C-RAN
L2SW	Layer-2 Switch
LAN	Local Area Network
LLR	Log Likelihood Ratio
LLS	Lower Layer Split
LTE	Long-Term-Evolution
MAC	Medium Access Control
MBH	Mobile Backhaul
MBS	Mobile Base Station
MC	Macro Cell
MCF	Multi-Core Fiber
MFH	Mobile Fronthaul
MIMO	Multiple-Input and Multiple-Output
MMF	Multi-Mode Fiber
NAK signal	Negative-Acknowledgment signal
NG-PON1/XG-PON	Next Generation PON 1
NG-PON2	Next Generation PON 2
NNI	Network-Network Interface
ns-3	Network Simulator 3
OBSAI	Open Base Station Architecture Initiative
OFDM	Orthogonal Frequency Division Multiplexing
OLT	Optical Line Terminal
ONU	Optical Network Unit
PDCP	Packet Data Convergence Protocol
PDS	Passive Double Star
PE	Frame Preemption
PHY layer	Physical layer
PON	Passive Optical Network
P-ONU	Primary-ONU
PUSCH	Physical Uplink Shared Channel
RAN	Radio Access Network
RF	Radio Frequency
RLC	Radio Link Control
RR	Round Robin
RRH	Remote Radio Head
RTT	Round Trip Time

---

SBS	Secondary Base Station
SC	Small Cell
SDN	Software Defined Network
SIEPON	Service Interoperability in EPON
SNI	Application Service Network Interface
S-ONU	Secondary-ONU
SP	Strict Priority
SpC	Spot Cell
SPP	Split-PHY Processing
SR-DBA	Status Reporting DBA
TAS	Time Aware Shaper
TBS	Transport Block Size
TDD	Time Division Duplex
TDM	Time Division Multiplexing
TSN	Time Sensitive Network
TTI	Transmission Time Interval
UDP	User Datagram Protocol
UE	User Equipment
UNI	User Network Interface
UpPTS	Uplink Pilot Time Slot
VDSL	Very High-bit-rate Digital Subscriber Line
VoIP	Voice over IP
VR	Virtual Reality
WDM	Wavelength Division Multiplexing



# Contents

Chapter 1	Introduction	1
1.1	Trends in Network Usage . . . . .	1
1.2	Network Architecture . . . . .	2
1.3	Time Sensitive Networking . . . . .	3
1.4	Access Network . . . . .	4
	1.4.1 Trends in Access Network . . . . .	4
	1.4.2 Optical Access Network . . . . .	5
	1.4.3 Mobile Access Network . . . . .	8
1.5	Purpose of Studies . . . . .	9
1.6	Thesis Organization . . . . .	12
Chapter 2	Bandwidth Allocation Scheme in Time Sensitive Network	15
2.1	Introduction . . . . .	15
2.2	Overview of Time Sensitive Network . . . . .	15
2.3	Radio Access Network Architecture . . . . .	16
2.4	Mobile Fronthaul Characteristics . . . . .	18
	2.4.1 Overview . . . . .	18
	2.4.2 Functional Split Mobile Base Station and Burst Generation . . . . .	19
	2.4.3 Latency Requirement . . . . .	21
2.5	Time Sensitive Network Based Mobile Fronthaul . . . . .	22
	2.5.1 Network Topology and Multiplexing Scheme . . . . .	22
	2.5.2 Time Sensitive Network Accommodating MFH and Secondary Services . . . . .	23
	2.5.3 Bandwidth Allocation Scheme in TDM-PON for Mobile Fronthaul . . . . .	24
	2.5.4 Layer-2 Bridged Network for Mobile Fronthaul . . . . .	28
2.6	Conclusion . . . . .	30
Chapter 3	Accommodation of TDD-based Fronthaul and Secondary Services	31
3.1	Introduction . . . . .	31
3.2	Accommodation of TDD-based MFH in TDM-PON . . . . .	31
3.3	Proposed TDM-PON Architecture . . . . .	33
3.4	Principle of Operation . . . . .	35
	3.4.1 Unallocated Interval Estimation in MFH Link by Using Traffic Monitor . . . . .	35
	3.4.2 Bandwidth Allocation Scheme . . . . .	37

3.4.3	Discovery Technique using Unallocated Interval . . . . .	38
3.5	Numerical Simulation . . . . .	38
3.5.1	Simulation Setup . . . . .	38
3.5.2	Simulation Results of Multiple Accommodations . . . . .	41
3.6	Experiments with 10G-EPON . . . . .	44
3.6.1	Allocatable Throughput for S-ONUs in 10G-EPON . . . . .	44
3.6.2	Experimental Setup . . . . .	45
3.6.3	Instantaneous Throughput and Latency . . . . .	46
3.6.4	Latency Distribution for TDD-based MFH . . . . .	48
3.6.5	Number of Accommodated P-ONUs . . . . .	48
3.6.6	Number of Accommodated S-ONUs and Throughput with Various TDD Patterns . . . . .	50
3.7	Conclusion . . . . .	51
Chapter 4	Auto-Recovery from Estimation Error for TDD-based Fronthaul	53
4.1	Introduction . . . . .	53
4.2	Challenging Issues . . . . .	53
4.3	Principle of Proposed TDM-PON System . . . . .	54
4.3.1	TDD Pattern Estimation . . . . .	54
4.3.2	Automatic Recovery from TDD Pattern Estimation Error . . . . .	59
4.4	Numerical Simulation for TDD Pattern Estimation . . . . .	59
4.4.1	Simulation Setup . . . . .	60
4.4.2	Simulation Result . . . . .	61
4.5	Automatic Recovery from TDD Pattern Estimation Error . . . . .	62
4.5.1	Experimental Setup . . . . .	62
4.5.2	Experimental Result . . . . .	64
4.6	Conclusion . . . . .	66
Chapter 5	Time Aware Shapers for Low-Latency Bridged Network	67
5.1	Introduction . . . . .	67
5.2	Forwarding Method of Mobile Fronthaul Signal in Time Sensitive Network . . . . .	68
5.3	Time Aware Shaper . . . . .	69
5.4	Base Station Types . . . . .	71
5.5	Factors of Latency and Decrease in Bandwidth . . . . .	71
5.6	Gate Shrunk Time Aware Shaper . . . . .	72
5.7	Numerical Evaluation . . . . .	73
5.7.1	Mobile System Condition . . . . .	74
5.7.2	TSN Condition . . . . .	74
5.7.3	Results . . . . .	76
5.8	Conclusion . . . . .	77
Chapter 6	Conclusion	79
Bibliography		83

# Chapter 1

## Introduction

### 1.1 Trends in Network Usage

Internet service has been widely spread not only to business use case but also to use cases of general households. It has become an indispensable social infrastructure in our life and corporate activities.

Trends in the number of Internet users and the population penetration rate in Japan are shown in Fig. 1.1 [1]. The number of Internet users in 2016 was 100.8 million which is 380 thousand more than that in 2015, and the population penetration rate was 83.5% in 2016. It can be seen from Fig. 1.1 that both of them increased moderately while amount of change decreased gradually.

The purpose of using the Internet service is shown in Fig. 1.2 [1]. People under 40 are considered to be the main consumer of future Internet contents. Many of them use “social network service” and “video posting service” frequently. Further video services are expected to become active in the future, due to the spread of virtual reality (VR) service or the like. Therefore, the increase in Internet traffic volume is expected to accelerate even if the increase in the number of users stagnates.

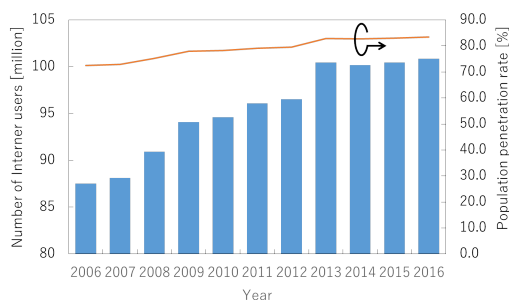


Fig. 1.1 Trends in the number of Internet users and population penetration rate [1].

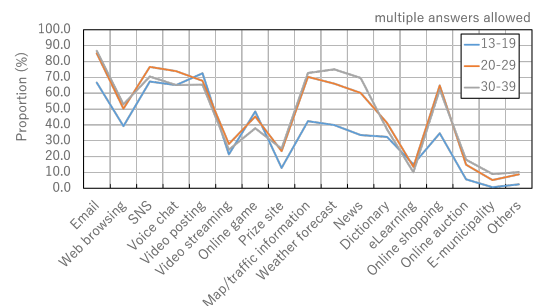


Fig. 1.2 Purpose of using Internet service [1].

## 1.2 Network Architecture

We describe a network architecture and a trend in transmission technology to support an enormous data traffic that will continue to grow in the future. Figure 1.3 shows a conceptual diagram of the network configuration. A network is roughly divided into three hierarchical structures; a core network, a metro network, and an access network. Transmission technologies in each network have different requirements. The requirements for transmission technologies are different depending on the network structures.

In the core and metro networks, large amount of data traffic from many subscribers is multiplexed and transmitted. In the current network system, the maximum transmission capacity can be 8 Tbps ( $100\text{Gbps} \times 80$  wavelength channels) by using an optical fiber having the characteristics of wide-band and low loss in the transmission path [2], [3].

There are two types of increase in capacity enhancement; increase of modulation level and extension of the multiple spaces. In the field of modulation level increase, a digital coherent system was proposed in 2005 as a breakthrough of transmission capacity expansion [4]. After that, the research and the development of the digital coherent technology has been accelerated, and a 100-Gbps class transmission system employing 25-Gbaud dual polarization multiplexed quadrature phase shift keying (DPM-QPSK) signal has been introduced [2]. Moreover, a 400-Gbps class transmission system employing 25-Gbaud DPM 16 quadrature amplitude modulation (DPM-16QAM) signal with two frequency subcarriers has been reported with a result of a field trial [5].

Regarding the extension of the multiple spaces, not only wavelength division multiplexing (WDM) but also signal multiplexing technique using multi-core and multi-mode fiber (MCF/MMF) has been proposed [6], [7]. The MCF is an optical fiber with multiple cores in one cladding. The MMF is an optical fiber in which there are multiple propagation paths (modes) in one core. The transmission capacity per one optical fiber can be increased since the transceiver can transmit different data signal through each core and/or mode. In March 2018, spatial division multiplexed transmission over 2,500 km using 12-core, and 3-mode fiber was reported [8].

On the other hand, an access network is also called a subscriber network, and it refers to a section of approximately 20 km from the central office (CO) in the terminal point of the whole network to the user office. A part of the access network becomes the interface when the user actually uses the network. The number of transmission devices is enormous compared with the core network, and its transmission medium and topology are also diversified. Therefore specifications of the subscriber network are designed mainly by the economical point of view rather than the enhancement of system capacity in the case of core networks.

Moreover, the diversification of network contents accelerates demands for services with lower latency. For example, there are factory automation and audio/video networks. Recent low latency service is becoming necessary not only in wired but also in wireless networks. In mobile service, the fifth generation mobile communication system (called 5G) requires end-to-end latency of 1 ms or less. Standardization of time sensitive network (TSN) has progressed with the purpose of enhancing the low latency performance[9]. In the next section, we describe the trend in TSN.

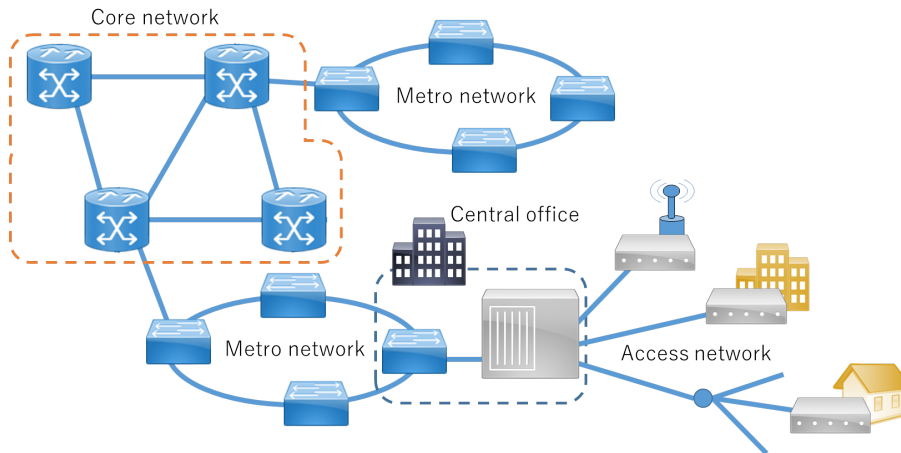


Fig. 1.3 Conceptual diagram of network configuration.

Table 1.1 Time sensitive network specifications for various application examples [11].

Network features	Video streaming	Automotive radar	Factory automation	Professional audio/video	Radio access network
Bandwidth	100 Mbps	1 Gbps	100 Mbps	100 Mbps	>10 Gbps
Latency	1 s	1 ms	100 $\mu$ s	10 $\mu$ s	100 $\mu$ s/250 $\mu$ s
Jitter	100 ms	20 ns	100 ns	10 ns	32 ns
Cycle time	Burst	10 ms	< 1 ms	Continuous	< 1 ms
Time synchronized	No	Yes	Yes	Yes	Yes

### 1.3 Time Sensitive Networking

TSN is an extension of the Ethernet AVB (Audio Video Bridging) standard [10] which has been introduced to audio/video, in-vehicle network or the like. We show the applications and their specifications for TSN in Table 1.1. The case of a general video streaming service is also shown in Table 1.1 for comparison. For an automotive radar, low-latency is needed since an automatic driving system demands a quick response to an obstacle. For factory automation, low latency performance is required since a precise operation is required and the devices need to be synchronized in the factory. A professional audio/video service synchronizes with multiple speakers and broadcasts video in a closed space such as a theater. The TSN for radio access network (RAN) which provides connections from mobile base stations (MBSs) to central office (CO) or between MBSs, has been also studied [12]. A future RAN requires the end-to-end latency of 1 ms or less [13]. Wired network in the RAN requires more stringent conditions since the end-to-end latency of 1 ms or less includes the radio propagation time and wireless signal processing time. Moreover, cost-effective systems are needed because many MBSs will be densely deployed. That is, realizing cost-effective time sensitive access network will be significant. In the next section, we outline the access network trend and technology.

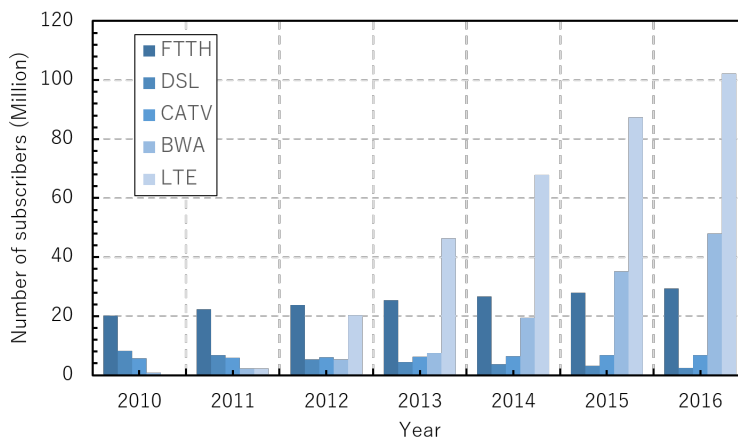


Fig. 1.4 Number of subscribers to broadband access in Japan [1].

## 1.4 Access Network

### 1.4.1 Trends in Access Network

Figure 1.4 shows the trends in the number of subscribers to broadband access in Japan, based on “white paper information and communications in Japan” of the Ministry of Internal Affairs and Communications [1]. Growth in the number of subscribers for metal lines tends to slow down, while the growth in fiber-to-the-home (FTTH) service is increasing. According to the Japanese census of 2015, the total number of households in Japan was approximately 53.3 million including 18.4-million single households [14]. The number of the FTTH subscribers in 2015 was 28 million, and it was approaching the total number of family households in Japan. Therefore, it seems difficult to further increase the number of FTTH subscribers.

The number of subscribers of mobile communication lines has been rapidly increasing since 2012. In 2010, NTT docomo launched up “Xi” service employing long-term-evolution (LTE). Moreover, the transmission speed was dramatically improved since the service employing 800 MHz and 1.5 GHz bands started.

A smartphone iPhone 5 [15] released in 2012 by Apple Inc, was able to use the LTE service; consequently the number of LTE subscribers has increased explosively.

NTT docomo has introduced “PREMIUM 4G” service since 2015 to increase the transmission speed. Since 18 May 2018, NTT docomo has expanded the service to increase the bit rate of up to 988 Mbps by employing 1.7 GHz and 3.5 GHz bands, the modulation format of 256QAM, and the  $4 \times 4$  multiple-input and multiple-output (MIMO) technique. Figure 1.5 shows the number of MBSs deployed by NTT docomo in Japan up to 2016 [29]. In 2020, 5G will be introduced, and it is expected that the number of user equipment and number of the MBSs will increase more and more [16]. The reason that the number of the MBS increases will be described in section 1.4.3.

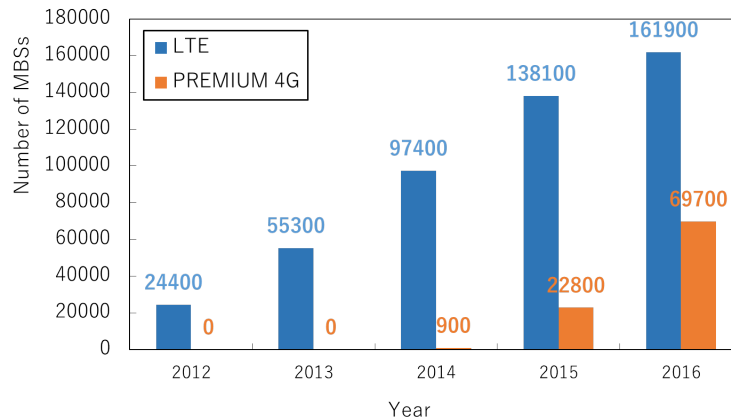


Fig. 1.5 Number of base stations deployed by NTT docomo [29].

## 1.4.2 Optical Access Network

### Passive optical network architecture

Figure 1.6–1.8 show examples of configurations for an optical access system. The optical access system is generally classified into two types; a single star type and a double star type. The single star type is a point-to-point connection in which the CO and the subscriber are directly connected by single optical fiber as shown in Fig. 1.6. The service with the single star type is mainly used for mass and business users. It is connected from the CO to the building management office by the optical media converter. The business user constructs a local area network (LAN) in the building. NTT EAST supports the bit rate of 1Mbps to 1Gbps for the business use case. As other services, the bandwidth from 50 to 100 Mbps are allocated to each subscriber in multi-dwelling houses by very high-bit-rate digital subscriber line (VDSL) system using existing telephone wires. By using the VDSL system, cost-effective broadband service for mass users can be provided since the optical equipment can be shared by many subscribers in the multi-dwelling houses.

The double star type is a point-to-multipoint connection in which subscribers share a part of the optical fiber and the equipment located in the CO. The double star type is further divided into two types; an active double star (ADS) type and a passive double star (PDS) type. The PDS is also called a passive optical network (PON). In the ADS, a device such as a concentrator that needs a power supply is arranged in both nodes at the CO and the subscribers. In the PDS, a device that does not need power supply, such as an optical splitter or wavelength multiplexer/demultiplexer, is placed in the relay node.

The PDS that can provide a service without power supply is a system superior to ADS. The PDS is actually introduced as a commercial system. For example, NTT EAST provides “FLET’S HIKARI” service with the bit rate of up to 1 Gbps. Hereinafter, it is described as PON instead of PDS.

The PON is categorized into two types: time division multiplexing PON (TDM-PON) and a wavelength division multiplexing PON (WDM-PON).

A TDM-PON shown in Fig. 1.7 was first proposed in 1987 by British Telecommunica-

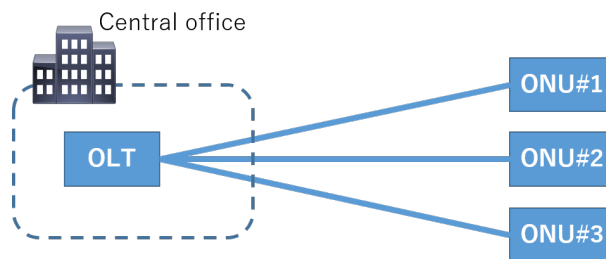


Fig. 1.6 Single star connection.

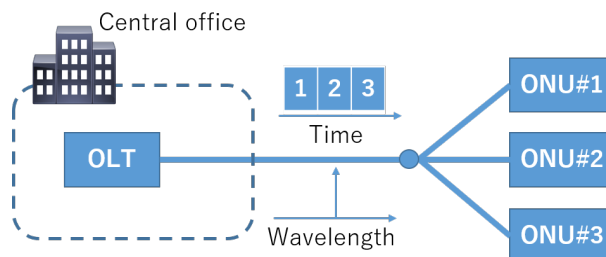


Fig. 1.7 TDM-PON.

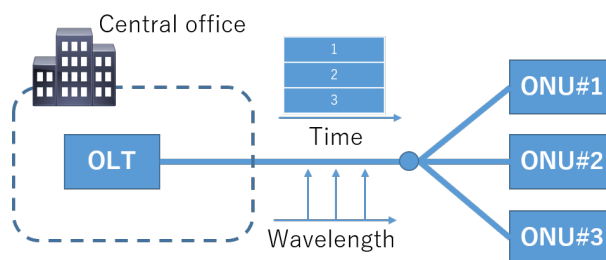


Fig. 1.8 WDM-PON.

tions plc to provide subscribers with new broadband services in addition to telephone line services [17]. In TDM-PON, a signal multiplexing is performed on a packet-by-packet. The destination is specified by using the identifier assigned to the packet after receiving the user signal. Hence, the technique for ensuring the confidentiality of the user information is required. On the other hand, PON has a highly economic efficiency because not only the optical fiber but also an optical line terminal (OLT) in the CO is shared. In addition, the same type of optical network unit (ONU) arranged in the subscriber can be used for all of the subscribers. That is, it is not complicated to realize a plug-and-play function by which a service can be started just after a terminal is connected to the system. The TDM-PON is widely used for mass users secured by encryption technology because an access network service is strongly required to be low priced.

A WDM-PON as shown in Fig. 1.8 was proposed by Bell Laboratories in 1988 [18]. Each user signal is superimposed on different wavelengths, and optically wavelength demultiplexed when receiving the signals. Therefore, there is the high confidentiality of user information. Furthermore, it is suitable for providing a high-speed bandwidth guarantee service since one subscriber occupies one wavelength. On the other hand, only optical

fiber and an optical splitter are shared, and different OLT is required for each subscriber.

A standardization of TWDM-PON has been discussed as a new optical access scheme focusing on the high economy of TDM and the scalability of WDM.

#### Global standardization

Global standardization of the optical access system is carried out by two organizations of “The Institute of Electrical and Electronics Engineers (IEEE)” and “International Telecommunication Union Telecommunication standardization sector (ITU-T)”. Figure 1.9 shows standardization trend of PON system in IEEE and ITU-T with the trend of Ethernet. Ethernet is the most popular signal transmission protocol for LAN. In the PON system proposed by IEEE, the Ethernet frame is forwarded on the PON link without de-encapsulating. In the ITU-T-based PON system, the arbitrary type of the frame is encapsulated by the GEM (Gigabit PON (G-PON) encapsulation method) frame or the like, and the frame is forwarded on the PON link. The PON system has been standardized 6 or 7 years after the standardization of the Ethernet protocol. In Japan, a broadband PON (B-PON) was commercially introduced in 2001. A Gigabit Ethernet PON (GE-PON) standardized by IEEE was introduced in 2004. In recent years, an installation of the GE-PON system to not only Japan but also Asian countries is proceeding.

On the other hand, the G-PON standardized by ITU-T in 2004, has been commercially introduced by Verizon Communications Inc. France Télécom (FT) which is a telecommunications company in France, has introduced the G-PON system.

The GE-PON system supports the bit rate of only 1.25 Gbps for both uplink and downlink transmission. The G-PON system supports the two types of the bit rate. The first one supports the bit rate of 1.25 Gbps for the uplink and 2.5 Gbps for the downlink. The other one supports the bit rate of 2.5 Gbps for both uplink and downlink transmission. The propagation distance is set at 20 km or less for the 32-branch GE/G-PON system by the limitation of the optical transceiver.

A PON system with high bit rate was standardized. In IEEE, the standardization in 10G-EPON system has been completed in 2009 [19]. The bit rate of the 10G-EPON system is the two types; 10 Gbps for both uplink and downlink transmission, and 1.25 Gbps for uplink and 10 Gbps for downlink transmission. Since 2010, a framework of a service interoperability in EPON (SIEPON) has been discussed to improve the compatibility among equipment vendors.

In ITU-T, a next generation PON (NG-PON1/XG-PON) and an NG-PON2 were standardized in 2010 and 2015, respectively [20]. NG-PON1 has the bit rate of 2.5 Gbps for uplink and 10 Gbps for downlink transmission. The target of the NG-PON2 includes not only the mass users but also a business user and mobile backhaul/fronthaul. The number of the wavelength channels is 4 (including 8 as an option). The bit rate per one wavelength channel is 10 Gbps for both uplink and downlink transmission.

In IEEE, a standardization of a 100-Gbps class PON system has also started since IEEE 802.3ca task force was established on December 2015 [21]. 100G-EPON employs WDM technology in the case of NG-PON2 and it was agreed that the bit rate per wavelength is 25 Gbps and the number of wavelength channels is up to 4. The ONUs having seven types of the combination of the data rate; 25/10G, 25/25G, 50/25G, 50/50G, 100/25G, 100/50G, and 100/100G for downlink/uplink, have been prepared in order to increase the maximum data rate step by step [22].

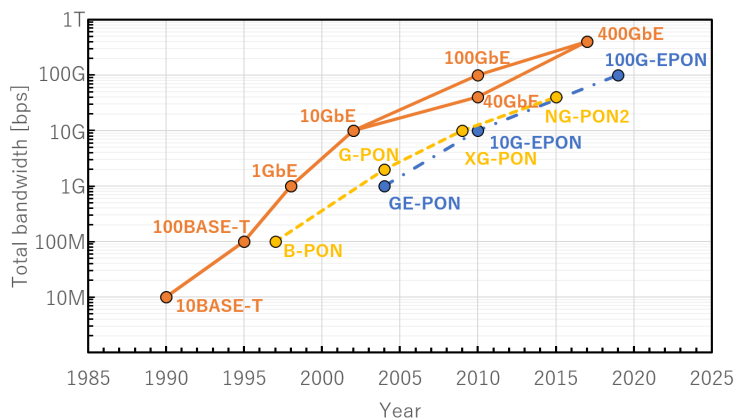


Fig. 1.9 Standardization trends in PON system and Ethernet.

In the future optical access system, the standardization will support not only an increase in the maximum transmission capacity but also the various requirements [23]. For instance, it will support flexibility of system configuration, improvement of transmission distance, device availability and low latency.

### 1.4.3 Mobile Access Network

The number of LTE subscribers is rapidly increasing with the spread of smartphones as discussed in Section 1.4.1. Moreover, the mobile data traffic will increase at an annual average rate of 40% from 2014 to 2017 with the spread of video applications such as Youtube and Netflix [24]. In the future, various things such as home appliances, automobiles, buildings and factories will be connected to the Internet, and the number of terminals connected to the Internet will explosively increase. These applications are called Internet of Things (IoT). IoT devices are characterized by connecting to the Internet without human intervention. Referring to the marketing results conducted by IHS Technology, the number of IoT devices connected to the Internet in 2016 was 17.3 billion [1]. A compound average growth rate (CAGR) from 2016 to 2021 will be 15.0%, and in 2020 there will be about 30 billion IoT devices which are expected to double the current number.

In summary, the following two points are important in future mobile access systems.

- (a) Increase in a wireless transmission data rate
- (b) Increase in a wireless system capacity per unit area

For (a), we need to use a higher frequency band to improve the wireless data rate. The influence of the phase noise becomes conspicuous when a higher frequency band is used. The frequency synthesizer is influenced by the phase noise. Thus, the mobile operator should set the radio parameters such as sub-carrier spacing taking the influence of the phase noise into consideration [25], [26]. A beam forming technique using many antenna elements is expected to improve the point (a). The propagation distance of the radio signal from the MBS can be extended by employing this technique. Moreover, each beam can be allocated to each user when the many antenna elements construct massive MIMO. Thus, the number of the users accommodated by an MBS is also increased.

For (b), there is a limit to the number of user equipment (UE) per unit area that can

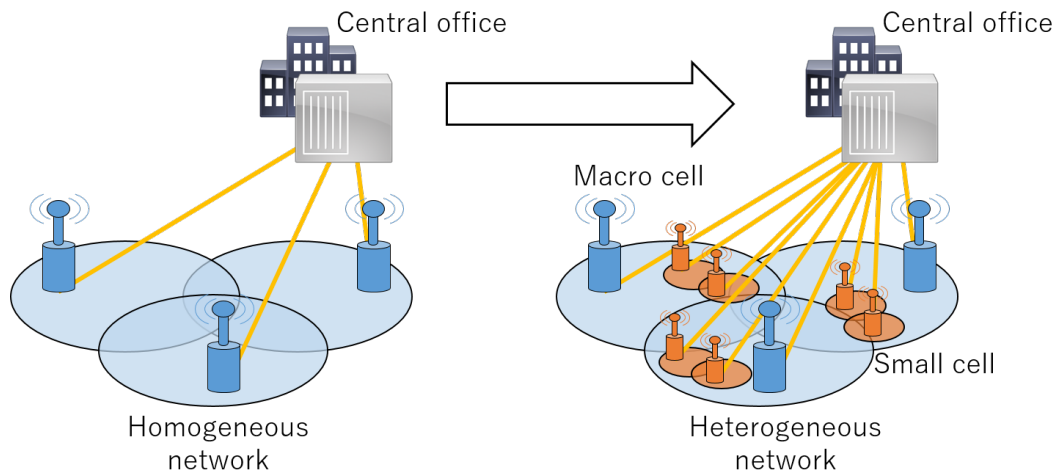


Fig. 1.10 Heterogeneous network.

be accommodated by one MBS when the cell formed by the MBS covers a wide area having the radius of several kilometers. Therefore, it is possible to increase the number of UE that can transmit more user signal per unit area by densely deploying the MBS with narrower coverage of the radius of a few hundred meters. In this thesis, such a small coverage cell is called a small cell (SC). The transmission capacity per UE is increased by increasing the density of the MBSs forming the SC in the high mobile traffic demand area.

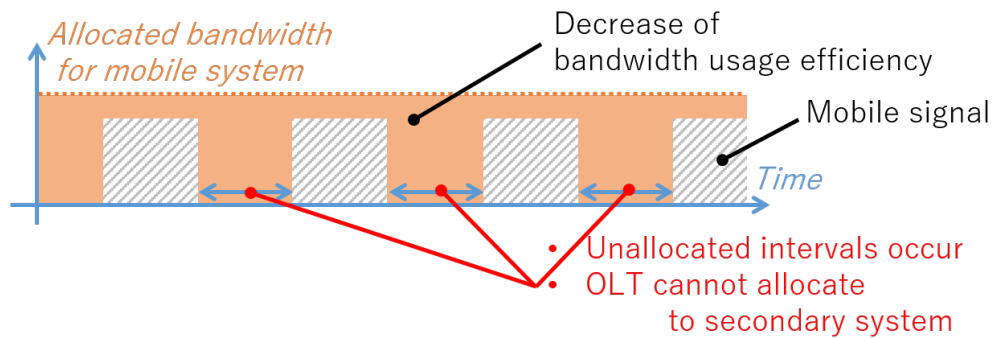
A heterogeneous network (HetNet) arranging SC-MBSs on macro cell (MC) with a large coverage area are useful since it is difficult to cover all service areas with only SC-MBSs. The HetNet structure is shown in Fig. 1.10. In HetNet, control plane and user plane are separated [27], thereby it is possible to reduce the number of handover [28] since the wide-area MC carries out transmission and reception of the control signal.

A centralized radio access network (C-RAN) architecture is useful for employing a HetNet. In the C-RAN, the SC-MBS is divided into two functions; a baseband processing unit (BBU) and a remote radio head (RRH). The BBU is generally located at the CO and the RRH is deployed on the antenna site. The BBU is directly connected to the RRH by an optical fiber and the optical link is called mobile fronthaul (MFH).

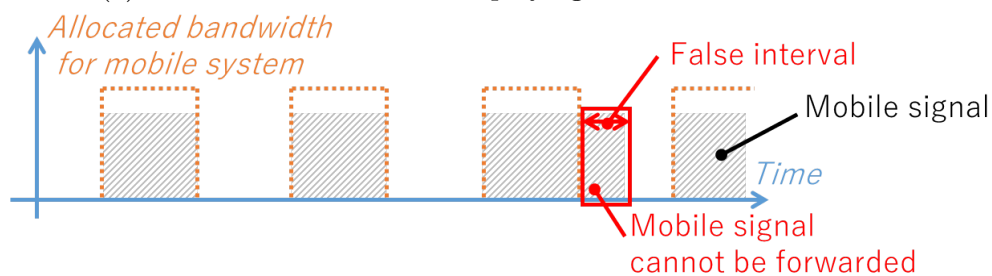
The number of MFH links will explosively increase when many RRHs will be deployed. Therefore, reducing the cost of optical links constructing a wireless network will be an important issue. Thus, the TSN-based RAN has been discussed in IEEE 802.1CM[12].

## 1.5 Purpose of Studies

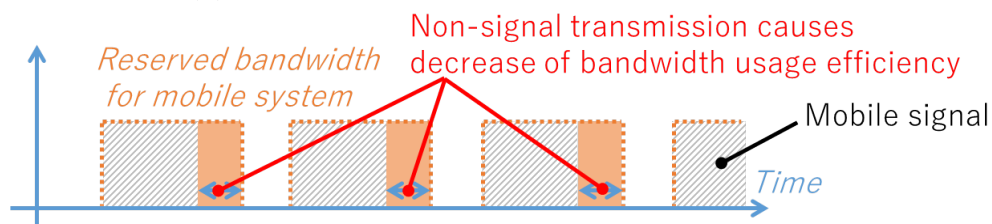
The goal is to establish bandwidth allocation schemes that can improve the accommodation efficiency in TSN for MFH. In terms of the cost effectiveness, we study to employ a layer-2 bridging system using layer-2 switch (L2SW), and TDM-PON system, on TSN. In the TSN-based MFH, it is not suitable to utilize only the MFH link since there is a huge queueing delay. The RRHs send the burst signals to the BBU at the same time because of the time synchronization among the RRHs. The burst MFH signals arrive at a network



(a) Decrease of BUE when employing conventional TDM-PON.



(b) Occurrence of estimation error in TDM-PON.



(c) Decrease of BUE when employing L2 bridging system.

Fig. 1.11 Issues of bandwidth allocation scheme for realizing TSN accommodating MFH and secondary services.

node such as the ONU or L2SW. The burst MFH signals are buffered in the network node until other burst MFH signals that arrive earlier can be forwarded. This waiting time causes a huge queueing delay. Therefore, we consider the TSN accommodating an MFH link as a highest priority service, and FTTH, public wireless LAN, and mobile backhaul (MBH) as a lower priority services. Hereinafter, such lower priority services are called to as secondary services. By multiple service accommodations, it is possible to easily increase the number of users in the TSN. However, there are two issues when those networking systems accommodate the MFH link and the secondary services: decreases in the bandwidth usage efficiency (BUE) in the TSN and in throughput of the secondary signal when employing conventional bandwidth allocation schemes.

Figure 1.11 shows these issues of bandwidth allocation schemes for realizing a TSN accommodating MFH link and secondary services.

For an uplink transmission in the TDM-PON as shown in Fig. 1.11 (a), the signals of the secondary systems cannot be forwarded even though there is an unallocated period of the MFH link in the TSN. In the TDM-PON, this is because the OLT manages the amount of

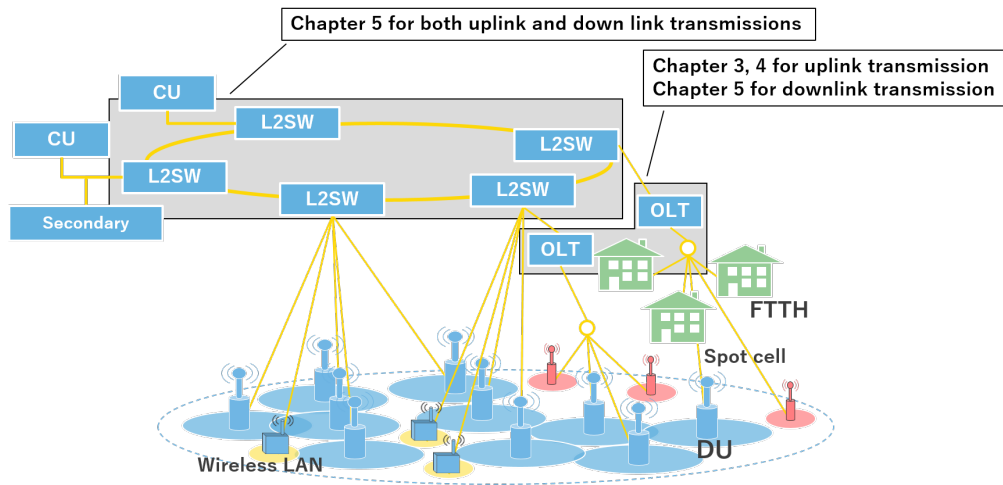


Fig. 1.12 Network architecture with proposed systems.

data and the data sending time for the uplink. The conventional OLT cannot distinguish the unallocated interval from the allocated one in the MFH link. This is because wireless access system and optical access network are operated by different operators. In this case, the operators of the optical access network cannot get information such as the timing of the unallocated interval, and the amount of the allocating bandwidth from wireless access operators. Thus, the OLT needs to allocate enough bandwidth continuously to the MFH link in order to suppress the latency for the MFH signal. The OLT allocates a small bandwidth to the secondary systems. Therefore, for the uplink transmission of the secondary system, the OLT needs to estimate the unallocated interval of the MFH link without remodeling the mobile system. Moreover, a recovery scheme is also needed when the unallocated interval changes or an error in the estimation occurs as shown in Fig. 1.11 (b). If unallocated interval cannot be correctly estimated, the OLT allocates full bandwidth to the secondary system during the period in which the MFH signal exists. This interval is defined as a false interval. Next, the OLT starts to allocate the bandwidth to the MFH link at the next uplink interval of the MFH link that the OLT recognizes as an uplink interval of the MFH link. During the period from the false interval to the uplink interval of the MFH link, the MFH signal is buffered in the ONU. This will result in a huge latency for the MFH link. The same issue occurs when an operator of the mobile system changes the transmission timing of the wireless signal.

In the layer-2 bridged TSN, we employ a function of a time aware shaper (TAS) [30] to an L2SW in order to preferentially send an MFH signal. The TAS scheme writes time on a timetable in the L2SW. The L2SW can forward the MFH signal and the forwarding of the secondary signal is halted during the reserved time. This reserved time cannot be released even when the MFH signal does not arrive at the L2SW as shown in Fig. 1.11 (c). That is, the BUE decreases when the amount of data of the MFH signal is small. Therefore, a scheme for releasing bandwidth is required.

The final goal is to establish bandwidth allocation schemes to solve the above issues.

## 1.6 Thesis Organization

This thesis consists of 6 chapters.

Chapter 2 describes the definition of the TSN and a RAN accommodated in the TSN. The requirements and characteristics of an MFH link for the MBS are introduced. In addition, a decrease in the accommodation efficiency is described when constructing a TSN that only accommodates an MFH link. Thus, the accommodation of the MFH link and secondary services in the same TSN is studied. Then, the network topology and the multiplexing scheme required to construct a cost-effective TSN are selected. The issues of the TSN are the decrease in the throughput of the secondary system and the BUE, which can be overcome by establishing a bandwidth allocation scheme.

Figure 1.12 shows the TSN architecture of the proposed system and maps the objective areas of the proposed schemes described in the following chapters.

Chapter 3 devotes to propose and demonstrate a bandwidth allocation scheme in a TDM-PON for an MFH link and secondary services. The MBS employs a time division duplex (TDD) scheme. First, the characteristics and technical issues of the TDD-based MFH are introduced. Techniques by which the OLT can estimate the unallocated intervals and allocate the bandwidth to the secondary system during the unallocated interval are proposed. In the estimation method, the OLT estimates the head of the MFH signal burst. The mobile operator sends a test signal when the MBS is first deployed. The OLT starts to estimate the unallocated interval on the basis of the test signal. The details of the proposed scheme and the principles of operation are described. The results of the numerical simulation, experiments, and theoretical evaluation are given. Finally, the performance of the throughput and latency for the MFH and secondary systems when employed in the proposed scheme is indicated.

Chapter 4 describes a technique to automatically recover the impact of the TDD estimation error in the TDM-PON for the MFH when supporting the secondary services. The OLT distinguishes the unallocated interval from the transmission interval of the MFH link, and allocates the bandwidth to the secondary system during the unallocated interval. However, there is an issue that the OLT cannot obtain the configuration of the uplink and the downlink when the mobile system changes the configuration of the uplink and downlink during operation. In addition, the OLT cannot allocate bandwidth to the secondary system when the estimation of the unallocated intervals also fails. This chapter proposes an automatic recovery scheme, where the OLT allocates the bandwidth for detecting the change in the configuration of the uplink and downlink. An estimation scheme of the configuration without requiring a test signal is also proposed. The proposed estimation scheme is evaluated by numerical simulation and experiments, and the effectiveness of the proposed bandwidth allocation scheme is confirmed experimentally. Finally, the improvement in the time from detection to restoration is indicated.

Chapter 5 deals with a layer-2 bridged network employing a TAS that accommodates the MFH and secondary services. First, the issue of the decrease in BUE when employing

the TAS is described. In this chapter, a novel TAS with a high BUE is proposed using the MFH characteristics. The details of the proposed scheme and the principles of operation are described, and the results of numerical simulation are given. The proposed TAS scheme improves the throughput and latency of the secondary service while maintaining low latency transmission in the MFH.

Chapter 6 summarizes the above results.



## Chapter 2

# Bandwidth Allocation Scheme in Time Sensitive Network

### 2.1 Introduction

Our goal is to realize flexible bandwidth allocation scheme for time sensitive network (TSN) accommodating mobile fronthaul (MFH) and secondary services. This chapter describes a TSN and a radio access network (RAN) architecture in detail. MFH characteristics in the future RAN are also described. Furthermore, we clarify an issue that TSN accommodating only MFH link has limitations on the number of MBSs which can be accommodated. The realizing the cost-effective TSN accommodating the MFH link and the secondary services will be needed. Then, we will clarify that the technical issues are decreases in bandwidth usage efficiency (BUE) and in throughputs of secondary systems in the TSN. To overcome these issues, we denote the necessity of novel bandwidth allocation schemes, and the system requirements in the TSN accommodating the MFH link and the secondary systems.

### 2.2 Overview of Time Sensitive Network

The purpose of the TSN standard is to support a low latency of less than a few milliseconds for the bit rate of 1 Gbps or more. In order to satisfy this requirement, the TSN standard includes the functions of time synchronization, forwarding control, frame preemption, and ingress shaping/policing. With these features, the TSN standard will evolve into a higher-speed networking technology that can be fully adapted to automotive applications for realizing automated operation and industrial applications for the realization of Industry 4.0.

In the TSN, the requirements are quite different depending on the contents. Note that most of the TSN standards refer to layer-2 bridged network systems. That is, the technique of the TSN standard does not apply to the other network systems such as a passive optical network (PON) system.

The term “Time sensitive network” in this thesis has a wider meaning than that defined in standardization. Even if PON or other multiplexing schemes are used in a layer-2 bridged network, the network can be called a “TSN” when low-latency forwarding is

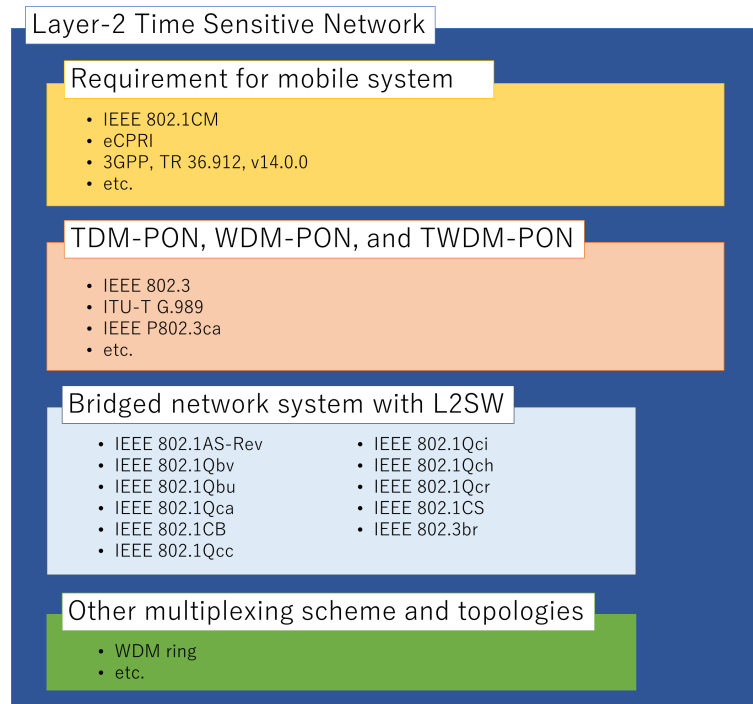


Fig. 2.1 Overview of layer-2 time sensitive network.

required. Fig. 2.1 shows the overview of a TSN.

Usage of TSN for MFH has been done since 2014 at IEEE 802.1CM[12]. The TSN for MFH includes various types of characteristics. IEEE 802.1CM has not standardized new technologies for the functions of the layer-2 bridged network system, but has discussed some requirements for the MFH. Examples of these are latency, jitter, and frame-loss rate. MFH link needs to be low cost since it is also included in the range of optical access network. Therefore, if it can satisfy the requirement of 802.1CM by using PON or other multiplexing schemes, this network can be regarded as a TSN for MFH.

However, the MFH has unique characteristics other than those specified in IEEE 802.1CM. The burst signals arrive at the central unit (CU) from the distributed units (DUs) at the same time. A queuing delay in the network node occurs when the TSN attempts to accommodate the MFH signals from the multiple DUs. In this case, the number of DUs that can satisfy the latency requirement is limited in the TSN. In general, the network cost per a user terminal is lowered by increasing the number of the accommodated user terminals in the network. That means it is necessary to consider accommodation of secondary services in order to construct a cost-effective TSN for MFH. The following sections describe the reasons that this mobile system has special characteristics.

## 2.3 Radio Access Network Architecture

As a method to form a cell on an antenna site, there are two types of RAN architectures; a distributed RAN (D-RAN) and a centralized RAN (C-RAN). The D-RAN architecture

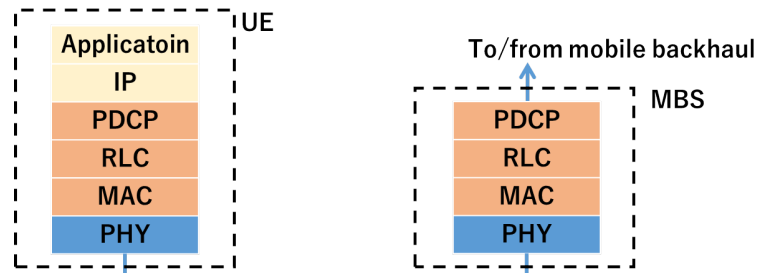


Fig. 2.2 Radio protocol stack in user-plane.

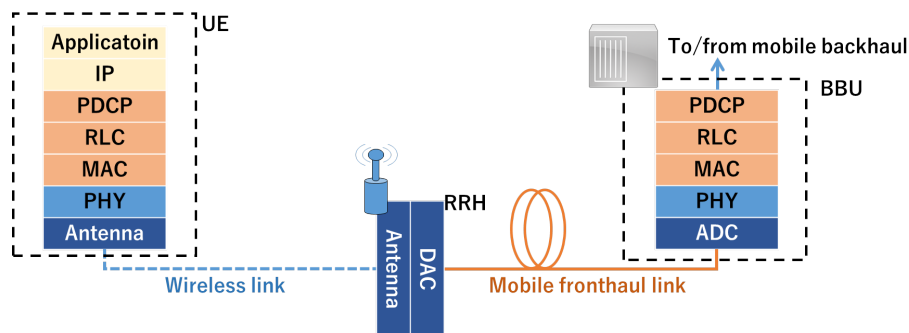


Fig. 2.3 C-RAN concept.

is constructed of a mobile base station (MBS) of an all-in-one type. Figure 2.2 shows a protocol stack in user plane for a general MBS [31]. A physical (PHY) layer in layer-1 decides modulation and channel encoding types in accordance with wireless scheduling information forwarded from a medium access control (MAC) function. Layer-2 functions include MAC, radio link control (RLC), and packet data convergence protocol (PDCP). The MAC function controls wireless resource allocation and a hybrid automatic repeat request (HARQ). The RLC function performs a retransmission control and a packet ordering. The PDCP function compresses, decompresses, and encrypts an Internet protocol (IP) packet header. The radio resource control (RRC) function in layer-3 manages a handover control. One MBS in the D-RAN includes all functions of the protocol stack.

Another is a C-RAN architecture in which the MBS is divided into a baseband processing unit (BBU) and a remote radio head (RRH). C-RAN architecture is shown in Fig. 2.3. The BBU is generally located at a central office (CO) and the RRHs are deployed on the antenna sites. The RRH includes functions of the antenna and digital-to-analog/analog-to-digital converters (DAC/ADC). The BBU includes other upper layer functions and ADC/DAC.

Mobile operators can employ either architecture depending on the required wireless transmission capacity and demand for a cooperative operation. The RRHs can perform cooperative operations with neighboring RRHs when employing the C-RAN since the BBU managing each RRH is located in the same CO. In addition, there are advantages to reduce MBS costs and the power consumption since the RRH does not include upper layer functions.

In the C-RAN, the link between the BBU and RRH is directly connected by an optical

Table 2.1 Cell types.

	Macro cell	Small cell	Spot cell
Wireless data rate	< hundreds Mbps	< several Gbps	< dozens Gbps
RAN type	D-RAN/C-RAN	C-RAN	D-RAN
Latency	100 $\mu$ s	100 $\mu$ s	A few milliseconds
Cell size	< several kilometers	< hundreds meters	< dozens meters

fiber. The optical link is called MFH. The signal format in the MFH link will be described in the next section. The link between the MBS and the core network is called a mobile backhaul (MBH).

In the MFH link, however very high capacity with low latency is required.

In addition, the RAN architecture can be roughly divided into three types in terms of the cell forming; macro cell (MC), small cell (SC), and spot cell (SpC). In the future RAN, a heterogeneous network (HetNet) will be employed as described in Chapter 1. In this network, the SC based MBSs (SC-MBSs) are deployed on the MC. The SC-MBSs have a narrower coverage with a radius of only a few hundred meters and are densely deployed in order to increase the ability to accommodate the desired number of the user equipment (UE). The SC-MBS forwards the signal in the user plane and performs the signal transmission with the neighboring SC-MBSs in cooperation. Thus, employing the C-RAN is suitable for the SC-MBS.

Meanwhile, the MBS with higher frequency bands will be locally deployed in the area where the mobile traffic demand is concentrated such as at a stadium and event venue. Such a MBS is called “spot cell” MBS (SpC-MBS).

The specification in these MBSs is shown in Table 2.1. This thesis focuses on the SC-MBS because many of the SC-MBSs are densely deployed. The next section describes the characteristics of an MFH link.

## 2.4 Mobile Fronthaul Characteristics

### 2.4.1 Overview

For transmission in the MFH link, a digital radio over fiber (D-RoF) is generally employed. Figure 2.3 illustrates a D-RoF concept. For an uplink transmission, the RRH converts a wireless analog signal into the signal with a digital waveform by an ADC. The digital signal is forwarded to the BBU through the optical fiber. The BBU reconverts the digital signal into the wireless analog signal. The D-RoF has the tolerance for fiber-nonlinearity and noise compared with an analog-RoF (A-RoF). Moreover, the mobile operator can use the general optical transceiver for the D-RoF link. There are common public radio interface (CPRI) [32] and open base station architecture initiative (OBSAI) [33] as the optical transceiver and interface for the MFH link. The optical bit rate in the D-RoF system is calculated from a sampling frequency, the number of quantization bits, and the number of streams for multiple-input and multiple-output (MIMO). For example, when the wireless bit rate is 150 Mbps for long-term-evolution (LTE) case, there are a system

bandwidth of 20 MHz and  $2 \times 2$  MIMO streams. In this case, the optical bit rate is as below,

$$\begin{aligned} \text{Optical bit rate} &= 20 \text{ (system bandwidth, MHz)} \times 1.536 \text{ (over sampling)} \\ &\times 15 \text{ (quantization, bits)} \times 2 \text{ (in - and quadrature - phase parts)} \\ &\times 2 \text{ (streams)} \times 1.33 \text{ (overhead)} \\ &\simeq 2.45 \text{ (Gbps)}. \end{aligned}$$

That is, the MFH link is required 16 times wireless bit rate [34]. To suppress the optical transmission rate in the MFH link, the redefinition in the split point between the BBU and the RRH is studied [35]–[43]. Note that in the functional split MBS, the block of the upper layer functions is called a CU and the block of the lower layer functions is called a DU. The MFH signal is packetized by Ethernet frames when the functional split MBS is employed. Thus, the functional split MBS can contribute the MFH networking with packet forwarding. Next section describes the functional split MBS.

## 2.4.2 Functional Split Mobile Base Station and Burst Generation

This section describes MFH characteristics when an MBS employs new functional split. Note that we describe a lower layer split (LLS) MBS. In the LLS case, the MBS is divided into MAC and PHY layers or Intra-PHY layers. In the case of a higher layer split (HLS) MBS, the signals of the HLS-MBSs regarding as secondary can be accommodated in the TSN with the signals of the LLS-MBSs since latency requirement is not strict.

Figure 2.4 depicts a functional block of the PHY layer in an MBS [43]. When a CPRI is applied to both the CU and the DU, the MBS is split between a radio frequency (RF) front-end and a function of a fast Fourier transform (FFT) [32]. This is a common case in the LTE service. Here, we can expect the cost of the MBS to decrease, since the DU has few functions. However, in recent years, by increasing the wireless transmission capacity, wider bandwidth of MFH is required, although such a bandwidth expansion is not desirable. To suppress increase of bandwidth for MFH, a new functional split point has been proposed [35]–[43]. Also, CPRI group has published a new CPRI called an eCPRI [43]. The eCPRI has some options regarding a newly functional split point that replace the CPRI. The use of the eCPRI reduces the cost of the MFH link because the MFH bandwidth is reduced. The newly functional split MBS will be compatible with PON and bridged network systems because the MFH signal will be packetized in a layer-2 frame.

In the eCPRI, options D, I<sub>U</sub> and I<sub>D</sub> are better functional split points at which the PON and the bridged network are employed. Here, we describe characteristics of the data amount and burst type for each option.

With option D, the MBS splits the function between the medium access control (MAC) layer and the PHY layer. Figure 2.5 shows a time chart of an uplink signal transmission with option D. First, the UE sends the wireless signal with an orthogonal frequency division multiplexed (OFDM) symbol in a physical uplink shared channel (PUSCH) to a DU. The DU buffers the wireless signal for one transmission time interval (TTI) when the DU receives the wireless signal. After buffering the wireless signals for one TTI, the DU including all of the PHY functions demodulates and decodes the wireless signal and generates the burst MFH signal. The burst MFH signal is packetized using Ethernet

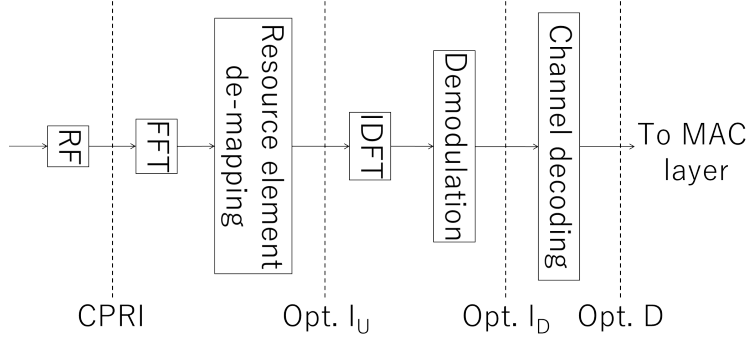


Fig. 2.4 Functional blocks in PHY layer [43].

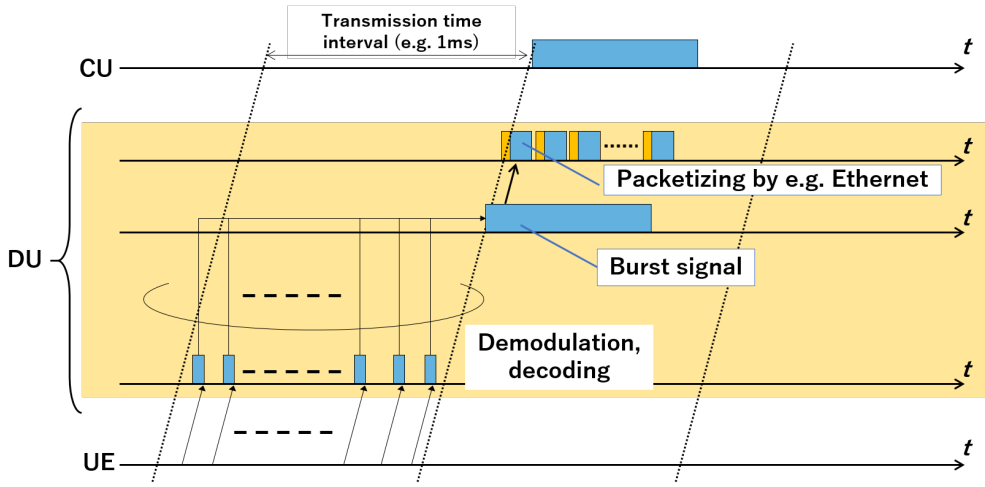


Fig. 2.5 Burst signal generation in DU.

frames. The packetized burst MFH signals are forwarded to the CU through the MFH link. The amount of MFH data  $D_{mfh}$  in 1TTI is as follows,

$$D_{mfh} = N_{lay} S_{tbs}, \quad (2.1)$$

where  $N_{lay}$  is the number of multiple-input and multiple-output (MIMO) layers, and  $S_{tbs}$  is the transport block size.

With option I<sub>U</sub>, the DU and the CU are divided within the PHY layer. With the eCPRI, the functional block of the PHY layer is divided between a resource element (RE) de-mapper and the function of an inverse discrete Fourier transform (IDFT). The amount of MFH data  $D_{mfh}$  in 1TTI is as follows,

$$D_{mfh} = N_{lay} N_{iq} N_q N_{rb} N_{sc} N_{sym}, \quad (2.2)$$

where  $N_{iq}$  is the number of in- and quadrature-phase parts (=2),  $N_q$  is the number of quantization bits of the in- and quadrature-phase parts,  $N_{rb}$  is the number of resource blocks in a wireless system bandwidth,  $N_{sc}$  is the number of subcarriers in a resource block, and  $N_{sym}$  is the number of OFDM symbols in a physical uplink shared channel (PUSCH).

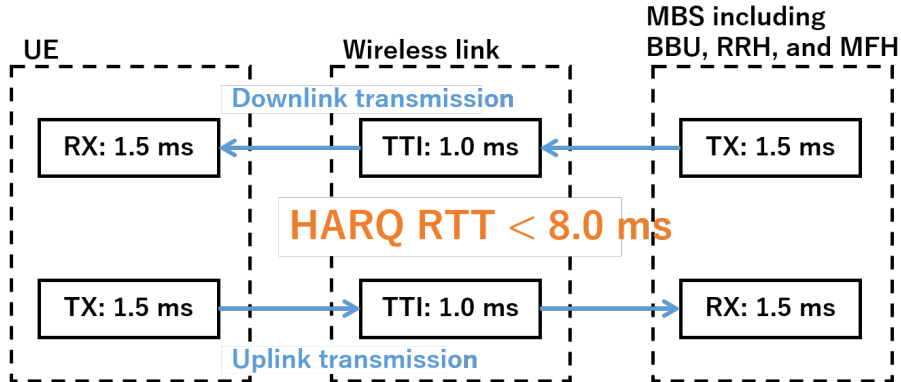


Fig. 2.6 Latency requirement for HARQ.

The option  $I_D$  in eCPRI is only recommended for the downlink signal. To further reduce bandwidth, for option  $I_D$ , K. Miyamoto *et al.* [40] proposed split-PHY processing (SPP) for the uplink transmission. In this case, the amount of MFH data  $D_{mfh}$  in 1TTI is as follows,

$$D_{mfh} = N_{lay}N_{mod}N_{q-LLR}N_{rb}N_{sc}N_{sym}, \quad (2.3)$$

where  $N_{mod}$  is the modulation order,  $N_{q-LLR}$  is the number of quantization bits for log likelihood ratio (LLR).

### 2.4.3 Latency Requirement

The MBS requires the strict specification for the latency due to a hybrid automatic repeat request (HARQ) process in the case of the LLS. Here, we describe the HARQ process defined in the third generation partnership project (3GPP) release 14 [44]. HARQ is error correction method combined ARQ with feed forward error correction (FEC). If the data signal cannot be correctly received, the data signal is divided into several data blocks and retransmitted and it is integrated with the first transmitted data to verify correctness. The transmission rate can be increased since a part of the data signal is retransmitted. The time limit from sending a user signal to receiving acknowledgment (ACK)/ negative-acknowledgment (NAK) response signal for the HARQ process is defined as 8 ms in frequency division duplex (FDD) case. Therefore, the round trip time (RTT) is required 8 ms or less. Figure 2.6 shows the latency requirement for the UE, the wireless link, and MBS. The UE needs to perform the signal sending and receiving process within 3 ms. In this case, the TTI is set to 1 ms. The MBS should perform the signal processing within 1.5 ms for sending and receiving, respectively. In the C-RAN, The 1.5-ms processing time includes each processing time of the RRH, BBU and the propagation time in the MFH link. The total processing time excluding the propagation time in the MFH link is described 1 ms as a reference value. Thus, the latency requirement for the MFH link is 0.5 ms. The actual requirement is set to 250  $\mu s$  [42] or 100  $\mu s$  [43] with a margin.

Table 2.2 Network topology and multiplexing scheme for mobile fronthaul networking.

	TDM-PON	WDM-PON	Bridged network	WDM bridged network
Topology	Star	Star	Ring/Mesh/Bus	Ring
Channel	Share	Occupation	Share	Occupation
Latency	Huge	Low	Middle	Low
Scalability	Low	High	Low	High
Cost	Low	High	Low	High

## 2.5 Time Sensitive Network Based Mobile Fronthaul

### 2.5.1 Network Topology and Multiplexing Scheme

This section describes a network topology and multiplexing scheme for the MFH networking as a TSN.

Although the latency requirement in the MFH link is very stringent, some latency for the MFH signal is allowed if it is within the specified range. In addition, there is a requirement in a time variation (timing jitter) for MFH signal forwarding. The timing adjustment method has been proposed [45]. Using this method, the timing adjuster [45], in the CU, DU, or first connected node stamps a time information on the MFH signal frame. The node receiving the stamped frame refers to the time information and then buffers the stamped frame. The node then forwards the buffered frame to the CU or DU at the preset time. By employing the timing adjuster [45] to enter and exit nodes of the network, the MFH link can be more effectively networked.

MFH networking with various multiplexing schemes and topologies has been studied. Representative studies of multiplexing scheme in the MFH network are summarized in Table 2.2. A PON system will be a better solution if a number of small cell DUs are to be deployed within a radius of less than a few hundred meters [46].

In particular, there is no interference between the MFH signals having independent channels when a wavelength division multiplexing (WDM) scheme is employed. Thus, the low latency transmission can be realized when employing the WDM scheme. In addition, the WDM-PON has high scalability since the operator can set any transmission data rate per each wavelength channel. However, the WDM system has a higher cost since different light sources for each wavelength will be needed. Moreover, there is a limitation in the number of wavelength channels which can be multiplexed since the bit error rate is affected by the reflection at fusion points and optical splitters [47].

Time division multiplexing (TDM) schemes have also been studied [45], [48]–[53]. A general TDM-PON system suffers from a huge transmission waiting time of more than one milliseconds when sending the MFH signal. The details concerning the transmission waiting time are described in next section. There are several ways to solve this issue [45], [48]–[54]. Optimally, all of the optical network units (ONUs) which are connected to the DUs can use the same type of the optical transceiver at the same wavelength. When that is the case, we can achieve a cost-effective MFH network.

A bridged network with a layer-2 switch (L2SW) is one of the solutions. The low-latency network can be realized since L2SW does not suffer from transmission waiting time. Note that a packet serialization causes a delay when packet multiplexing is employed in the bridged network. In addition, the L2SW requires a power supply, unlike the PON system, and there is a limitation in the placement location.

A WDM bridged system has been studied mainly in Europe [55]–[57]. It also requires a different transceiver for each wavelength which is, as stated above, costly.

In the access network, the most important factor in deciding the transmission method is cost-efficiency. Therefore, the TDM-PON and the bridged network are better solutions compared to WDM systems. The number of wavelength channels can be increased by employing the WDM scheme if the bandwidth is insufficient. The next section describes the related features in the TDM-PON and the bridged network which are required to construct the TSN.

### 2.5.2 Time Sensitive Network Accommodating MFH and Secondary Services

The architecture of the time sensitive network (TSN) employed in this thesis is shown in Fig. 2.7. We construct the TSN by using both PON and a layer-2 bridged network systems because these two network systems are known as the most-cost effective systems. A TSN would be feasible in the following network configurations:

1. Only a TDM-PON system
2. Only a layer-2 bridged network system
3. Both TDM-PON and a layer-2 bridged network systems

In fact, it is difficult to construct the TSN with only MFH service. This is because the burst wireless signals arrive at the MFH simultaneously and a queuing delay occurs since the MFH signals have the same priority. For example, the length of one burst MFH signal is  $100 \mu\text{s}$  when the burst MFH signals of 1 Gbps from 4 DUs arrive at the relay node and the transmission capacity in the MFH link is assumed to be 10 Gbps. In this case, the last forwarded burst MFH signal waits for roughly  $300 \mu\text{s}$  at the relay node. This queuing delay is not compatible with the MFH latency requirement. Thus, the total number of the accommodated users needs to be increased by accommodating the MFH and secondary services in the TSN. However, the TSN has other issues of decreases in BUE and throughputs of the secondary services when we construct the TSN accommodating both the MFH link and the secondary services.

In this thesis, we study the bandwidth allocation schemes for improving the BUE and throughputs of the secondary systems. In a related work, there is a network resource control for preparing network slices for each RAN service [58]. In this case, the network is dynamically shared by multiple services and the network resource is dynamically allocated to each slice. For another example, the software defined network (SDN) controller focuses on the PON system as a bandwidth control target [59].

The difference between our studies and the network sliced system [58], [59] is whether it is controlled in a distributed manner or in a centralized manner. Strict time management of bandwidth allocation in the proposed scheme must be performed by each OLT or L2SW, but the amount of the allocating bandwidth can be calculated by an external controller. The distributed control is currently performed for general TDM-PON system and L2SW. For this reason, we consider the distributed control in terms of rapid introduction and ease



Table 2.3 Mobile backhaul requirements.

Access type	Latency	Throughput
Fiber Access 1 (Non-Ideal)	10–30ms	10M–10Gbps
Fiber Access 2 (Non-Ideal)	5–10ms	100M–1Gbps
Fiber Access 3 (Non-Ideal)	2–5ms	5M–10Gbps
Fiber Access 4 (Ideal)	2.5 $\mu$ s without propagation delay	< 10Gbps

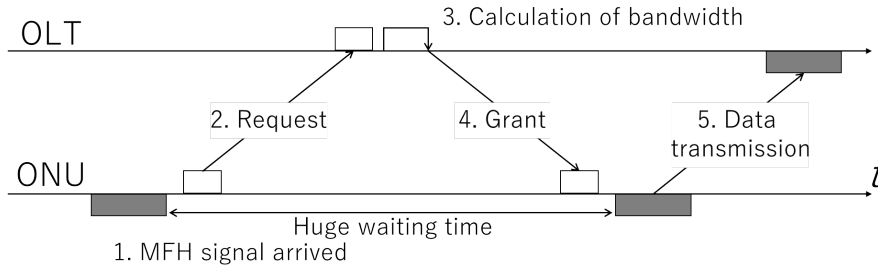


Fig. 2.8 Time chart of conventional DBA [62].

transmission waiting time between requesting the data transmission and being granted permission to send. The transmission waiting time in the ONU is a critical problem since the latency requirement for the MFH link is very strict, e.g. 250  $\mu$ s [42] or 100  $\mu$ s [43].

The DBA techniques reducing the MFH latency have been proposed. Moreover, considering the accommodation of the MFH and the secondary services in the TDM-PON, we also have to secure bandwidth allocated to the secondary system. In this section, we describe the related DBA schemes.

#### Status Reporting Dynamic Bandwidth Allocation Scheme

Conventional status reporting DBA (SR-DBA) suffers from a huge transmission waiting latency [62]. Figure 2.8 shows the time chart of the conventional DBA scheme. First, the ONU transmits a signal requesting that a data signal be forwarded. After receiving the request signal from the ONU, the optical line terminal (OLT) calculates the bandwidth and the time. The OLT then allocates the bandwidth and the transmittable time and the ONU can transmit the data signal. The waiting time until the ONU transmits the data signal is typically more than a few milliseconds. A conventional TDM-PON employed the SR-DBA does not satisfy this requirement since the required latency in an MFH link has been defined as 250  $\mu$ s [42] or 100  $\mu$ s [43]. On the other hand, the OLT can flexibly allocate the bandwidth to the secondary system because the ONU send the signal buffering state to the OLT. That is, the OLT can allocate all bandwidth to the secondary systems when the MFH is not forwarded.

#### Cooperative Dynamic Bandwidth Allocation Scheme

To satisfy the latency requirement, a cooperative DBA scheme has been proposed [48]–[53]. Figure 2.9 shows the time chart of the cooperative DBA. In [48], the CU forwards wireless

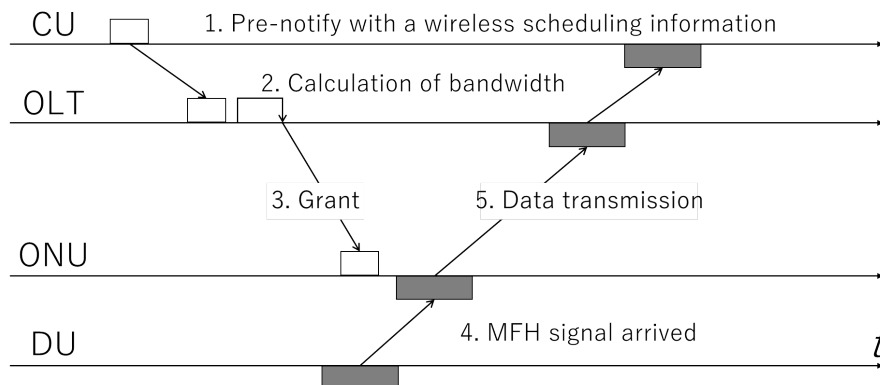


Fig. 2.9 Time chart of cooperative DBA [48], [50].

scheduling information to the OLT through the cooperative interface [50]. The OLT calculates the bandwidth in the PON link based on the wireless scheduling information. The OLT allocates the bandwidth to the ONU, and then the ONU receives the MFH signal from the DU just at that time. Thus the transmission waiting time is minimized.

S. Zhou *et al.* [53] proposed a wireless scheduling scheme with a high BUE and low latency. The use of the proposed mobile scheduler eliminates the need for conventional PON scheduling.

Employing those DBA schemes [48], [53] enables the transmission waiting time of a TDM-PON based MFH link to be optimally minimized. Moreover, the OLT can flexibly allocate the bandwidth to the secondary system because the OLT receives the information of the non-transmission interval from the CU.

In [48] and [53], however, the CU and the OLT exchange the information of the amount of the allocated wireless bandwidth. Generally speaking, wireless access system and optical access network are operated by different operators. Thus, it is difficult for the CU and the OLT to exchange the information since there are a confidentiality and a difference in operation policy between the operators. Meanwhile, in terms of the standardization, both optical and mobile systems need to be standardized by different standardization group. It is difficult to align the timing of standardization among different standardization bodies. In addition, the additional remodeling must be needed. The remodeling of the mobile system has low adoption advantages because it is necessary to exchange all the MBSs according to the specification of the optical system. Thus, we need to provide the PON based MFH without an additional interface if the CU cannot be remodeled.

### Statistical Dynamic Bandwidth Allocation Scheme

A statistical DBA scheme has been proposed as a method of bandwidth calculation in a PON link without a request signal [64], [65]. By employing the statistical DBA scheme, the cooperative interface is not needed and low-latency forwarding can be realized. The time chart of the statistical DBA scheme is shown in Fig. 2.10.

H. Bang *et al.* [64] proposed a technique for estimating the amount of buffer in an ONU without a request signal and reported an improvement of the BUE. A. Walid and A. Chen [65] proposed multiple methods for the statistical DBA scheme. The first method

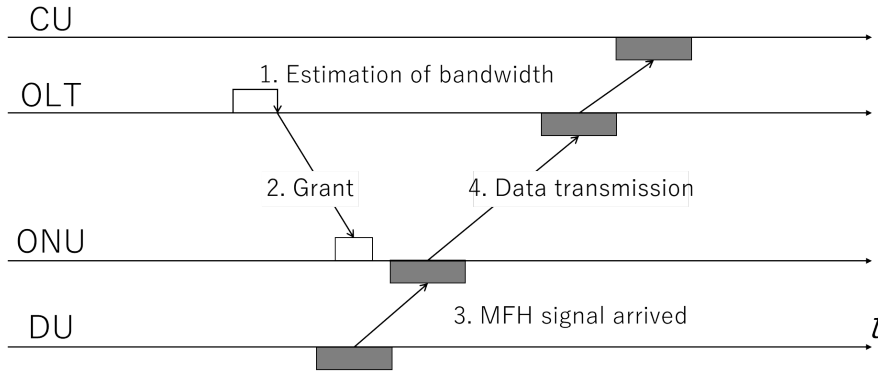


Fig. 2.10 Time chart of statistical DBA.

is the estimation of the buffer state in the ONU based on probability. The second method finds an exact solution for the buffer amount based on the input traffic model. The final method switches the DBA from/to the first allocation to/from the second allocation by using machine learning. This scheme focuses on BUE improvement rather than latency suppression. However, when accommodating a mobile system, the most important condition is to satisfy the latency requirement.

In our previous work, we proposed a statistical DBA scheme based on mobile traffic with a long day-by-day cycle [54]. The proposed DBA scheme allocates bandwidth based on average and standard deviation values.

The CU and DU can generate burst MFH signals instead of continuous signals for the 5G era and beyond as shown in section 2.4.2. The above DBA schemes [64], [65], and [54] do not consider the input of such a burst signal. The related studies cannot estimate the time of the burst traffic generation and so the bandwidth allocation starts at a different time from the burst generation. In other words, there is a very long transmission waiting time.

#### Fixed Bandwidth Allocation Scheme

Fixed bandwidth allocation (FBA) scheme allocates a constant bandwidth with a fixed interval continuously. There is the low BUE since the ONU is allocated the constant bandwidth regardless of the forwarding data volume. For instance, when total transmission capacity of the PON link is 10 Gbps and the DU has the maximum data rate of 1 Gbps, The OLT accommodates only 10 ONUs. Note that PON link overhead is not considered in the above simple calculation for the number of the ONUs which can be accommodated. However, the OLT allocates the small bandwidth to the secondary system since the OLT allocates the constant bandwidth to the MFH independent of the data amount. Thus, the throughput of the secondary system is reduced.

Here, we summarize the related DBA schemes in Table 2.4. The most important factors are BUE, low latency performance, and low cost when PON system is employed. Our goal is also described in Table 2.4. The optical network operator cannot exchange the information for the MBS with the mobile operator. The information for the MBS includes

Table 2.4 Comparison of technical advantages of bandwidth allocation scheme in TDM-PON.

	SR-DBA	Cooperative DBA	Statistical DBA	FBA	Study goal
Bandwidth usage efficiency*	High	High	Middle	Low	High
Latency for MFH link	Huge $\geq 1$ ms	Low $\leq 250$ $\mu$ s	Middle	Low $\leq 250$ $\mu$ s	Low $\leq 250$ $\mu$ s
Throughput of secondary system*	High	High	Middle	Low	High
Hardware remodeling	Unnecessary	CU, OLT	OLT	OLT	Only OLT

\*Quantitative value depends on the network system design.

Table 2.5 List of TSN standardizations for mobile fronthaul networking.

Standard	Title	Status	Last updated
IEEE 802.1CM	Time-Sensitive Networking for Fronthaul	Draft 2.2	14 Mar. 2018
IEEE 802.1AS-rev	Timing and Synchronization for Time-Sensitive Applications	Draft 7.0	29 Mar. 2015
IEEE 802.1Qca	Path Control and Reservation	Published	11 Mar. 2016
IEEE 802.1Qbv	Enhancements for Scheduled Traffic	Published	18 Mar. 2016
IEEE 802.1Qbu	Frame preemption	Published	30 Aug. 2016
IEEE 802.3br	Interspersing Express Traffic	Draft 2.3	22 Oct. 2015

the timing of the burst generation and wireless bandwidth allocation. Thus we need to establish a bandwidth allocation scheme to forward the MFH signal as highest priority service with low latency. In this case, the signals of the secondary services must not influence the MFH signal. Therefore, we employ the FBA scheme. The CU does not need to be remodeled when the OLT is employed to the FBA scheme. However, the OLT needs to allocate the bandwidth continuously to the ONUs connected to the DUs as the primary systems since the OLT is employed the FBA. Thus, the throughputs of the secondary systems are decreased. Moreover, the BUE also decreases because the OLT allocates the continuous bandwidth to the ONUs connected to the DUs even if the DUs do not transmit the MFH signals. Thus, we need to study the method of increasing the BUE and the throughput of the secondary system.

#### 2.5.4 Layer-2 Bridged Network for Mobile Fronthaul

A low-latency bridged network for the MFH has been standardized in IEEE 802.1 TSN [12]. A TSN for MFH has been discussed in IEEE 802.1CM [12]. IEEE 802.1CM is diverted the existing technologies from other IEEE standard rather than standardizing a new technology. In addition, it also defines as the values of frame loss rate, latency, and jitter. These definitions are also referred to CPRI [32] and eCPRI [43]. The goal of a TSN for MFH in IEEE 802.1CM is to guarantee low-latency forwarding and ensure redundancy

Table 2.6 Comparison of flow control methods in layer-2 bridged network.

	Strict Priority	Frame preemption	Time aware shaper	Study goal
Bandwidth usage efficiency*	High	High	Low	High
Latency for MFH link	High $\geq 250 \mu s$	Low $\leq 250 \mu s$	Low $\leq 250 \mu s$	Low $\leq 250 \mu s$
Throughput of secondary system*	High	High	Low	High
Time synchronization	Unnecessary	Unnecessary	Necessary	Unnecessary
Hardware remodeling	Unnecessary	All L2SWs	Partial L2SWs	Partial L2SWs

\*Quantitative value depends on the network system design.

without frame loss.

The TSN standardization related to MFH networking is shown in Table 2.5. IEEE 802.1AS–rev [66] defines the standardization for a function of a time synchronization in layer-2 bridged network. IEEE 802.1Qca [67] standardizes about a protocol of a path control in layer-2 bridged network. In IEEE 802.1Qbv [30], a bridged node has a time scheduler and each queue in bridged node set a time slot. The bridged node allocates the bandwidth to each queue and then bandwidth allocated queue can forward buffered frame at the allocated time. This function is called a time aware shaper (TAS). In IEEE 802.1Qbu [68] and IEEE 802.3br [69], a bridged node halts and divides the low-priority frame forwarding when the primary frame arrives. This function is called frame preemption (PE).

We summarize applicable methods of flow controls in Table 2.6. In a method of strict priority queuing (SPQ), primary frames in a specific queue are forwarded earlier than frames of other queues. However, the MFH frames are affected by the secondary frames when only employing the SPQ. This is because the frames of the secondary system are inserted between the MFH frames. That is, employing only the SPQ is not sufficient enough to forward the burst MFH signal since the huge latency occurs. The detail of this issue is described in section 5.2.

SPQ is also used in conjunction with a PE or a TAS. As of May 2018, PE has been approved in IEEE 802.1CM draft 2.2 as an option. For PE, we need two L2SWs at least to perform the PE function. All of the L2SW in the bridged network have to employ the PE since the PE function changes header information in the frame. One L2SW divides the secondary frame into two frames. The divided frames are combined when the divided frames arrive at another L2SW.

Meanwhile, TAS has not been approved in IEEE802.1CM due to the complicated operations. To employ the TAS, the bridged node needs to allocate the bandwidth strictly

in accordance with a time scheduler. Moreover, the L2SWs employed TAS in a bridged network have to be time-synchronized. As a merit of employing the TAS, the TAS can operate on a single node.

Here, we describe our goal as shown in Table 2.6. In the TSN for MFH, a hardware remodeling gives a large impact to a network operator because of increase in capital expenditure. Thus, we focus on the TAS scheme because the hardware remodeling has to be minimized.

The uses of PE and TAS have been studied to satisfy MFH requirements. In related work, a jitter-less scheduling scheme for a CPRI [32] stream has been proposed with the aim of employing a TAS for a MFH [70]. D. Thiele, et al. [71] reported evaluations of the worst delay for a priority stream by using a TAS.

As a next step, we need to improve the PE and the TAS to reduce the latency for the secondary system. This is because forwarding the signals of the secondary systems has not been considered in previous work [70], [71]. The TAS bridged node is helpful for reducing the latency of the primary stream but has a lower BUE than a node employing only the SPQ. Despite the low BUE, the secondary stream cannot be assigned any bandwidth and so the bandwidth is wasted. Thus we need to overcome the above issue to realize a converged network. The detail is described in Chapter 5.

## 2.6 Conclusion

First, we clarified the definition of TSN which is the research goal in this thesis. The characteristics in the MFH link that was the object of accommodation in TSN were described in detail. According to the characteristics in the MFH link, we showed that low latency is required despite the simultaneous occurrence of burst signals. To improve the accommodation efficiency, we described the necessity of the accommodation of the MFH link and the secondary services in single TSN. In addition, as the construction method of the TSN, we selected a TDM-PON system and a layer-2 bridged network system because of their cost effectiveness.

We indicated the significant issues when employing the TDM-PON and layer-2 bridged network systems. We reported that the TSN suffered from decreases in the throughput of the secondary system and the BUE. Finally, we showed the need to establish a bandwidth allocation scheme to improve the above issues.

For the TDM-PON system, we selected the FBA scheme from conventional bandwidth allocation schemes. We denoted a necessity of the estimation of the non-transmission intervals in the MFH link without CU remodeling to improve the throughput of the secondary systems and the BUE.

For the layer-2 bridged network system, we selected the TAS scheme from the techniques of the TSN standard. We denoted that TAS kept the reserved bandwidth for the MFH link for a preset time even after forwarding has been completed. This reserved time causes a decrease in the BUE.

The techniques to solve the above issues are described in Chapters 3, 4, and 5.

## Chapter 3

# Accommodation of TDD-based Fronthaul and Secondary Services

### 3.1 Introduction

A cost-effective mobile fronthaul (MFH) is needed because a lot of mobile base stations (MBSs) will be densely deployed in future radio access network (RAN). A time division multiplexing passive optical network (TDM-PON) is capable of reducing the network cost as the number of subscribers increases. However, the number of distributed units (DUs) that can be accommodated in a TDM-PON is limited since an MFH has a throughput of more than 1 Gbps. The accommodation of not only the MFH but also multiple services will enable us to construct a more cost-effective network that will in turn achieve cost-effective MFH. Therefore, we propose the accommodation of the MFH and secondary services in a TDM-PON. Our proposed TDM-PON allows us to increase the number of accommodated ONUs. We use a traffic monitor to capture the MFH signal and then estimate the unallocated interval of the MFH link in the PON domain by using the characteristics of the MFH signal. The signals of the secondary services are inserted in the unallocated interval of the MFH link. We estimate the unallocated interval by using this characteristic. In this chapter, we report simulation, experimental and theoretical results for our proposed technique obtained with a 10Gigabit-Ethernet PON (10G-EPON) prototype. Moreover, we also discuss the variation in throughput when we increase the number of optical network units (ONUs).

### 3.2 Accommodation of TDD-based MFH in TDM-PON

This section describes the overview of time division duplex (TDD) system and the characteristics of the TDD-based MFH link.

The TDD system flexibly switches the wireless bandwidth from the uplink to downlink and vice versa, with respect to the wireless sub-frame. Table 3.1 shows the component ratio of the uplink and downlink defined as Third Generation Partnership Project (3GPP) [72]. Here, we define the configuration as TDD pattern. A wireless frame is divided into ten sub-frames. There are 7 categories of TDD frame structure in 3GPP. In addition, the transmission interval of the sub-frame is called transmission time interval (TTI) in

Table 3.1 TDD pattern [72]. D: downlink sub-frame, U: uplink sub-frame, S: special sub-frame.

		Sub-frame number									
		0	1	2	3	4	5	6	7	8	9
Index	0	D	S	U	U	U	D	S	U	U	U
	1	D	S	U	U	D	D	S	U	U	D
	2	D	S	U	D	D	D	S	U	D	D
	3	D	S	U	U	U	D	D	D	D	D
	4	D	S	U	U	D	D	D	D	D	D
	5	D	S	U	D	D	D	D	D	D	D
	6	D	S	U	U	U	D	S	U	U	D

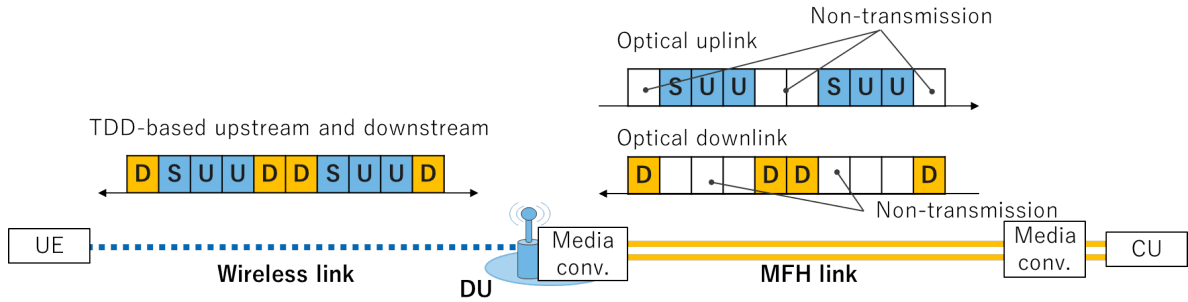


Fig. 3.1 TDD-based MFH characteristic.

general. Note that the special sub-frame includes an uplink pilot time slot (UpPTS), a downlink pilot time slot (DwPTS) and a guard time period (GP) [72]. In Table 3.1, the TDD-based mobile base station (MBS) is operated with the fixed optimal index. The index does not change dynamically per wireless frame. However, it could be changed with a long period (e.g. from morning to evening).

Figure 3.1 shows a general MFH link when an MBS employs the TDD scheme. A central unit (CU) is connected to a distributed unit (DU) by optical fibers. For the uplink transmission, the user equipment (UE) sends the wireless signal to the DU. After receiving the wireless signal, a media converter converts the wireless signal into the optical signal. The optical signals of the uplink and the downlink are forwarded through the different optical fibers. The periodical non-transmission interval occurs in the optical domain since the MBS employs the TDD scheme on the wireless transmission.

Figure 3.2 (a) shows a TDM-PON system accommodating TDD-based DUs. The neighboring DUs are time synchronized and use the same index to avoid signal collision. For the uplink transmission, the DUs simultaneously transmit the data signal to a CU. An ONU transmits the burst signal when the TDM-PON accommodates the packet based MBS as typified by the media access control (MAC) layer - physical layer (PHY) split [42]. A MAC-PHY split MBS is with a function for redefining the CU and the DU. In

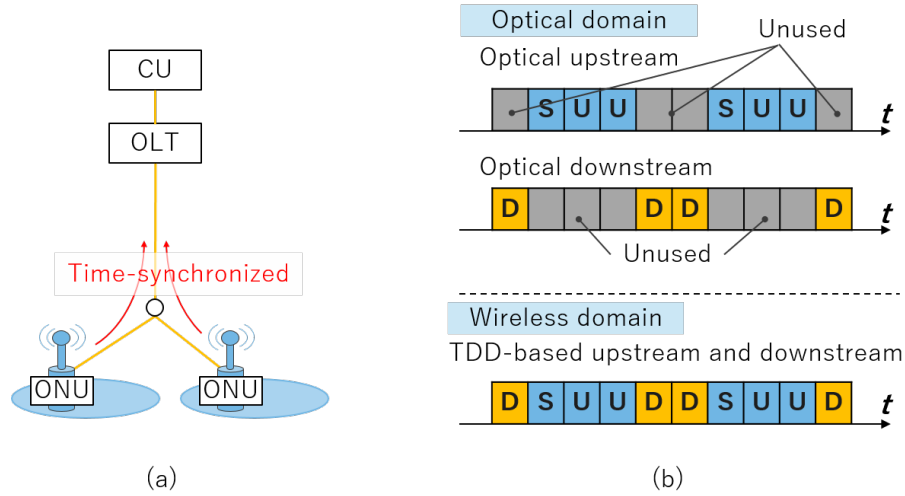


Fig. 3.2 TDM-PON system accommodating TDD-based RRHs. (a) Time synchronized transmission. (b) Unused interval in optical domain.

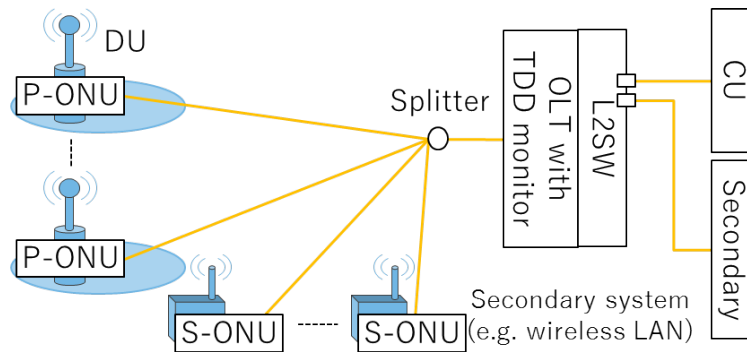
the MAC-PHY split MBS, the functions of the MAC and upper layers are in the CU, and those of the PHY and lower layers are in the DU. Therefore, a statistical multiplexing effect is not expected because a burst signal arrives at the ONU at the same time. The number of ONUs that can be accommodated in a TDM-PON is limited. This limitation was also described in Chapter 2.

In the optical transmission domain, the use of wavelength division multiplexing (WDM) systems is well known. The WDM scheme forms virtually independent links in single optical fiber by using the multiple wavelengths. For TDM-PON system, two different wavelengths are also used as the uplink and downlink, respectively. By using the two wavelengths in the optical domain and a single frequency band in the wireless domain, non-transmission periods occur when an optical system accommodates a TDD-based RRH as shown in Fig. 3.2 (b). Such an interval is defined as an “unallocated interval”. Bandwidth usage efficiency (BUE) in the TDM-PON is decreased because the unallocated intervals always appear.

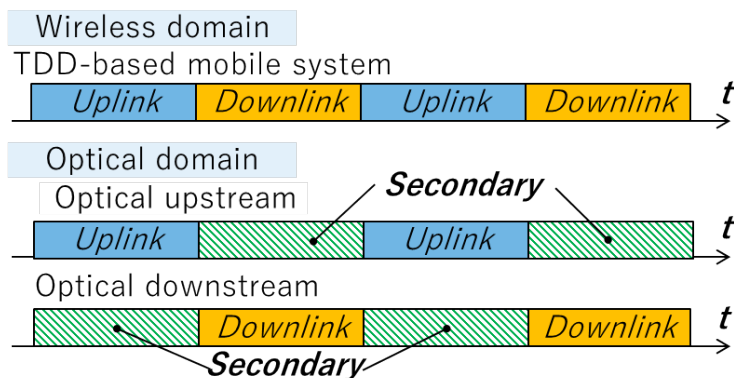
### 3.3 Proposed TDM-PON Architecture

We propose inserting the signal of secondary services in the unallocated intervals of the TDD-based MFH to increase the number of accommodated ONUs. Figure 3.3 (a) shows a proposed architecture based on TDM-PON and Fig. 3.3 (b) shows a time chart of proposed bandwidth allocation. The technique used for inserting secondary services is different for the uplink and downlink transmissions and is outlined below. Here, we define a Primary-ONU (P-ONU) as an ONU connected to an RRH, and a Secondary-ONU (S-ONU) as an ONU connected to a secondary system.

For the downstream direction, we employ priority control based on quality of service (QoS) at a layer 2 switch (L2SW) in an optical line terminal (OLT). The MFH signal, which is forwarded from a CU to an OLT, is preferentially transmitted to an ONU with



(a) Proposed architecture based on TDM-PON.



(b) Secondary system insertion.

Fig. 3.3 Concept of multiple accommodation technique.

ultra-low latency. As an additional way of decreasing the queuing latency in an L2SW, the techniques of frame preemption (PE) and time aware shaper (TAS) have been proposed [68], [30]. It is expected to achieve ultra-low latency transmission.

For the upstream direction, the OLT manages and calculates the uplink transmission schedule and the bandwidth allocation. After the calculation, the OLT sends a grant signal to the ONUs with the same time interval. This interval is defined as an “allocation cycle”. Then, the ONUs can transmit the data signal with the granted bandwidth at the granted time. The detail of the general bandwidth allocation scheme is described in Chapter 2. In the proposed architecture, the OLT must learn the period of the uplink unallocated interval of the MFH link. For this reason, our proposed technique estimates the period with a traffic monitor, and then the OLT allocates the bandwidth to the ONU on the basis of the estimated result. In this way the period is learned at the OLT without any additional interface or mechanism for notifying the timing of the unallocated interval from the CU. Thus, we proposed the use of a traffic monitor in the OLT to distinguish the timing of allocated intervals from that of the unallocated intervals. The bandwidth allocation scheme is described in Section 3.4.2.

---

**Algorithm 1** Unallocated interval estimation.

---

```

Set monitoring time
Traffic monitoring
Generating pseudo wireless frame
Searching for leading position of pseudo wireless frame
Set threshold
counter ← 0
while counter ≠ lengthofpseudowirelessframe do
  if traffic volume of TTI leading position > threshold then
    Set Sub-frame to uplink
  else
    Set Sub-frame as downlink
    Set Only array of leading position as uplink
  end if
  counter ← counter + 1TTI
end while

```

---

## 3.4 Principle of Operation

### 3.4.1 Unallocated Interval Estimation in MFH Link by Using Traffic Monitor

A TDD monitor which includes a traffic monitor and an estimator, is installed in an OLT as shown in Fig. 3.3 (a). We describe the operation of the unallocated interval estimation in Algorithm 1. First, the traffic monitor counts the uplink frames with respect to each ONU. The monitoring time is manually preset. The monitoring interval is also preset and is the same as the allocation cycle. In the second step, the monitored frames are summed up at regular intervals. The interval between summed up frames is the length of one wireless frame. Moreover, all of the summed up frames are superimposed so that they can be treated as one wireless frame (Line 3). For example, in the long-term-evolution (LTE), the length of the superimposed frame is 10 ms. The estimator uses this superimposed frame. When the estimator distinguishes the unallocated interval from the allocated interval, the OLT must obtain and estimate the leading position of the sub-frame.

To learn the leading position of the sub-frame, the estimator seeks the longest spells of non-data transmission and determines the switching point from the interval of the non-data transmission to that of the data transmission (Line 4). The switching point is the leading position of the sub-frame. This search algorithm is applicable for the MBS type of common layer 2 C-RAN (L2-CRAN) such as the MAC-PHY split [42] and split PHY processing (SPP) [40], [41]. For the L2-CRAN, the wireless signal is demodulated and decoded in the DU with respect to each 1 TTI. The demodulated and decoded wireless signal is forwarded in bursts into the MFH every 1 TTI. For unallocated interval estimation, the leading position of the unallocated interval is only needed. In this time, the data volume and variation are independent of the estimation. Thus the leading position can be learned by seeking the rising point of the sub-frame.

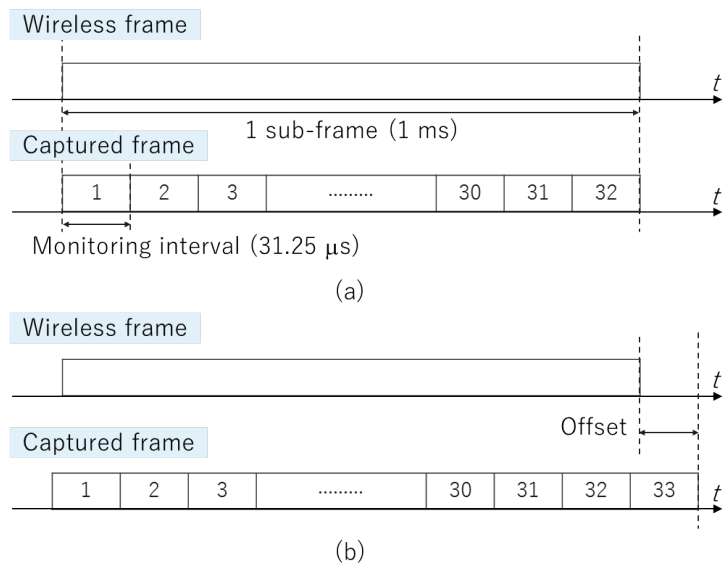


Fig. 3.4 Example for need of extra monitoring interval. (a) Phase synchronization between sub-frame and monitoring interval. (b) No synchronization between sub-frame and monitoring interval.

In the estimator, the threshold is set as a yardstick when distinguishing the unallocated interval from the allocated interval (Line 5). Note that the uplink and downlink are switched as a unit of the sub-frame. The data volume of the array of the leading position is compared with the threshold every TTI unit (Line 8).

When the volume of the array of the leading position exceeds the threshold (Line 8), the array of the leading position is considered as the allocated interval, and all of the arrays for 1 TTI from the leading position are set at the allocated interval (Line 9).

The same operation is employed for the next 1 TTI. Then, when the arrays of the leading position in the next 1 TTI are unallocated intervals, only the array of the leading position is reserved as an allocated interval (Line 10, 11). This is because the TDD-based DU is not completely phase-synchronized with the TDM-PON system and needs an offset between the leading position of the sub-frame and the allocation cycle of the TDM-PON system. The maximum offset is about one monitoring interval.

An example of the required offset is shown in Fig. 3.4. When the leading position of the sub-frame matches that of the monitoring interval as shown in Fig. 3.4 (a), it is possible to rebuild the sub-frame from the superimposed frame with the 32 monitoring intervals ( $32 \times 31.25 \mu\text{s} = 1 \text{ ms}$ ). However, when the leading position of the sub-frame does not match that of the monitoring interval as shown in Fig. 3.4 (b), an extra monitoring interval is needed ( $33 \times 31.25 \mu\text{s} = 1.03125 \text{ ms}$ ).

Our estimation approach is the above uncomplicated method. The estimation technique is applied when the MBSs are first deployed. The MBSs transmit test signals to confirm the connection between the DU and the CU. Then, a TDD test pattern corresponding to the TDD pattern can be transmitted. Therefore, the TDD pattern can be estimated by employing a simple estimation technique.

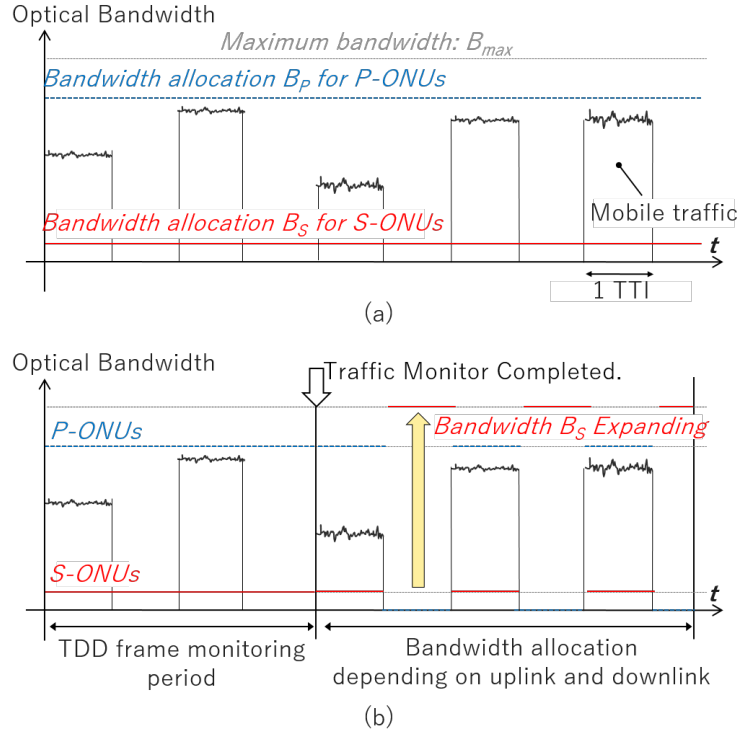


Fig. 3.5 DBA time chart of bandwidth allocation, (a) conventional FBA scheme. (b) proposed bandwidth allocation scheme.

### 3.4.2 Bandwidth Allocation Scheme

The proposed bandwidth allocation technique is compared with a conventional technique. Figure 3.5 (a) and (b), respectively, show the time chart of bandwidth allocation with the conventional fixed bandwidth allocation (FBA) and with the proposed bandwidth allocation scheme. The P-ONU is allocated a fixed bandwidth. The suffix ( $i$ ) indicates the unique identifier of the ONU. The OLT sends a grant signal to the ONUs. The ONUs transmit the data signal at the granted time. Then, the bandwidth  $B_S$  of all the S-ONUs is,

$$B_S = B_{full} - \sum_{i=1}^{N_P} b_P^{(i)}, \quad (3.1)$$

where  $B_{full}$  is the full bandwidth in the TDM-PON.  $N_P$  is the number of accommodated P-ONUs.  $b_P^{(i)}$  is the bandwidth of each P-ONU. The S-ONUs are commonly send the signal in accordance with the granted time and bandwidth.

If the proposed bandwidth allocation scheme is not applied as shown in Fig. 3.5 (a), the bandwidth  $B_S$  is only allocated according to Eq. 3.1. When the TDD monitor is operating, the type of optical bandwidth allocation is switched once the traffic monitor and the estimator have acquired information about the unallocated uplink interval as described by Algorithm 1.

The P-ONUs are unallocated when the TDD-based DUs are in the downlink state. Then, the bandwidth  $B_S$  of all the S-ONUs is,

$$B_S = B_{full}. \quad (3.2)$$

This permits an increase in the operable optical allocation bandwidth of the S-ONUs.

The bandwidth  $B_S$  is set based on the array data from the estimator. The array data is prepared with respect to each grant. For example, when the array of the first number grant in an allocation cycle indicates the allocated interval, the  $B_S$  is allocated according to Eq. 3.1. When the array of the second grant in the allocation cycle indicates the unallocated interval, the  $B_S$  is allocated according to Eq. 3.2.

### 3.4.3 Discovery Technique using Unallocated Interval

The TDM-PON needs to authenticate the connection of a new ONU. This procedure is called the discovery process. For the discovery process, the OLT activates the new ONU and measures the round-trip-time (RTT) between the OLT and the new ONU. The OLT sets an interval called a discovery window. During the discovery window, the ONU sends a signal carrying an authentication request at a random time. As regards the discovery window, when we assume that the distance between the OLT and the ONU is 20 km and the propagation time is 5  $\mu\text{s}/\text{km}$ , the RTT (= discovery window) is 200  $\mu\text{s}$ . While the discovery process is running, the OLT does not allocate connected ONUs to avoid any signal collisions between the new ONU and the connected ONUs. This causes a critical latency for the MFH accommodated in the TDM-PON. Thus, we propose a technique for reducing the latency caused by the discovery process when accommodating the MFH. Figure 3.6 and Fig. 3.7, respectively show the time chart and the operation flow of the proposed discovery process. Even while performing the discovery process, the discovery process transitions the standby mode when the MFH is in the uplink state. The discovery process transitions the operation mode when the MFH is switched to the downlink state. The maximum length of the discovery window depends on the length of the sub-frame. For instance, if the sub-frame length is 1 ms, the maximum length of the discovery window is 1 ms. The discovery window of 200  $\mu\text{s}$  is needed when the distance from the OLT to the ONU is 20 km. Thus, the proposed scheme can satisfy the requirement for the discovery process.

## 3.5 Numerical Simulation

### 3.5.1 Simulation Setup

The simulation parameters are shown in Table 3.2. For the parameters of the mobile system, we assume that the MBS is a MAC-PHY split model [42]. In the MAC-PHY split MBS, the data volume through the MFH is given as [42],

$$\text{Data volume} = TBS \times N_{CA} \times N_{MIMO}, \quad (3.3)$$

where TBS is the transport block size given in bytes that is transmitted per sub-frame.  $N_{CA}$  and  $N_{MIMO}$ , respectively, are the number of component carriers in the carrier

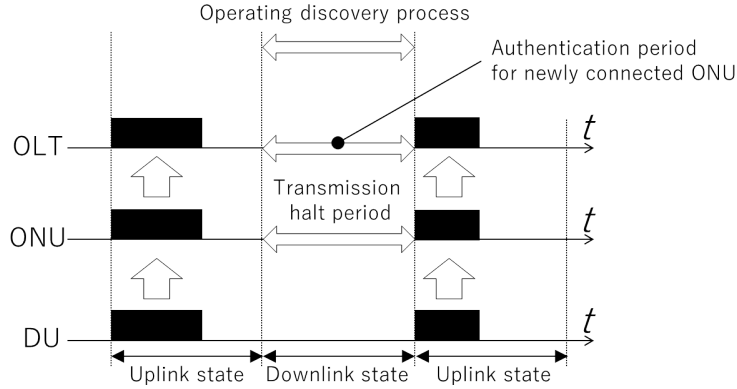


Fig. 3.6 Time chart of the proposed discovery process.

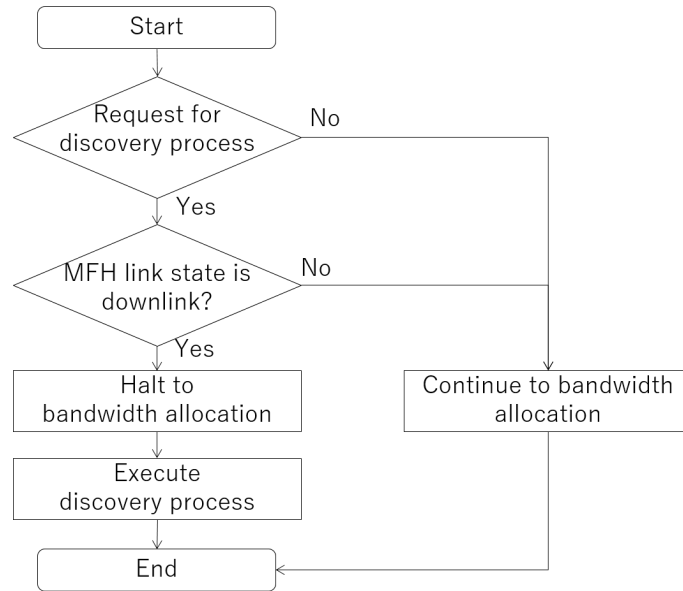


Fig. 3.7 Operation flow chart of the proposed discovery algorithm.

aggregation (CA) and the number of antennas per DU. This equation is also described in Eq. 2.1. We can expect the MFH signal to be packetized by using an Ethernet frame when the MAC-PHY split is employed. The DUs randomly send uplink signals to the CU. That is, the UE sends user datagram protocol (UDP) flows to each DU as intermittent data traffic. The intervals and durations of the bursts were exponentially distributed random variables. The average burst duration was 1.0 sec and the average burst interval was 5.0 sec. The data rates of the bursts were 2.0 Mbps. In addition, the TBS is calculated with the LTE module [73] of network simulator-3 (ns-3) [74]. Note that we generated the frequency division duplex (FDD) traffic by using ns-3. Finally, we converted the generated FDD traffic into TDD traffic based on the TDD frame pattern in Table 3.1. The index of the TDD pattern was set at No. 0. The maximum TBS size is 9422 bytes per millisecond in LTE. Thus, when considering Eq. 3.3 and Table 3.2, the maximum TBS size becomes

Table 3.2 Numerical simulation parameters.

Variable	Value
Num. of DUs (=P-ONUs)	4
Distance between DUs	100 m
Num. of UEs	50
Carrier frequency	2.0 GHz
System bandwidth	20.0 MHz/carrier
$N_{CA}$	5 carrier
$N_{MIMO}$	2 layers
Num. of S-ONUs	4
Simulation time	1.0 s
Monitoring time	10.0 ms
Optical bandwidth allocation cycle	125 $\mu$ s
FBA to P-ONU	1.0 Gbps/P-ONU
FEC	RS(255,223)
Guard time for laser on $T_{on}$	512 ns
Guard time for laser off $T_{off}$	512 ns
Synchronization time	1200 ns
Discovery window	250 $\mu$ s
Discovery cycle	100 ms

94220 bytes in 5G. The MFH capacity is assumed to be up to about 800 Mbps.

The data volume of the secondary system has a fixed size. The data size is 1.0 Gbps  $\times$  the bandwidth allocation cycle [s]. For the parameters of the TDM-PON system, the TDM-PON accommodates a total number of 8 ONUs. We performed a numerical simulation using a 10Gigabit-Ethernet PON (10G-EPON) system [19] as the TDM-PON. In this simulation, we did not consider the processing delay in the OLT or the propagating delay in the PON link. This is because such delays generally have a fixed value. In addition, the frame size is not considered. For the ONUs, the buffer size is infinity. Thus, the traffic data continue to be buffered in the ONU when the data traffic is congested. An optical bandwidth allocation cycle of 125  $\mu$ s is chosen to reduce the queuing delay in the ONU [75]. Here, we discuss the computational cost. The OLT needs to prepare an enough computational resource for estimating the period of the unallocated intervals. The OLT does not calculate the bandwidth to allocate to the ONU while estimating the period of the unallocated interval. This is because the OLT employs the FBA scheme during the period of the estimation. That is, most of the computational resource can be allocated to the estimation of the unallocated interval. After estimating the period of the unallocated intervals, the computational resource is allocated to the calculation of

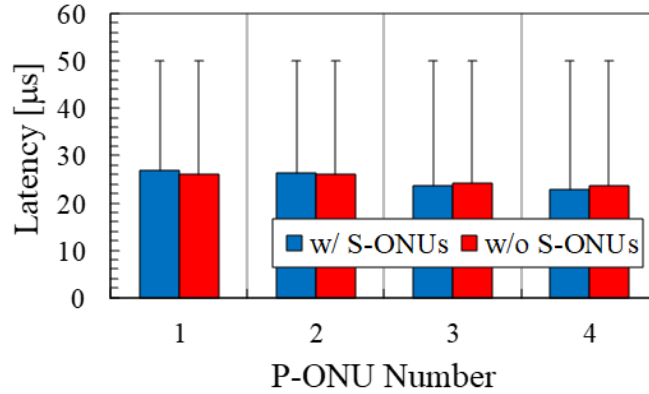


Fig. 3.8 Latency for P-ONUs.

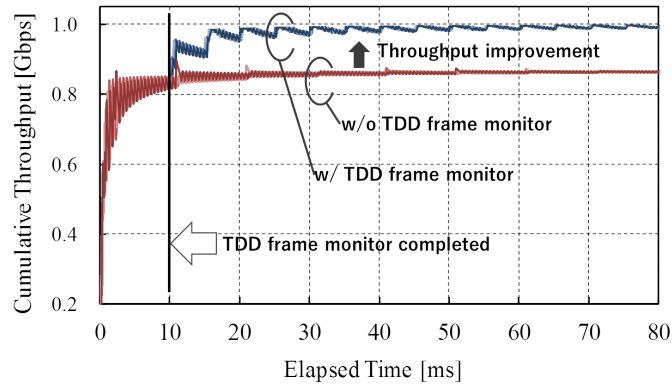


Fig. 3.9 Cumulative throughput of S-ONUs.

the bandwidth allocation. For the S-ONUs, it depends on the kind of employed dynamic bandwidth allocation (DBA) scheme. This means that only the DBA scheme requires computational resources. The discovery window in Table 3.2 enables the ONU to be authenticated through the 20 km distance between the OLT and the ONU when the propagation delay is assumed to be  $5 \mu\text{s}/\text{km}$ .

The discovery window value must be more than  $200 \mu\text{s}$  RTT because it must include the processing delay. Thus, the discovery window is set at  $250 \mu\text{s}$ . The discovery window is executed in the discovery cycle. While operating the discovery window, the OLT halts the DBA scheme.

### 3.5.2 Simulation Results of Multiple Accommodations

We report the evaluation results we obtained when employing the proposed technique. The proposed technique means the bandwidth allocation scheme with Eq. 3.2. The comparison target is a conventional allocation scheme. The conventional allocation scheme means the S-ONUs are allocated surplus bandwidth with Eq. 3.1 independent of the TDD-based MFH state. We evaluate the effect on the MFH latency and on the throughput of the S-ONUs.

### Latency Evaluation for P-ONUs

Figure 3.8 shows the result of the latency evaluation for the P-ONUs. Although the bandwidth allocation changes according to the MFH link state, the TDM-PON allows the MFH signal to be forwarded with no additional latency. The average latency of each ONU differs slightly. This is because the order of the uplink signal transmission is changed. With the proposed technique, when the TDD-based DU is in the downlink state, the OLT does not allocate the bandwidth. As the bandwidth allocation is halted, the order in which the bandwidth is allocated to each P-ONU is changed, so a slightly different latency jitter appears.

Nevertheless, the difference in the latency value with the proposed or comparison techniques is negligibly small and thus has no impact on this study.

The maximum latency is  $50.0 \mu\text{s}$ . The ONU which sends the signal in the last order induces such a maximum latency. In this simulation, 4 ONUs are accommodated in the TDM-PON and allocated a bandwidth of 1.0 Gbps. We assumed that the entire overhead is included in the 1.0 Gbps bandwidth. The total granted length  $L_{all}$  over which the ONU is able to send the uplink signal is,

$$L_{all} = \frac{T_{cycle}}{B_{full}} \sum_{N_P} b_P^{(i)}, \quad (3.4)$$

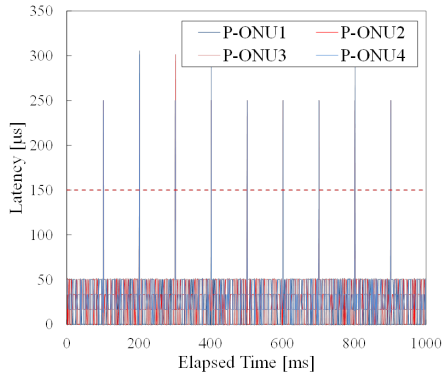
where  $T_{cycle}$  is the bandwidth allocation cycle. Then the total granted length  $L_{all}$  is  $50 \mu\text{s}$ . Therefore, this queuing delay is the maximum value. If the MFH signal is not forwarded with one allocation cycle, then the ONU sends the signal with the next bandwidth allocation cycle. In other words, the length of the allocation cycle directly affects the MFH latency and must be shortened. To ensure that the queuing delay in the ONUs is fair, the transmission order is changed with respect to each optical bandwidth allocation cycle. For this reason, the maximum latencies of all the ONUs are even.

### Throughput Evaluation for S-ONUs

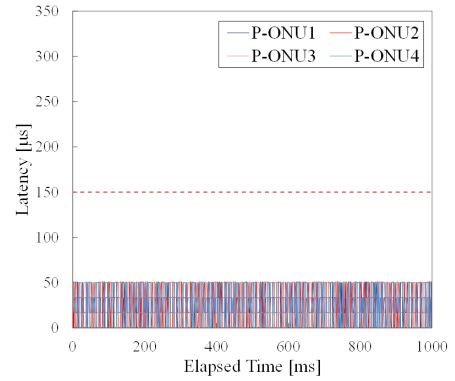
Next, we evaluated the throughput and latency of the S-ONUs. Figure 3.9 shows the elapsed time of the cumulative throughput with and without the proposed technique. The cumulative throughput  $T_P$  is defined as,

$$T_P = \frac{1}{t_e} \sum_{t=0}^{t_e} D_r[t], \quad (3.5)$$

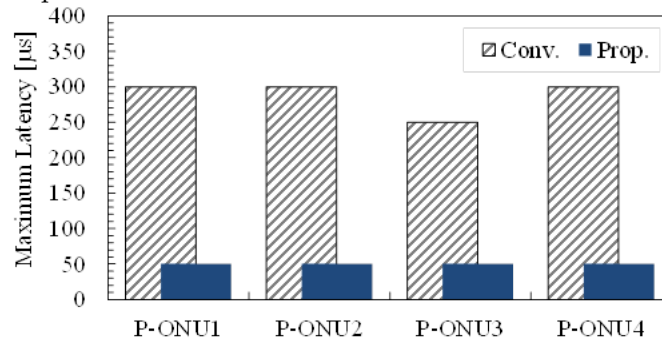
where  $D_r[t]$  is the data received at the OLT and  $t_e$  is the elapsed time. The throughput is gradually accumulated in the first 10 ms, and it is stable at around 0.85 Gbps. The cumulative throughput is the same value whether or not the proposed technique is employed. This is because the first 10 ms is the monitoring and estimation period. Therefore, the bandwidth allocation of the S-ONUs is performed in accordance with Eq. 3.1. After 10 ms, the throughput begins to increase with the proposed technique. Then, it remains stable at around 1.0 Gbps. The throughput decreases slightly with a 5 ms cycle. This is because bandwidth is also allocated to the P-ONUs. In addition, the proposed discovery process is also performed. The queuing delay (e.g. several ms) caused by the uplink state



(a) Time variation without proposed technique.



(b) Time variation with proposed technique.



(c) Maximum latency with/without proposed technique.

Fig. 3.10 Latency result caused by discovery process.

of the TDD-based MFH is longer than the delay ( $250 \mu\text{s}$ ) caused by the discovery process. In other words, the queuing delay is dominant for the latency of the ONUs.

#### Simulation Result of Discovery Technique

Figure 3.10 shows the evaluation result of the discovery process with the proposed technique. The comparison target is one where the discovery process is performed when the signals of the P-ONUs are forwarded. In Fig. 3.10 (a), a huge periodic latency appears while the discovery window is operated when the TDD-based DU is in the uplink state. From [42], the latency requirement is defined as  $250 \mu\text{s}$  including the propagation delay. It is assumed that the propagation delay between the OLT and the ONU is  $100 \mu\text{s}$  at a distance of 20 km. The processing latency in the TDM-PON must be less than  $150 \mu\text{s}$ . To accommodate the 20-km MFH link in the TDM-PON, the discovery window needs to operate for more than  $200 \mu\text{s}$ . On the basis of these requirements and results, the latency caused by the discovery process is a critical issue. In Fig. 3.10 (b), the discovery process is performed in the unallocated interval. The latency can be suppressed by comparison with Fig. 3.10 (a). In addition, the latency with the proposed technique satisfies the MFH requirement. The latency reduction of each P-ONU is summarized in Fig. 3.10 (c). The discovery latencies of all the P-ONUs can be suppressed.

## 3.6 Experiments with 10G-EPON

### 3.6.1 Allocatable Throughput for S-ONUs in 10G-EPON

The theoretical throughput of the S-ONU is calculated based on Eqs. 3.1 and 3.2 when employing a 10G-EPON. First, the granted data volume  $d_P^{(i)}$  per allocation cycle of a P-ONU is as follows:

$$d_P^{(i)} = \text{floor} \left( \frac{b_P^{(i)} T_{grant} d_{FEC}}{d_{FEC\_Payload}} \right) + d_{OH}, \quad (3.6)$$

$$D_P = \sum_{i=1}^{N_P} d_P^{(i)}, \quad (3.7)$$

where  $T_{grant}$  is the allocation cycle,  $d_{FEC}$  is the length of the Forward Error Correction (FEC) code word and  $d_{FEC\_Payload}$  is the length of the FEC payload. With a 10G-EPON,  $d_{FEC}$  is 248 bytes including a payload of 216 bytes and a 32-byte parity bit.  $d_{OH}$  is the total overhead including the laser on/off time, synchronous time and guard time.  $\text{floor}(x)$  indicates the floor function, which is the largest integer less than or equal to  $x$ . Next, the granted data volume  $d_S$  per allocation cycle of an S-ONU is

$$d_S = \text{floor} \left( \frac{B_{full} T_{grant} - D_P}{N_S} \right), \quad (3.8)$$

where  $N_S$  is the number of the S-ONUs. The net granted data volume  $d_S^{net}$  after subtracting the overhead is,

$$d_S^{net} = \text{floor} \left( \frac{d_S - d_{OH}}{d_{FEC}} \right) \times d_{FEC\_Payload}. \quad (3.9)$$

Moreover, the transmittable number of the Ethernet frames  $N_{frame}$  per an allocation cycle is as follows:

$$N_{frame} = \text{floor} \left( \frac{d_S^{net}}{d_{frame} + d_{pa} + d_{IFG}} \right), \quad (3.10)$$

where  $d_{frame}$  is the Ethernet frame size,  $d_{pa}$  is the length of the preamble and the  $d_{IFG}$  is the inter-frame gap size. Then, the throughput of the S-ONU is,

$$\text{Throughput} = \frac{d_{frame} N_{frame}}{T_{grant}}. \quad (3.11)$$

The throughput with the allocated and unallocated intervals is calculated from Eq. 3.11 and the parameters shown in Table 3.3. The calculated result is shown in Fig. 3.11. The throughput in the unallocated interval is expanded.

Table 3.3 Parameters for theoretical calculation and experiments.

Symbol	Definition	Quantity and Units
$B_{full}$	full bandwidth in TDM-PON	10 Gbps
$T_{grant}$	allocation cycle	31.25 $\mu$ s
$N_P$	number of P-ONUs	4 ONUs
$N_S$	number of S-ONUs	4 ONUs
$b_P^{(i)}$	allocated bandwidth for P-ONU <sup>(i)</sup>	1.0 Gbps
$d_{FEC}$	length of FEC code word	248 bytes
$d_{OH}$	overhead	2264 bytes
$d_{frame}$	Ethernet frame size for S-ONUs	128 bytes
$d_{pa}$	preamble size	8 bytes
$d_{IFG}$	IFG size	12 bytes

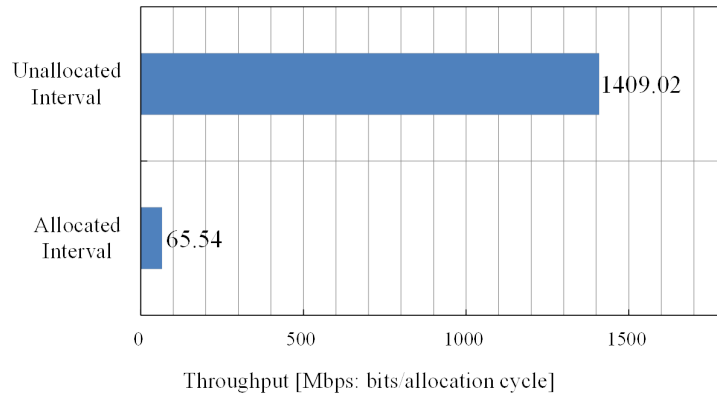


Fig. 3.11 Throughput calculation results for S-ONU in unallocated and allocated intervals.

### 3.6.2 Experimental Setup

Figure 3.12 shows an experimental setup based on the 10G-EPON system. The traffic monitor is implemented in an OLT using a field programmable gate array (FPGA). The FPGA board is Altera Arria II GX. The traffic monitor captures the upstream signal with respect to each allocation cycle from a signal processing function block. The unallocated interval of the MFH is determined by capturing the MFH upstream signal and calculated by a part of a DBA program in the OLT. The calculated result is sent to the bandwidth allocation function, which generates a grant signal based on the calculation result. The user network interface (UNI) ports of each ONU are connected to a local area network (LAN) analyzer. The LAN analyzer has a role as an uplink traffic generator. The application service network interface (SNI) port of the OLT is connected to another port

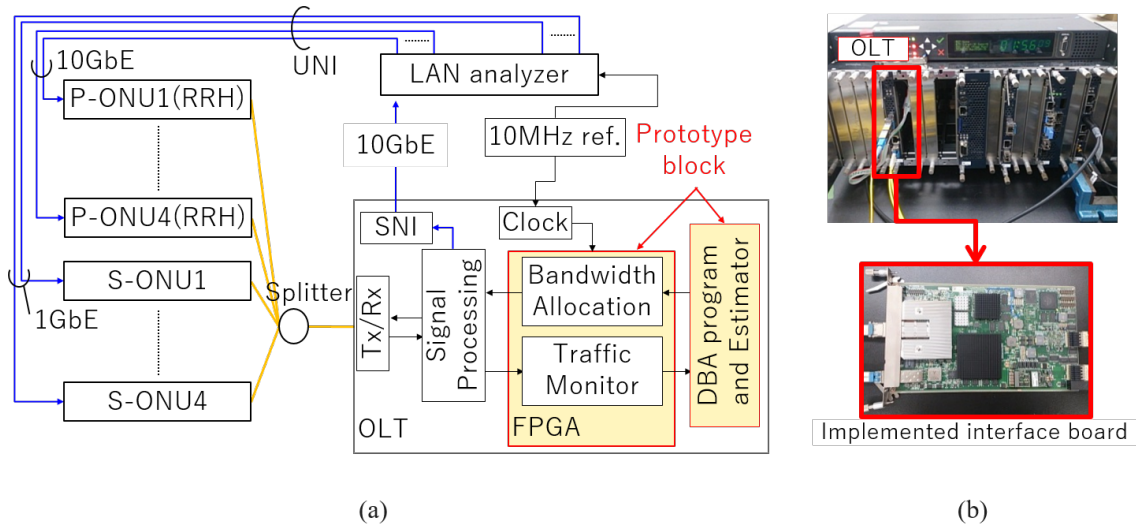


Fig. 3.12 Experimental setup based on 10G-EPON, (a) Functional block diagram of prototype system, and (b) Photograph of implemented interface board in OLT.

of the LAN analyzer. The LAN analyzer measures the latency and captures the layer-2 upstream signal. When all ONUs connect to the OLT at first, the OLT opens the discovery window and then the registration process runs. After the process, the LAN analyzer sends the Ethernet frame to each ONU. The granted bandwidths are allocated to 1000 Mbps for the P-ONUs and given by Eqs. 3.1 and 3.2 for the S-ONUs with an FBA. There are 4 P-ONUs and 4 S-ONUs. The allocation cycle is  $31.25 \mu\text{s}$ . Thus the ONU sends a data signal at intervals of  $31.25 \mu\text{s}$ . A monitoring time of 10 ms is needed to determine the unallocated interval of the MFH excluding the calculation time. The traffic model of the mobile system is assumed to be a MAC-PHY split MBS [39]. For this reason, the wireless data rate is the same as the optical data rate. The MAC layer data rate of the P-ONUs sent into the MFH is set at 800 Mbps. The mobile sub-frame is assumed to be 1 ms long. The ratio of the TDD pattern is assumed to be 3:2 (upstream: downstream), which means Index 1 of the TDD pattern in Table 3.1. The MFH upstream is generated for 3 ms and then halted for 2 ms, repeatedly. The generated frame length is fixed at 1250 bytes. For S-ONUs, the frame length is fixed at 128 bytes and the MAC layer data rate is 860 Mbps. Other experimental parameters are shown in Table 3.3.

### 3.6.3 Instantaneous Throughput and Latency

Figure 3.13 shows the result of the throughput measurements from the P-ONUs and the S-ONUs to an OLT. The use of a conventional FBA scheme is shown in Fig. 3.13 (a). The average throughput is defined as,

$$\text{Average throughput} = \frac{\text{Data volume}}{\text{Captured interval}}. \quad (3.12)$$

The captured interval is 10 ms. For P-ONUs, the measured average throughput is equal to the input average throughput ( $800 \text{ Mbps} \times 3 \text{ ms}/5 \text{ ms} = 480 \text{ Mbps}$ ). For S-ONUs,

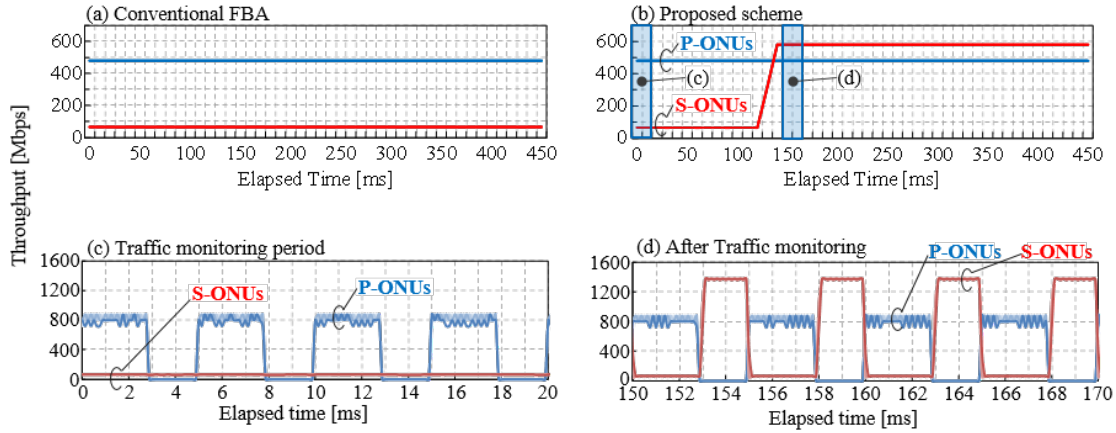


Fig. 3.13 Throughput measurements.

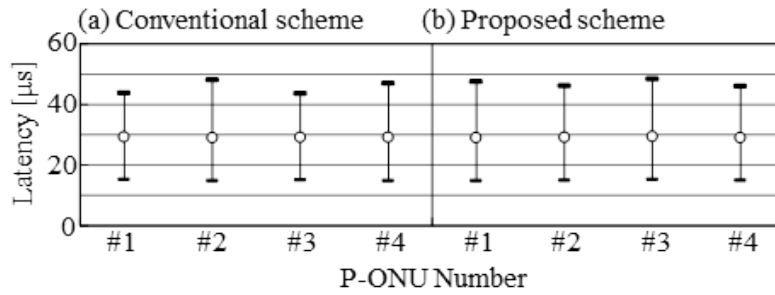


Fig. 3.14 Latency measurements for P-ONUs.

the average throughput is about 65.5 Mbps. Figure 3.13 (b) plots the measured average throughput at intervals of 10 ms when using the proposed scheme. Moreover, Fig. 3.13 (c) shows an extended graph of Fig. 3.13 (b) between 0 to 20 ms that includes the traffic monitor period. The average throughput is calculated at intervals of  $125 \mu\text{s}$ . The average throughput in the monitoring period is same as that in Fig. 3.13 (a). In Fig. 3.13 (b), the average throughput of the S-ONUs exhibits a ninefold increase after traffic monitoring. Figure 3.13 (d) is an extended graph of Fig. 3.13 (b) between 150 and 170 ms. This indicates the period after traffic monitoring. The y-axis indicates the average throughput at intervals of  $125 \mu\text{s}$ . Note that the S-ONU throughput is higher than the input throughput from the UNI port. This is because the data is buffered in the S-ONU when the P-ONUs are forwarded. The expanded throughput of the S-ONUs equals the theoretical value according to Eq. 3.11 and Fig. 3.11. The monitoring and calculation completion time is about 140 ms. The throughput of the secondary system is limited for only about 140 ms. After traffic monitoring, the secondary system continues to forward the data signal with the expanded throughput in operation. Figure 3.14 shows the latency measurements obtained with each P-ONU. Figure 3.14 (a) and (b) show the results obtained with the conventional FBA and the proposed scheme, respectively. The error bar indicates the maximum–minimum value. The latency is very low at less than  $60 \mu\text{s}$ .

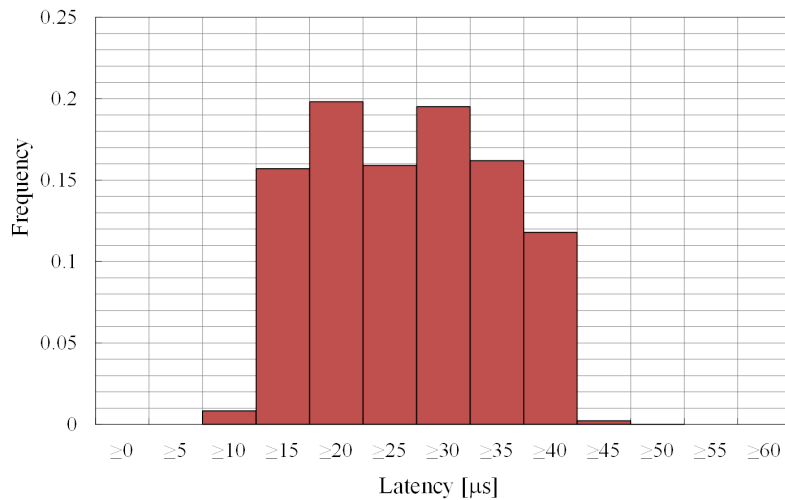


Fig. 3.15 Latency histogram for P-ONUs.

### 3.6.4 Latency Distribution for TDD-based MFH

We measured the latency histogram to confirm the long-term stability for the proposed system. The experimental setup and parameters are identical with those in Section 3.6.2. In Section 3.6.3, the measurement time was 450 ms. In this case, the operation time was 1.0 hour. For the convenience of the LAN analyzer, the aggregated total latency in the output port from the 10G-EPON to the LAN analyzer is measured.

Therefore, the signals from the S-ONUs are halted for the entire time. Figure 3.15 shows the result of the latency histogram measurement. The minimum latency was around 10.0  $\mu\text{s}$  because the processing delay occurred in the OLT. Latency jitter appeared due to the time lag between the time at which the data transmission to the OLT started and the time at which it arrived at the buffer in the ONU. The data signal can be forwarded to the OLT with the lowest latency when the ONU is granted the data transmission immediately after the data signal arrives at the buffer in the ONU. A higher latency appears when the data signal arrives at the buffer in the ONU soon after the data transmission to the OLT. The latency is accumulated when the data signal is forwarded with multiple allocation cycles.

Latency jitter certainly occurs. If the proposed TDM-PON accommodates a system where latency jitter is not allowed such as a Common Public Radio Interface (CPRI), a jitter absorption function should be implemented. Such a function has been already proposed [45].

### 3.6.5 Number of Accommodated P-ONUs

We calculate the dependence of the throughput variation on the number of accommodated ONUs to discuss the maximum number of ONUs. Figure 3.16 shows the calculation result. The parameters are given in Table 3.3. The throughput per P-ONU greatly varies

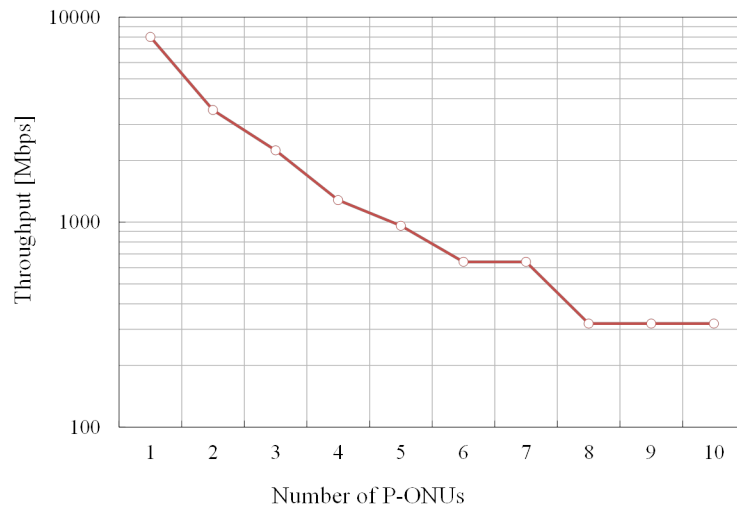


Fig. 3.16 Throughput per P-ONU depending on number of accommodated P-ONUs.

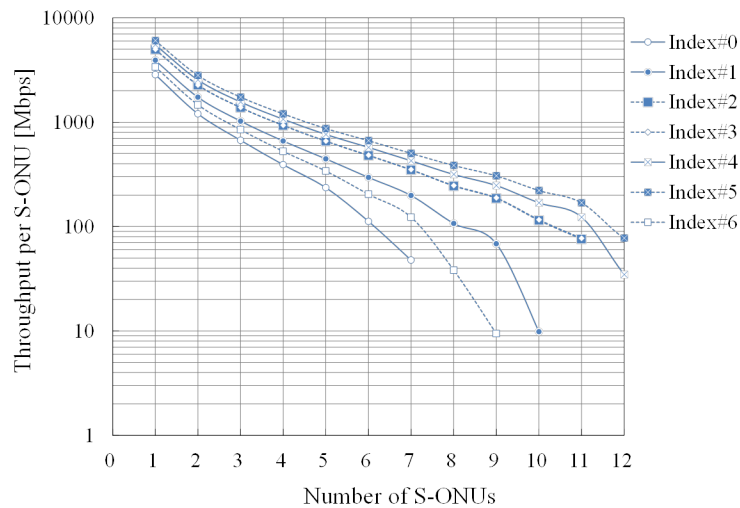


Fig. 3.17 Throughput per S-ONU depending on number of accommodated S-ONUs and type of TDD index.

depending on number of accommodated P-ONUs. Therefore, the maximum number of accommodated P-ONUs is greatly limited. For instance, 4 ONUs are accommodated when the wireless upstream data rate is 1.0 Gbps. Moreover, a technique for reducing the overhead has been proposed [76]. We can expect to increase the number of accommodated P-ONUs by employing such a technique. However, the number of the ONUs is still limited when only P-ONUs are accommodated.

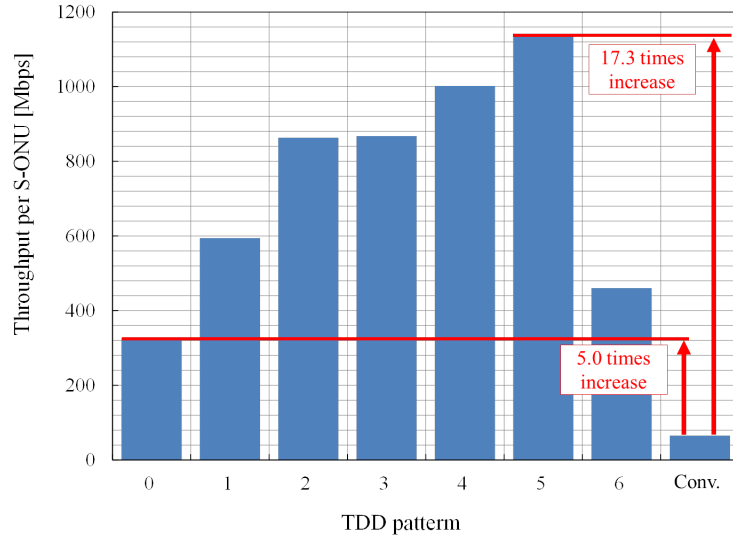


Fig. 3.18 Comparison of throughput of each TDD index and conventional method.

### 3.6.6 Number of Accommodated S-ONUs and Throughput with Various TDD Patterns

We also show the dependence of the throughput variation on the TDD pattern. The throughput variation per S-ONU with FBA as the number of accommodated S-ONUs increases is shown in Fig. 3.17. The parameters are shown in Table 3.3. The number of P-ONUs is assumed to be 4 and  $b_P = 1.0$  Gbps. The throughput is calculated for every type of TDD pattern. The throughput depends on the ratio of the TDD pattern. For example, the throughput becomes the worst in the case of the highest TDD pattern ratio of 4:1 (upstream: downstream), which means Index 0.

The number of S-ONUs that can be accommodated is determined by the throughput requirement. For example, the number is 2 when the throughput requirement is 1.0 Gbps, and the number is 6 when the throughput requirement is 100 Mbps. In this case, we employed the proposed bandwidth allocation scheme based on FBA. Thus, these values can be called the guaranteed bandwidth in other words. If the conventional DBA technique is employed to the S-ONUs, then the number of accommodatable S-ONUs will increase thanks to the statistical multiplexing effect.

Figure 3.18 shows a bar graph that directly compares the expanded throughput with the conventional throughput with 4 S-ONUs. The throughput is expanded up to 17.3 times and by a minimum of 5.0 times. These results were obtained when the proposed technique was integrated with a 10G-EPON. The throughput can be improved by employing Next Generation-PON2 (NG-PON2) [20], which reduces the overhead, for example the laser on/off time.

### 3.7 Conclusion

We proposed a TDM-PON system that accommodates a TDD-based MFH and secondary services. The proposed technique was evaluated with the numerical simulations and the experiments. We showed that our proposed technique makes it possible to superimpose the signal of the secondary services on the unallocated interval of the TDD-based MFH.

We reported the feasibility of the proposed bandwidth allocation method and the discovery process by the numerical simulation. After that, we demonstrated the operation of the proposed technique with a 10G-EPON prototype by experiments. The signal of TDD-based MFH is forwarded with an average low latency of  $30 \mu\text{s}$  and the throughput of the secondary services is expanded ninefold with TDD index 1. We discussed the number of accommodatable ONUs using a numerical calculation. For ONUs connected to DUs, the maximum number is 4 P-ONUs when a 1000 Mbps throughput is needed. For ONUs connected to secondary systems, the maximum number is 6 S-ONUs when a 100 Mbps throughput is guaranteed. In fact, the total number of 10 ONUs can be accommodated if the above conditions are satisfied. Furthermore, T(W)DM-PON has a higher potential. We expect that the total number of ONUs can be increased by employing a mobile DBA [48] or a DBA with statistical traffic analysis [54] for P-ONUs, and a conventional DBA [63] for S-ONUs with the statistical multiplexing effect.



## Chapter 4

# Auto-Recovery from Estimation Error for TDD-based Fronthaul

### 4.1 Introduction

In the previous chapter, we proposed a technique that accommodates time division duplex (TDD)-based mobile fronthaul (MFH) and secondary services in the same time division multiplexing passive optical network (TDM-PON). The signals of secondary services are forwarded in the unallocated interval of the MFH link. The use of our proposed technique achieves higher bandwidth usage efficiency (BUE) in the PON link.

In the previous chapter, we studied searching method and a bandwidth allocation scheme. The searching method explores the unallocated interval and a head of the transmission time interval (TTI). The use of the proposed techniques improves the throughputs of the secondary services without additional latency for the mobile system, and the number of accommodated optical network units (ONUs) can be increased.

However, with the proposed method, we did not consider the possibility that the searching method is erroneous. When the searching method fails, the MFH signal is affected by additional latency with our previously proposed technique.

In this chapter, we propose a new searching method based on the coefficient of the correlation between captured uplink MFH signals and the seven types of preset patterns defined by the third generation partnership project (3GPP) [72]. In the following, we will call the 3GPP-defined preset patterns as TDD patterns. We propose a novel automatic recovery scheme from estimation error. The recovery scheme is effective when TDD pattern estimation fails. Here, we define these errors as the TDD pattern estimation error. When the optical line terminal (OLT) detects the TDD pattern estimation error, the OLT resets the bandwidth allocation to its initial state. After resetting the bandwidth allocation, the OLT starts to re-estimate the TDD pattern.

### 4.2 Challenging Issues

As regards the techniques for accommodating the MFH and secondary services, there may be an unexpected delay to the MFH signal when the TDD pattern estimation fails as shown in Fig. 4.1. Then the P-ONU cannot forward the MFH uplink signal to the OLT

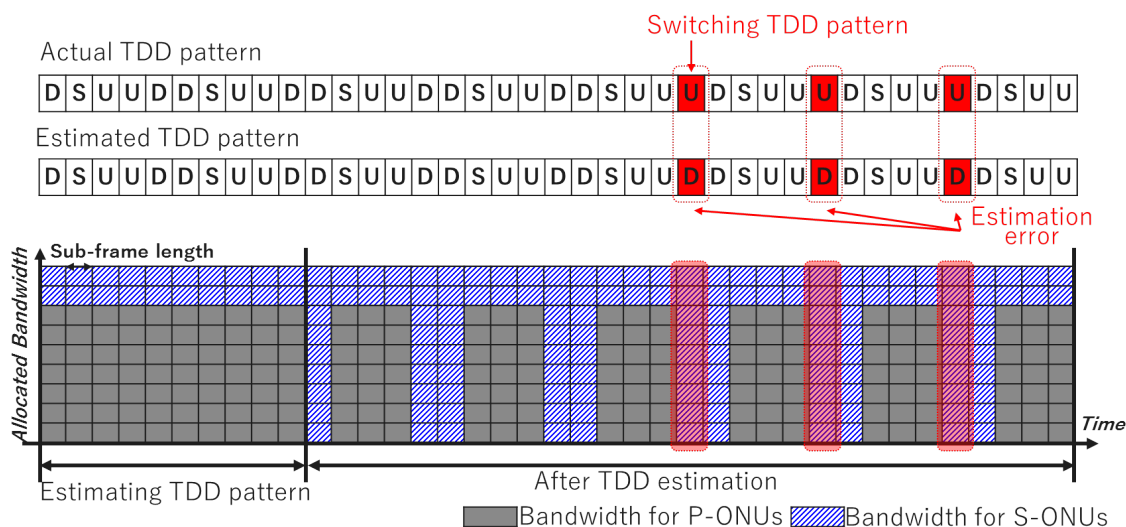


Fig. 4.1 Bandwidth allocation procedure.

within the acceptable latency. This is because the OLT halts the bandwidth allocation to the primary-ONU (P-ONU) when it recognizes the interval as an unallocated interval.

In this case, the huge latency for the mobile system becomes permanent since the OLT cannot reset the bandwidth allocation.

Therefore, we propose a TDD pattern estimation error recovery scheme. Moreover, the TDD pattern estimation in our previous work assumes that the test signal is forwarded from the distributed unit (DU) to the central unit (CU) when the DU is installed. The OLT captures the test signal and estimates the TDD pattern simply. However, the test signal is not always forwarded when the OLT resets the bandwidth allocation. Thus, the OLT needs to estimate the TDD pattern from the actual mobile traffic between the CU and the DUs in operation. These techniques are described in the next section.

### 4.3 Principle of Proposed TDM-PON System

This section describes two techniques for dealing with a TDD pattern estimation error. The first one is a TDD pattern estimation technique, which uses the captured uplink MFH signal. The second one is a bandwidth allocation scheme which the OLT can detect the TDD pattern estimation error to automatically switch the bandwidth allocation to the FBA scheme.

#### 4.3.1 TDD Pattern Estimation

The previous proposed scheme described in Chapter 3 was not assumed that the TDD pattern is switched. The novel scheme that the mobile operator sends the test signal is needed when the OLT re-estimates the TDD pattern using the previous proposed estimation scheme. It is difficult for all the mobile operator to correspond to such a scheme. Thus, an estimation method of the TDD pattern without the test signal is needed. In

**Algorithm 2** Overall operation flow in OLT

---

```

 $T_{resol} \leftarrow T_{ba}$ 
 $N_{ds} \leftarrow T_{wf}/T_{resol}$ 
UplinkMfhTrafficMonitor( $T_{mon}, T_{resol}$ )
 $DS1[N_{ds}] \leftarrow \text{MakeWirelessFrame}()$ 
SearchBeginningSubFrame() [77]
 $DS2[N_{ds}] \leftarrow \text{Threshold}(DS1[N_{ds}])$ 
 $DS3[N_{sub}] \leftarrow \text{PatternMatch}(DS2[N_{ds}])$ 
CalculateCoefficientCorrelation( $DS3[N_{sub}]$ )

```

---

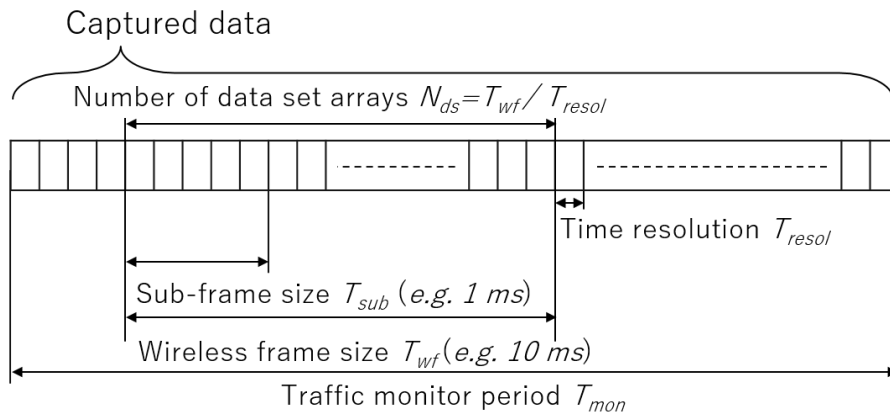


Fig. 4.2 Relationship between each time variables and data array.

this section, we describe TDD pattern estimation without a test signal.

The overall flow of the proposed scheme is given by Algorithm 2. The final goal of the algorithm is to calculate the correlation factor between the captured MFH signal and the TDD pattern shown in Table 3.1. The TDD pattern, which has the largest correlation factor among seven types, is selected as the estimation result. The variables are shown in Table 4.1. Most of the algorithm contributes preparing data sets  $DS1[N_{ds}]$ ,  $DS2[N_{ds}]$ ,  $DS3[N_{sub}]$ . The correlation of the TDD pattern is not calculated directly with the captured MFH signal but it is calculated with the prepared data set  $DS3[N_{sub}]$  to improve estimate accuracy. We take this rule into account when making the data set. Ultimately, the only data set requires  $DS3[N_{sub}]$ . In the following, to assist the reader to understand, as the first step,  $DS1[N_{ds}]$  and  $DS2[N_{ds}]$  are created in order. Then,  $DS3[N_{sub}]$  is created from  $DS2[N_{ds}]$ .

The relationship between each time variable and the elements of the data set is shown in Fig. 4.2. For initialization, the monitoring resolution  $T_{resol}$  is set the same as the bandwidth allocation cycle  $T_{ba}$ . The number of elements  $N_{ds}$  is  $T_{wf}/T_{resol}$ . Note that  $T_{wf}$  must be divisible by  $T_{resol}$ .  $T_{wf}$  means the time length of the wireless frame.

**Uplink Traffic Monitoring and Frame Fragmentation**

The OLT captures the uplink frames forwarded from the ONUs during the monitoring time  $T_{mon}$ . The captured uplink frames are stored in a captured data array  $CapArray[N_{mon}]$ .

Table 4.1 Variables for TDD pattern estimation

Variable	Definition
$T_{resol}$	Traffic monitor resolution
$T_{mon}$	Traffic monitor period
$T_{wf}$	Wireless frame size
$T_{sub}$	Sub-frame size
$N_{mon}$	Number of captured data
$N_{ds}$	Number of data sets
$N_{sub}$	Number of sub-frames in a wireless frame
$CapArray[N_{mon}]$	Captured data array
$DS1[N_{ds}]$	Data array after fragmentation
$DS2[N_{ds}]$	Data array after threshold process
$DS3[N_{sub}]$	Data array with pattern match
$E_{bs}$	Element of beginning of sub-frame
$Th_{upper}, Th_{lower}$	Threshold for preparing DS2
$C_{up}$	Constant value as uplink sub-frame
$C_s$	Constant value as special sub-frame
$C_{down}$	Constant value as downlink sub-frame

**Algorithm 3** MakeWirelessFrame()

---

```

i ← 0
while i <  $N_{ds}$  do
  j ← 0
  while  $j \times N_{ds} \leq N_{mon}$  do
     $DS1[i] \leftarrow CapArray[i + j \times N_{ds}]$ 
    j ← j + 1
  end while
  i ← i + 1
end while

```

---

The number of elements  $N_{mon}$  of the  $CapArray[N_{mon}]$  is  $T_{mon}/T_{resol} (> N_{ds})$ . The monitored array is fragmented by the number of data sets  $N_{ds}$ . The OLT adds the entire fragmented array to a  $DS1[N_{ds}]$ . Algorithm 3 shows this flow.

**Search of Beginning of Sub-frame**

As shown in Section 3.2, the uplink and downlink are switched every sub-frame. The OLT needs to distinguish the uplink or downlink every sub-frame. At this time, since the OLT does not receive information about the sub-frame receiving time from the CU, the OLT needs to calculate the start and end times of each sub-frame. Thus the OLT extracts

**Algorithm 4** Threshold( $DS1[N_{ds}], DS2[N_{ds}]$ )

---

```

 $N \leftarrow 0$ 
 $DS2 \leftarrow \{C_{down}\}$ 
while  $N \neq N_{ds}$  do
  if  $DS1[N] \geq Th_{upper}$  then
     $DS2[N] \leftarrow C_{up}$ 
  else if  $DS1[N] \geq Th_{lower}$  then
     $DS2[N] \leftarrow C_s$ 
  end if
   $N \leftarrow N + 1$ 
end while

```

---

the beginning element  $E_{bs}$  of the sub-frame from  $DS1[N_{ds}]$ . We use the start position searching technique from Chapter 3 and [77]. The OLT searches for the element that switches from the longest zero interval in the array to non-zero. This element is defined as  $E_{bs}$ . The reason for searching for the beginning of the sub-frame is because it is assumed that the MFH signal is generated as a burst signal from the beginning of the sub-frame.

Here, we assume that a mobile base station (MBS) model is a new functional split model, which is e.g. a MAC-PHY split [42],[39]. In particular, in the option of splitting between MAC and PHY and the option of splitting the function in intra PHY called lower layer split (LLS), the MFH traffic occurs in burst form. At this time, our proposed method is effective.

#### Preparation of Data Set with Threshold Processing

To suppress the error of the TDD pattern estimation, we prepared the  $DS2[N_{ds}]$  as shown in Algorithm 4. First, the OLT performs threshold processing on all the elements of the  $DS1[N_{ds}]$ . Two thresholds  $Th_{upper}$  and  $Th_{lower}$  are used. When the target array  $DS1[N] > Th_{upper}$ , the target array  $DS2[N]$  sets  $C_{up}$ .  $C_{up}$  indicates the possibility of the uplink sub-frame is high. When  $Th_{lower} \leq DS1[N] \leq Th_{upper}$ , the  $DS2[N]$  sets  $C_s$ .  $C_s$  indicates that it is more probable for this sub-frame to be uplink signal. When  $DS1[N] < Th_{lower}$ , the  $DS2[N]$  sets  $C_{down}$ .

#### Preparation of Data Set Depending on TDD Pattern

Next, we prepare  $DS3[N_{sub}]$  based on the TDD pattern by using  $DS2[N_{ds}]$ .  $N_{sub}$  is the number of sub-frames in a wireless frame. For instance, when  $T_{wf}$  is 10 ms and  $T_{sub}$  is 1 ms, then  $N_{sub}$  is 10.

Algorithm 5 shows the flow of the  $DS3[N_{sub}]$  preparation and performs with respect to each sub-frame. The initial value of all the elements of  $DS3$  is  $C_{down}$ . The value of the element in  $DS3$  is determined in accordance with some conditional branching with  $DS2$ . Algorithm 5 is performed with the loop processing in sub-frame length increments. When the target array  $DS2[j]$  is  $C_{up}$ , the OLT refers to the previous element  $DS2[j - 1]$ , the element after one sub-frame  $DS2[j + N_{ds}/N_{sub}]$ , and the next element  $DS2[j + 1]$ . Note that for the sake of simplicity, the modular operation is omitted in sentence. The reason for referring to the previous element  $DS2[j - 1]$  is to prevent erroneous recognition of the previous sub-frame data as the target sub-frame data. The reason for the incorrect

**Algorithm 5** PatternMatch( $DS2[N_{ds}], DS3[N_{sub}]$ )

---

```

 $N \leftarrow \text{Elementofbeginningofsubframe}$ 
 $i \leftarrow 0$ 
 $DS3 \leftarrow \{C_{down}\}$ 
while  $i \neq N_{ds}$  do
   $j \leftarrow i + N \bmod N_{ds}$ 
  if  $DS2[j] = C_{up}$  then
    if  $DS2[(N_{ds} + j - 1) \bmod N_{ds}] < C_{up}$  or
     $DS2[(N_{ds}/N_{sub} + j) \bmod N_{ds}] = C_{up}$  or
     $DS2[(j + 1) \bmod N_{ds}] = C_s$  then
       $DS3[j \bmod (N_{ds}/N_{sub})] \leftarrow C_{up}$ 
    end if
  else
    if  $DS2[j] = C_s$  then
      if  $DS2[(N_{ds} + j - N_{ds}/N_{sub}) \bmod N_{ds}] \geq C_s$  and  $DS2[(j + N_{ds}/N_{sub}) \bmod N_{ds}] \geq C_s$  then
         $DS3[j \bmod (N_{ds}/N_{sub})] \leftarrow C_{up}$ 
      else
        if  $DS2[(N_{ds} + j - 1) \bmod N_{ds}] = C_{down}$  then
           $DS3[j \bmod (N_{ds}/N_{sub})] \leftarrow C_s$ 
        end if
      end if
    end if
  end if
   $i \leftarrow i + N_{ds}/N_{sub}$ 
end while

```

---

recognition is that the OLT and the CU are asynchronous. Since the start timing of the bandwidth allocation cycle  $T_{ba}$  of the OLT and that for the sub-frame cycle do not coincide, there is a possibility that the last data of the previous sub-frame and the head data of the target sub-frame are overlapped in one array. Since the MFH link has a characteristic whereby the MFH signals are stored in the leading array of the sub-frame [78], the OLT refers to the previous element  $DS2[j - 1]$ . Next, as a reason for referring to the element after one sub-frame  $DS2[j + N_{ds}/N_{sub}]$  and the next element  $DS2[j + 1]$ , as shown in Table 3.1, when there is a high possibility that the next sub-frame is in the uplink state, there is a high possibility that the target sub-frame is also in the uplink state. When the next element  $DS2[j + 1]$  is  $C_{up}$ , since the MFH signals are stored in from the beginning of the sub-frame in order, there is a high possibility that it is an uplink.

The above reference, the target element  $DS3[j \bmod (N_{ds}/N_{sub})]$  is distinguished  $C_{up}$  or not according to the above reference. The purpose of this process is to avoid recognizing the data of the previous sub-frame as the data of the target sub-frame. This is because the start times of the TTI and bandwidth allocation cycles are not the same.

When the target array  $DS2[j]$  is  $C_s$ , the OLT refers to the previous and next sub-frames. The values of both sub-frames are more than  $C_d$ , and the target array is set at

$C_{up}$ . This is because the target sub-frame is definitely the uplink sub-frame when both the previous and next sub-frames are either the uplink sub-frame or the special sub-frame.

Then, if the target element does not meet the above condition, the OLT refers to the previous element.

When the value of the previous array  $DS2[j-1]$  is  $C_{down}$ , the target array  $DS3[j]$  is  $C_s$ . When the target sub-frame is  $C_{down}$ , it is set at  $C_{down}$  without processing.

#### Calculation of Coefficient of Correlation

After preparing  $DS3$ , the OLT calculates the coefficient of correlation for  $DS3$  and the seven types of TDD patterns. We used the sample correlation coefficient  $r_i$ ,

$$r_i = \frac{\sum_{n=1}^{N_{sub}} (DS3[n] - \overline{DS3})(Tdd^i[n] - \overline{Tdd^i})}{\sqrt{\sum_{n=1}^{N_{sub}} (DS3[n] - \overline{DS3})^2 \sum_{n=1}^{N_{sub}} (Tdd^i[n] - \overline{Tdd^i})^2}}. \quad (4.1)$$

From the calculation result, the TDD pattern with the largest correlation coefficient value is set as the TDD pattern estimation result.

### 4.3.2 Automatic Recovery from TDD Pattern Estimation Error

Section 3.4.2 described the normal operation flow. Here, we propose a bandwidth allocation recovery scheme when the TDD pattern is switched.

Figure 4.3 shows a time chart for the proposed scheme. The OLT automatically executes a sequence of actions from detecting the estimation error to restarting the bandwidth allocation with the switched TDD pattern. In the unallocated interval, the OLT allocates the bandwidth  $b_D^{(i)}$  to detect the estimation error for the P-ONU. The OLT can detect the estimation error when the P-ONU forwards the frame to the OLT using the bandwidth  $b_D^{(i)}$ . This is because frame forwarding using the bandwidth  $b_D^{(i)}$  does not occur during normal operation. The total bandwidth  $B_S$  allocated to all the secondary ONUs (S-ONUs) is then derived as follows,

$$B_S = B_{all} - \sum_{i=1}^{N_P} b_D^{(i)} \quad (4.2)$$

The usable bandwidth for the S-ONUs is slightly decreased. The bandwidth  $b_D^{(i)}$  can be the small amount as long as one Ethernet frame can be forwarded. This is because the bandwidth  $b_D^{(i)}$  is used for estimation-error detection. In normal operation, the bandwidth allocation procedure is the same as that without the proposed scheme. When the TDD pattern is switched, the OLT detects the estimation error from the uplink signal with the bandwidth  $b_D^{(i)}$ . Then the OLT resets the bandwidth allocation to its initial state and re-estimates the TDD pattern with the traffic monitor. After the estimation, the OLT restarts the bandwidth allocation.

## 4.4 Numerical Simulation for TDD Pattern Estimation

As mentioned in section 4.2, the test signal is not always sent from DU when the OLT needs to estimate the TDD pattern. Section 4.3.1 describes the low-complexity TDD pattern

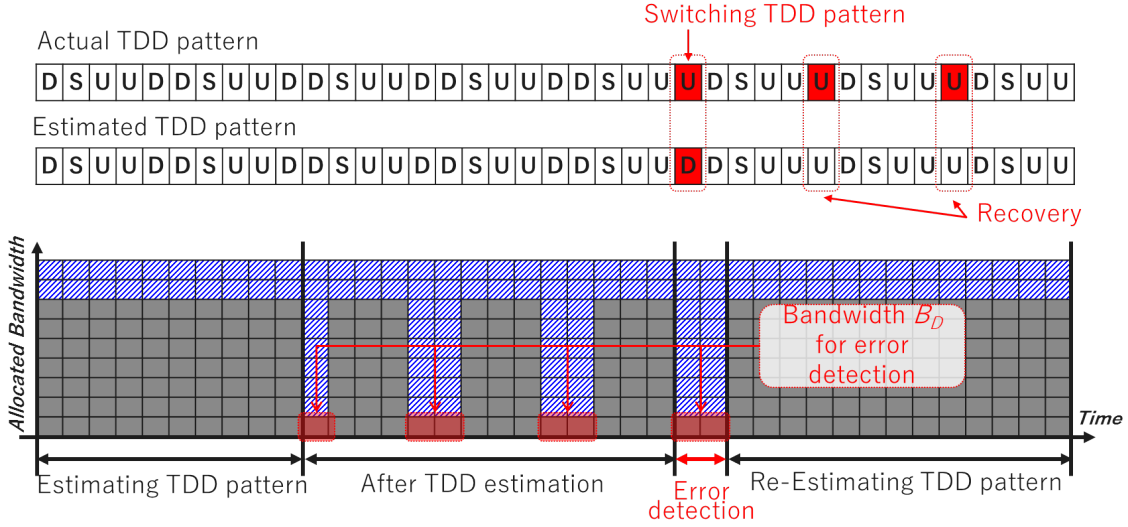


Fig. 4.3 Proposed error detection procedure.

estimation technique. It is necessary to confirm the traffic acquisition time duration range to ensure sufficient estimation accuracy when employing the algorithm proposed in section 4.3.1. This section clarifies how long a period is needed to estimate the TDD pattern by using a numerical simulation. The traffic close to the real mobile traffic fluctuates depending on the number of UE and the amount of the data on the basis of the exponential distribution.

A numerical simulation is used since it is difficult to undertake an experiment with fluctuating mobile traffic because the local area network (LAN) analyzer must be time-synchronized with the OLT and generate the fluctuating mobile traffic. Therefore, this paper divides the roles of simulation and experiment for the TDD pattern estimation as follows. The numerical simulation clarifies the MFH traffic acquisition time necessary for the estimation. In the experiment, after obtaining the MFH traffic, we confirm the computation time to reflect on the bandwidth allocation.

#### 4.4.1 Simulation Setup

We assume that the MBS is a MAC-PHY split type [42]. The data volume through the MFH link is given as follows [52],

$$\text{Datavolume} = TBS \times N_{CA} \times N_{MIMO}. \quad (4.3)$$

where TBS is the transport block size given in bytes that is transmitted per sub-frame.  $N_{CA}$  and  $N_{MIMO}$  are the number of component carriers in the carrier aggregation (CA) and the number of antennas per DU, respectively. We expect the MFH signal to be packetized by using an Ethernet frame when the MAC-PHY split is employed. The Ethernet frame size is assumed to be 1500 bytes. As simulation parameters, the DUs randomly send uplink frames to the CU. That is, the UE sends UDP flows to each DU as intermittent data traffic. The intervals and durations of the bursts were exponentially

Table 4.2 Numerical simulation parameters

Variable	Value
Num. of UEs	5, 10
Num. of iteration	10000 times
Maximum TBS size	9422 bytes
$N_{CA}$	5
$N_{MIMO}$	2
$T_{resol}$	31.25 $\mu s$
$T_{wf}$	10 ms
$Th_{upper}$	$MaximumTBSsize/14$
$Th_{lower}$	0
$C_{up}$	40
$C_s$	30
$C_{down}$	10

distributed random variables. The average burst duration was 1.0 s and the average burst interval was 5.0 sec. The data rates of the bursts were 2.0 Mbps. In addition, the TBS is calculated with the long-term-evolution (LTE) module [73] of the network simulator-3 (ns-3) [74]. Note that we generated the frequency division duplex (FDD) traffic by using ns-3. Finally, we converted the generated FDD traffic into TDD traffic based on the TDD frame number in Table 3.1. The parameters used for the numerical simulation are shown in Table 4.2. The maximum TBS size was 9422 bytes per 1 millisecond in LTE. The number of the UEs was assumed to be 5 or 10. One sub-frame was composed of 14 symbols in the LTE. In the special sub-frame, the uplink communication was performed using one of 14 symbols. Thus 1/14 of the maximum TBS size was set as the threshold  $Th_{upper}$ . When the MFH was in the downlink state, we assumed that no uplink traffic was generated. Thus  $Th_{lower}$  was 0. If the management signal between the CU and the DU such as the loss of the MFH signal is regularly forwarded, the  $Th_{lower}$  is set bigger than the data volume of the management signal.  $C_{up}$ ,  $C_s$ , and  $C_{down}$  are arbitrary values, but they have the property of an interval scale. Although  $C_s$  cannot be perfectly determined as the uplink, since the possibility of the uplink is very high, the value is set close to the  $C_{up}$ . We calculated the estimation success probability dependence on traffic monitoring time. Here, as a standard value of estimation success probability, we assumed that it withstands actual operation when the probability exceeds 99.7%.

#### 4.4.2 Simulation Result

Figure 4.4 shows the numerical simulation results. As for 5 and 10 UEs, the cumulative distribution function (CDF) was 0.997 when we captured the uplink frame for about 12 s and about 8 s, respectively. These results show that capturing the frame for ten and

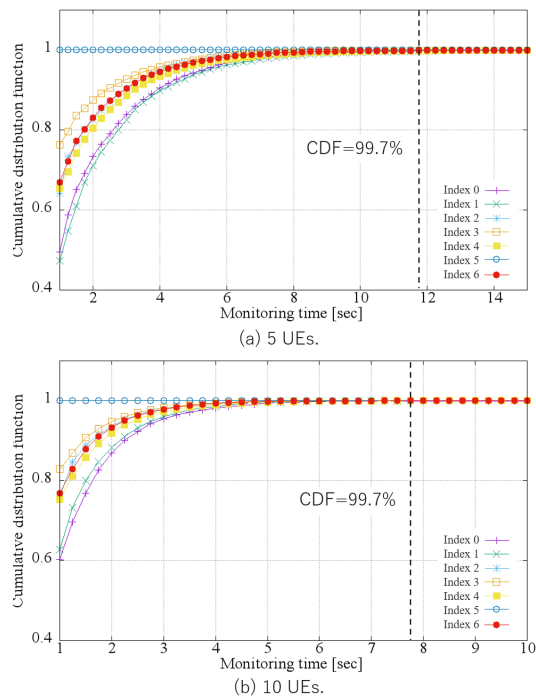


Fig. 4.4 CDF depending on monitoring time. Index numbers represent TDD patterns described in Table 3.1.

several seconds enables the OLT to estimate the correct TDD pattern with high accuracy even under actual operation conditions. For the automatic recovery scheme, the OLT switches from the bandwidth allocation to the FBA scheme when detecting the TDD pattern estimation error. After switching the bandwidth allocation scheme, the OLT captures the uplink MFH signal to re-estimate the TDD pattern. The OLT allocates bandwidth to the P-ONUs continuously while re-estimating the TDD pattern. That is, the MFH signal can be forwarded with low latency.

## 4.5 Automatic Recovery from TDD Pattern Estimation Error

Section 4.2 mentions the impact of switching the TDD pattern on the MFH signal. The technique used to detect such an error is described in section 4.3.2. In this section, we report an experimental result where the estimation error detector and bandwidth re-allocator implemented in the 10G-EPON prototype actually operate. Moreover, we implement the algorithm proposed in 4.3.1 for the 10G-EPON prototype. We confirm the real-time computation time to reflect on the bandwidth allocation.

### 4.5.1 Experimental Setup

Figure 4.5 shows a photograph of the OLT prototype and the experimental setup. The proposed estimation error detection function is implemented on a host central processing unit (CPU) in the 10G-EPON prototype. The traffic monitor and the bandwidth alloca-

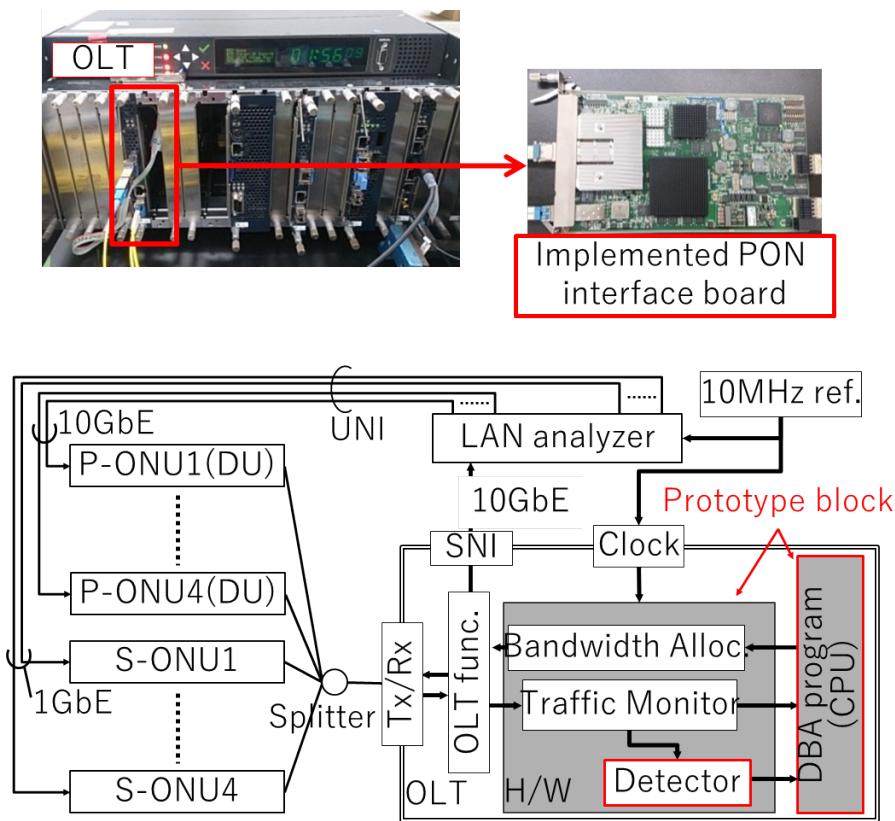


Fig. 4.5 Photograph of OLT and PON interface with FPGA board and experimental setup.

tion functions are also implemented on a field-programmable gate array (FPGA) board. The FPGA board is an Altera Arria II GX. The bandwidth allocation function emits a grant signal. The calculation of the amount of bandwidth and the TDD pattern estimator are implemented on the host CPU. The TDD pattern estimation algorithm is newly coded. The TDD pattern estimation is performed with respect to each polling cycle  $T_{poll}$ . After TDD pattern estimation, the traffic monitor continues to capture the uplink MFH signal and forwards the estimation error detection in the host CPU. The estimation error detection calls the dynamic bandwidth allocation (DBA) program in the host CPU when the TDD pattern estimation error is detected.

A local area network (LAN) analyzer has arbitrary uplink Ethernet frame generation and frame capture functions. Each port of the LAN analyzer is connected to the ONUs through a user network interface (UNI) and to the OLT through an application server-network interface (SNI). The OLT is frequency synchronized with the LAN analyzer by using a 10-MHz clock reference.

Table 4.3 shows the experimental parameters. The LAN analyzer inputs TDD simulated Ethernet frames into the P-ONUs through the UNI. The S-ONUs receive the Ethernet frames continuously from the LAN analyzer. While the OLT allocates the bandwidth to each ONU depending on the TDD pattern, the LAN analyzer switches the ratio between the uplink and downlink and captures the uplink data signal before and after instant switching. We capture the Ethernet frames using the LAN analyzer. From the captured

Table 4.3 Experimental parameters

Variable	Value
Number of P-ONUs $N_P$	4
Number of S-ONUs $N_S$	4
Bandwidth allocation cycle $T_{ba}$	125 $\mu$ s
Number of grants $N_g$	4
Bandwidth for uplink MFH transmission $b_P$	1.0 Gbps/P-ONU
Bandwidth for error detection $b_D$	250 Mbps/P-ONU
Input peak throughput for P-ONU	800 Mbps/P-ONU
Input peak throughput for S-ONU	860 Mbps/S-ONU
Frame size for P-ONU	625 bytes
Frame size for S-ONU	128 bytes
Ratio of uplink and downlink	Before 2:8 (10ms) After 4:1 (5ms)
Uplink traffic capturing period	10 ms
Estimation polling cycle $T_{poll}$	250 ms

frames, we count the number of Ethernet frames for every wireless frame length  $T_{wf}$  (10ms) or bandwidth allocation cycle  $T_{ba}$ . After counting the number of frames, we calculate the time variation of the throughput. Here, since the memory capacity of the LAN analyzer required for the frame capture is limited, only the frames from 1 P-ONU and 1 S-ONU are captured. We assume the MBS to be a MAC-PHY split model type [42],[39]. In addition, we measure the time variation of the average latency with a 1-s resolution.

## 4.5.2 Experimental Result

### Time Variation

Figure 4.6 shows the time variation of the throughput for a P-ONU and an S-ONU depending on the TDD pattern. As shown in Fig. 4.6 (a), the time resolution is 10 ms, which is the same as the length of the wireless frame  $T_{wf}$ . Figure 4.6 (b)-(d) show the results after enlarging each period with a 125- $\mu$ s resolution as same as the bandwidth allocation cycle  $T_{ba}$ . For section 'A' as shown in Fig. 4.6 (a) and (b), this section indicates the TDD pattern estimation period. The TDD pattern estimation takes about 86 ms, and the allocated bandwidth for the S-ONU is expanded as shown in section 'B'. Since the TDD pattern estimation is performed every 250-ms polling cycle, it is completed within at least a " $T_{poll}$  + calculation time". Note that the TDD pattern estimation was completed at about 86 ms in Fig. 4.6 (b) because the start time of the polling cycle was set at "-164 ms + calculation time". Since the polling works regularly, a case where the estimated time is short can occur. When the OLT needs to obtain the uplink data signal with few seconds to estimate the TDD pattern as shown in Fig. 4.4, the traffic monitor captures

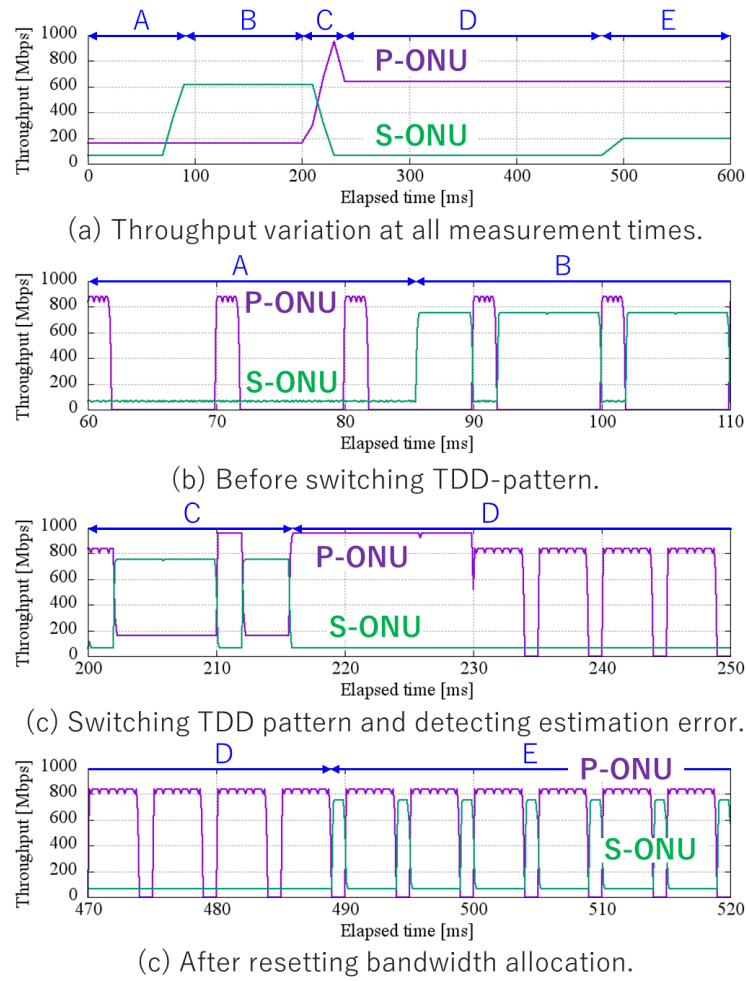


Fig. 4.6 Time variation of throughput depending on TDD pattern.

the uplink data signal in the multiple polling cycles. For instance, when the polling cycle is "250 ms" and the OLT needs a signal with a 12-second duration, the traffic monitor only needs to capture the "48-times" polling cycles.

This time, we switched the TDD pattern at 200 ms. Figure 4.6 (c) shows the result of switching the TDD pattern at 200 ms. In section 'C', estimation error occurs because the OLT recognizes the TDD pattern before switching. At about 202 ms, the P-ONU forwards the uplink Ethernet frames to the OLT by using the bandwidth  $b_D$ . At about 216 ms in section 'D', the OLT initializes the bandwidth allocation. There is a processing time of about 14 ms between detecting the estimation error and resetting the bandwidth allocation. Since one wireless frame is 10 ms, it is possible to transition to the normal state simply by discarding two wireless frames. This processing time depends on the FPGA performance. Therefore, if a higher-performance FPGA is used, there is a possibility that only one wireless frame needs to be discarded. After the bandwidth allocation reset, the OLT re-captures the uplink Ethernet frames and re-estimates the TDD pattern for section 'D' in Fig. 4.6 (d). From section 'D', the estimation time is about 270 ms because the

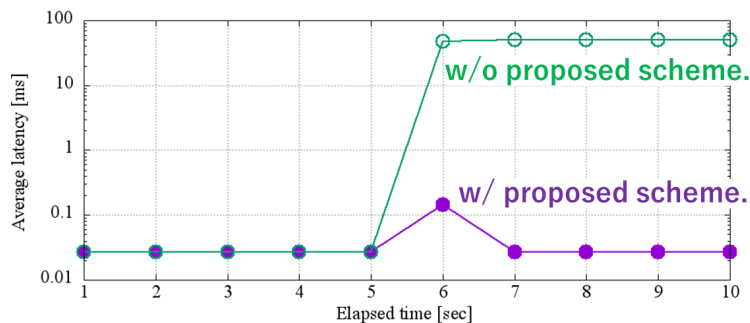


Fig. 4.7 Comparison of average latency performance.

estimation polling cycle is set at 250 ms and the calculation time is about 20 ms. Although the calculation time depends on the performance of the FPGA board, it is sufficiently shorter than the traffic monitoring time. After re-estimation, the OLT restarts allocating bandwidth to the P-ONUs and the S-ONUs depending on the TDD pattern after switching for section 'E'.

#### Comparison of Average Latency

Figure 4.7 compares the average latency performance with and without the proposed schemes. We switched the TDD pattern at 6 sec. Note that the average latency is the value every 1 second interval. While operating without the proposed scheme, the average latency continued to worsen. When employing the proposed scheme, although the P-ONU suffers from a huge latency at 6 sec, the OLT can automatically recover from estimation error and restore normal operation.

## 4.6 Conclusion

We have studied an accommodation of TDD-based MFH and secondary services in the same TDM-PON. In this chapter, we proposed two novel techniques; the first is a new estimation method based on the coefficient of correlation between the monitored uplink frame and the preset TDD pattern. The second is an estimation error recovery scheme. With the estimation method, TDD pattern estimation was possible even in the absence of a test signal transmission. We demonstrated the feasibility by numerical simulation. When the OLT captures the uplink signal within about 15 s and the number of UEs is 5, the estimation success rate reaches 0.997. For the recovery scheme, when the estimation error of the TDD pattern is incorrect, an additional bandwidth for error-detection is allocated to the P-ONU to prevent the delay influencing the MFH link. The OLT reallocates the bandwidth to the P-ONU when detecting the estimation error. We reported an experimental result regarding the feasibility of the recovery scheme that used a 10G-EPON prototype. We showed that recovery can be executed within approximately 14 ms of detecting the estimation error.

## Chapter 5

# Time Aware Shapers for Low-Latency Bridged Network

### 5.1 Introduction

This chapter studies a bandwidth allocation scheme in time sensitive bridged network accommodating mobile fronthaul (MFH) and secondary service. In IEEE802.1CM, strict priority (SP) forwarding is introduced as a quality of service (QoS). The layer-2 switch (L2SW) suppresses the queuing delay and timing jitter by employing the SP. However, there is a special case that the L2SW cannot suppress the queuing delay even if employing the SP. A burst MFH signal is packetized using Ethernet frames. In this case, the frame of the secondary signal is inserted between the frames of the burst MFH signal. That is, the length of the burst MFH signal is extended. This extension causes the additional latency for the MFH link.

Frame preemption (PE) and time aware shaper (TAS) can be employed to the L2SW in order to suppress the queuing delay and the timing jitter. In IEEE802.1CM, the PE and the TAS are considered as the options. It is necessary to exchange all the L2SWs constituting the bridge network when employing the PE. This is because each node segments or combines packets. Meanwhile, it is not necessary to exchange all the L2SWs when employing the TAS. Therefore, we focus on employing the TAS.

However, employing the TAS causes the decrease of the bandwidth usage efficiency (BUE). The TAS reserves the time slot for the primary flow and keeps the time slot until passing set time. To improve the BUE, we propose a gate shrunk TAS (GS-TAS). The GS-TAS inserts a gate shrunk frame (GS-frame) at end of the MFH burst signal. The reserved time slot is released when a L2SW with the GS-TAS receives the GS-frame. We indicate the latency reduction for the secondary signal without affecting the MFH signal. The latency reduction of the secondary signal is equivalent to the improvement of the BUE.

Figure 5.1 shows the application of the proposed GS-TAS. The TDM-PON system can be employed for the downlink transmission.

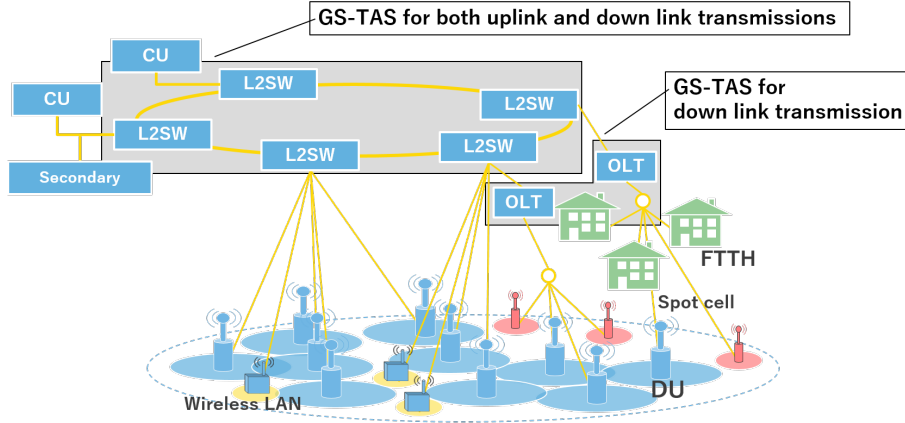


Fig. 5.1 Applicable target of the proposed GS-TAS.

## 5.2 Forwarding Method of Mobile Fronthaul Signal in Time Sensitive Network

In IEEE802.1CM, MFH signal is forwarded in the bridge network as the primary flow and queuing delay and timing jitter can be suppressed. Generally, the MFH signal is not affected by other secondary signals. Here, we denote the special case that the secondary signals give the delay to the MFH signal. When the L2SW is forwarding the secondary signal and then the MFH signal arrives at the L2SW, the MFH signal is buffered in the primary queue until the secondary signal forwarding is completed. For example, we assume the frame length of the secondary signal of 1500 bytes, link rate of 10 Gbps. The queuing time is as below,

$$\text{Queuing time} = 1500 \text{ (bytes)} \times 8 \text{ (bit/byte)} / 10 \text{ (Gbit/sec)} = 1.2 \text{ (\mu s)}.$$

In this case, queuing time is small value. That is, the MFH signal is slightly affected by forwarding the secondary signal. However, the queuing time causes the significant issue when the MFH signal is bursty.

An example of an important problem that occurs when the MFH signal is bursty is shown. We assume the parameters of the MFH signal: data amount of 94220 byte ( 2 antennas, 5 carrier aggregation, and 100 resource block (RB)), inter frame gap (IFG) of  $0.5 \mu\text{s}$ , and frame length of 1500 bytes/frame. In this assumption, the number of the MFH frames is 63. Thus, the burst duration of the MFH signal is as below,

$$\begin{aligned} \text{Burst duration} &= 1532 \text{ (bytes)} \times 63 \text{ (frames)} \times 8 \text{ (bit/byte)} / 10 \text{ (Gbit/sec)} \\ &\quad + 0.5 \text{ (\mu s)} \times (63 - 1) \\ &= 108.2 \mu\text{s}. \end{aligned}$$

When this burst MFH signal arrives at the L2SW, we assume the case where the secondary signal is congested. The frame of the secondary can be inserted between the frames of the MFH signals as shown in Fig. 5.2. As a worst case, when frames of the secondary signal

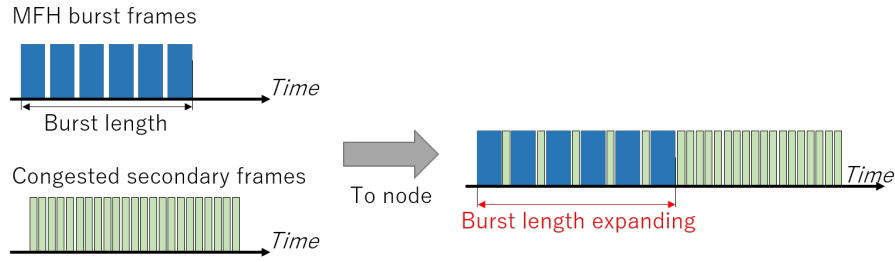


Fig. 5.2 Influence of latency on MFH signal by secondary signal.

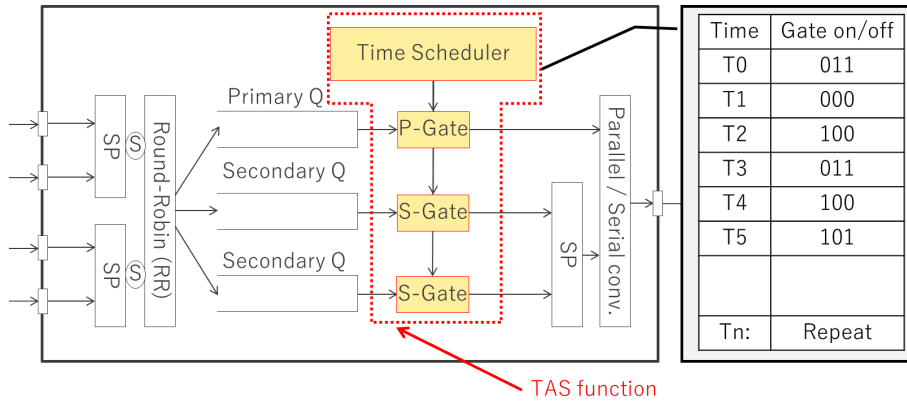


Fig. 5.3 Layer-2 switch configuration with time aware shaper, SP: Strict priority, S: Shaper, Q: Queue, P-Gate: Primary gate, S-Gate: Secondary gate.

is inserted in all the inter-frame of the MFH signal, the burst duration of the MFH signal is as below,

$$\begin{aligned}
 \text{Burst duration} &= 1532 \text{ (bytes)} \times 63 \text{ (frames)} \times 8 \text{ (bit/byte)} / 10 \text{ (Gbit/sec)} \\
 &\quad + 1.2 \text{ (\mu s)} \times (63 - 1) \\
 &= 151.6 \mu\text{s}.
 \end{aligned}$$

The 43.4- $\mu\text{s}$  latency for MFH signal occurs. Therefore, the PE or the TAS has to be employed to the L2SW when the MFH signal is bursty.

### 5.3 Time Aware Shaper

TAS function is installed in the node as shown in Fig. 5.3. TAS function includes time scheduler and gate functions. Time scheduler reads a time table and manages the open and closed states of each gate function in accordance with reserved information. Time table in the time scheduler is set by network controller which manages a flow routing design in the bridged network as shown in Fig. 5.4. First, the network controller designs the route of the MFH flow. In the layer-2 bridged network, the network operator can set the route by adding the virtual LAN tag in the frame header. After setting the MFH flow route, the network controller reserves time slots to each L2SW. The time scheduler writes the reservation time in the time table when each L2SW receive the information to reserve

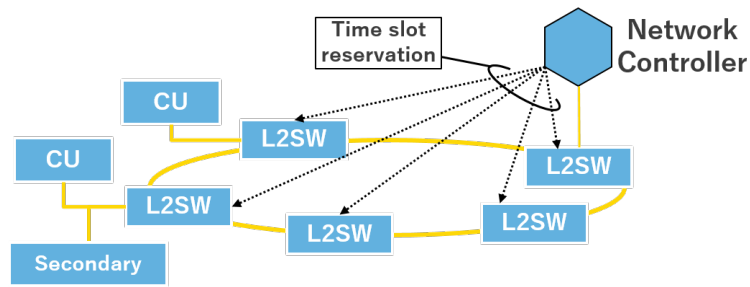


Fig. 5.4 Time sensitive network architecture with network controller, CU: Central unit, L2SW: Layer-2 switch.

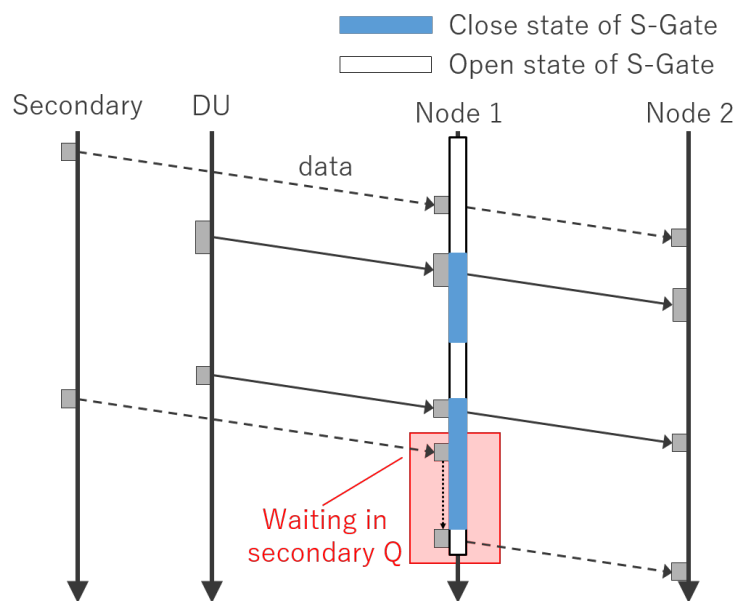


Fig. 5.5 Time chart of TAS operation.

the time slot. The gate function is in the open state and the signal can be forwarded, when the reservation time comes. For the TAS operation, the time scheduler has to manage accurate time information. Thus, each node needs to be time-synchronized.

Figure 5.5 shows the sequence of the TAS operation. When secondary gates (S-Gate) connected to the secondary queues are in the open state and a primary gate (P-Gate) connected to the priority queue is in the closed state, the secondary data frame is forwarded to the next node. If the gate state is inverted, the priority data frame can be forwarded. Note that we assume that the priority and secondary queues accommodate the MFH and secondary streams, respectively.

The forwarded time is completely orthogonal between each gate. A higher priority stream is forwarded and a lower priority stream is kept in the queue in the open state class when some gates are simultaneously in the open state. When the gate of the secondary queue is closed and a secondary data frame arrives in the queue, it is kept waiting until the gate state is switched.

## 5.4 Base Station Types

We assume that the MBS, which is accommodated in the bridged network, is a functional split model cited by section 2.4.2.

With the MBS with opt. D, the wireless signal is demodulated and decoded in the DUs with respect to each TTI cycle. The MFH stream is generated with a burst. The burst size is variable depending on the mobile traffic volume. For the opt.  $I_D$ , the demodulator is in the DU and the decoder is in the CU. The DU demodulates the wireless signal with respect to each sub-frame. Thus, as well as the MAC-PHY split model, the bursty traffic is also generated. As a result, there is unused bandwidth because the TAS reserves a fixed bandwidth.

## 5.5 Factors of Latency and Decrease in Bandwidth

This section summarizes factors related to the latency and the decrease of the bandwidth in TSN for the MFH. When one stream is input into a node  $n$ , then the delay  $d_n(t)$  is derived,

$$d_n(t) = p_n + f_l + s_l + q_{l,c}(t) + g_{l,c}(t), \quad (5.1)$$

where the time variable  $t$  is the current time. The  $n$  is a node identifier.  $p_n$  is processing delay.  $l$  indicates a link identifier.  $f_l$  is the forwarding delay between each node. In fact the optical fiber length is changed slightly by changes in temperature but in this thesis we treat it as a fixed length for simplicity.  $s_l$  is serialization delay.  $c$  is an identifier of the class of each queue.  $q_{l,c}(t)$  is the queuing delay in the node when the TAS gate is open.

$g_{l,c}(t)$  is a waiting delay caused by closing the gate.  $g_{l,c}(t)$  is derived as below,

$$g_{l,c}(t) = \begin{cases} T_{n,c,x} + w_{n,c,x} - t & (T_{n,c,x} \leq t < T_{n,c,x} + w_{n,c,x}) \\ 0 & (T_{n,c,x} + w_{n,c,x} \leq t < T_{n,c,x+1}), \end{cases} \quad (5.2)$$

where the  $x$  is a gate opening number.  $T_{n,c,x}$  is the gate open time by switching the gate state. The next gate open time is  $T_{n,c,x+1}$ .  $w_{n,c,x}$  indicates the window size in the open state. These definitions of the variables are shown in Fig. 5.6. In Fig. 5.6, only one class is described, but the time scheduler and gate perform the scheduling for all the classes. We discuss the reserved bandwidth for the MFH stream. We define the bandwidth reservation rate  $R_{n,c}^{(p)}$  as,

$$R_{n,c}^{(p)} = \sum_x \frac{w_{n,c,x}}{T_{tti}} \quad (5.3)$$

where an index  $(p)$  is an indicator of the priority stream.  $T_{tti}$  is the transmission cycle of the MFH stream. The window opens more than once within the transmission cycle  $T_{tti}$ . For this reason, the summing calculation is performed depending on the number of windows  $w_{n,c,x}$ .

In fact, the forwarded stream does not use all of the reserved windows because the data size of the MFH stream is variable. Here, we define the bandwidth occupancy as the ratio of the length of the reserved windows to that of the forwarded streams.

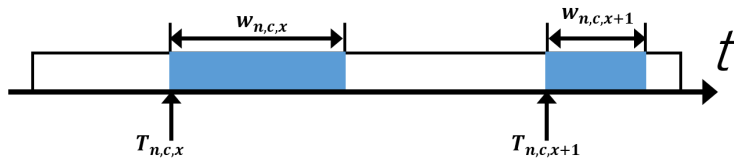
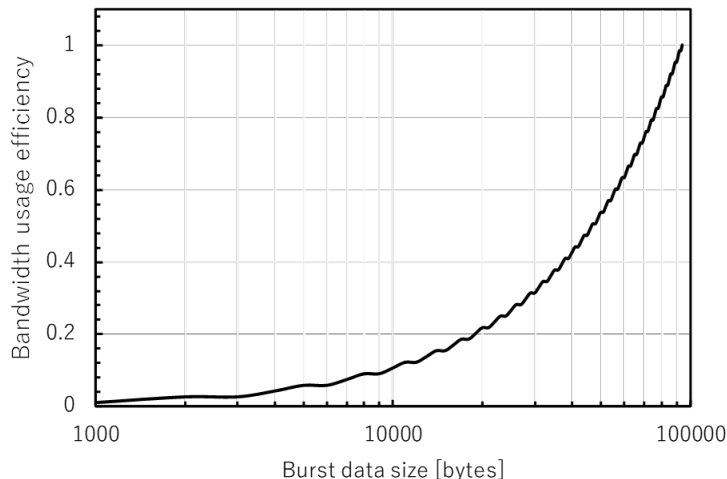
Fig. 5.6 Definition of the  $T_{(n,c,x)}$  and the  $w_{(n,c,x)}$ .

Fig. 5.7 Bandwidth usage efficiency.

Table 5.1 BUE calculation parameters.

Item	Value
Reservation window	94220 bytes
Wire rate	10 Gbps
Inter frame gap	0.5 $\mu$ s
Ethernet frame header	32 byte

Figure 5.7 shows the calculated bandwidth occupancy and Table 5.1 shows the calculation parameters. Since the data size of the MFH stream is variable, the forwarding stream is not always at the maximum data rate. There is a possibility that the reserved bandwidth is wasted.

## 5.6 Gate Shrunk Time Aware Shaper

Figure 5.8 shows the sequence of the proposed TAS operation. A GS-frame is added at the end of the MFH stream as shown in Fig. 5.9. When the proposed TAS node receives the GS-frame, the window  $w_{n,c,x}$  is shrunk. Briefly, the gate connected to the priority queue is switched to the closed state thus enabling a secondary stream to be forwarded to the next node. Since the time scheduler and the GS-frame control the gate state, all streams can

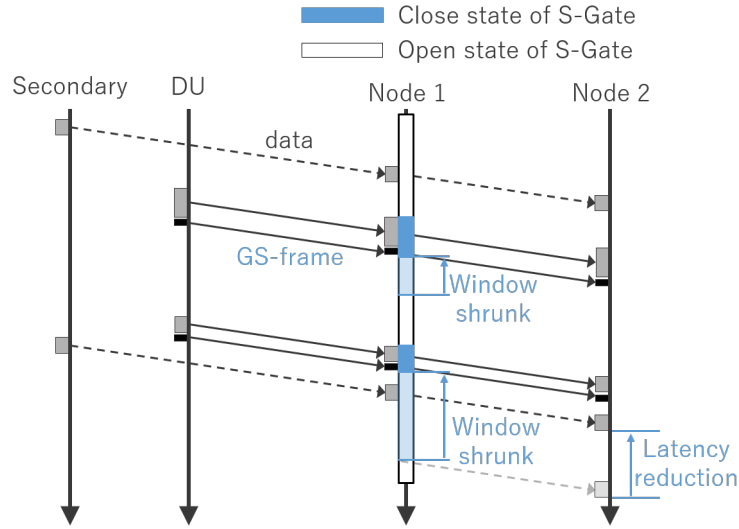


Fig. 5.8 Time chart of proposed TAS operation.

be effectively forwarded. Figure 5.10 shows a bridged node architecture with the proposed TAS. A GS-frame receiver is incorporated as an additional function. The GS-frame in the priority queue is extracted to the GS-frame receiver. Then, the GS-frame receiver transmits the information received by the GS-frame to the time scheduler. A GS-frame with a MFH stream is forwarded to the next node where it is also used.

The MFH stream with the opt.  $D$  or  $I_D$  is the bursty traffic. Therefore, the transmission end time in the window  $w_{n,c,x}$  is the end of the MFH stream and it is easy to add the GS-frame. For the CPRI, since the continuous bit stream is forwarded in the MFH, the effectiveness of our proposed technique is thin.

For the proposed TAS, the window  $w_{n,c,x}$  becomes a function with a burst size  $v$  of the MFH (priority) stream as a variable. Thus, the  $R_{n,c}^{(p)}$  in 5.3 becomes the function of the variable of the burst size as follows,

$$R(v)_{n,c}^{(p)} = \sum_x \frac{w(v)_{n,c,x}}{T_{tti}}. \quad (5.4)$$

The bandwidth reserved rate  $R(v)_{n,c}^{(np)}$  of a non-priority stream is derived in an opposite equation,

$$R(v)_{n,c}^{(np)} = 1 - R(v)_{n,c}^{(p)}, \quad (5.5)$$

where the index  $(np)$  represents the indicator of the non-priority stream.

## 5.7 Numerical Evaluation

We evaluate the latency performance and the BUE with a numerical simulation. Table 5.2 shows the parameters.

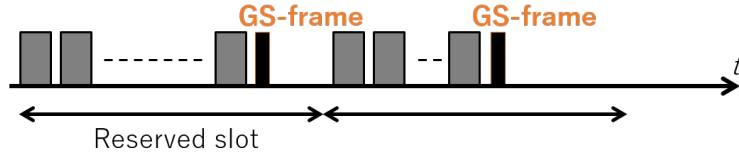


Fig. 5.9 GS-frame adding to fronthaul streams.

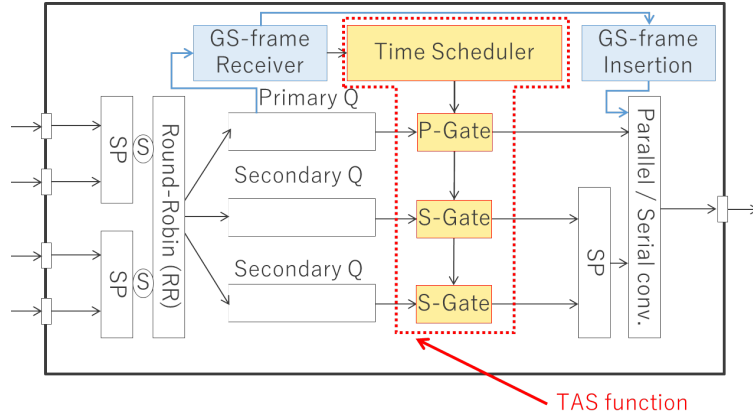


Fig. 5.10 Bridged node with proposed TAS function.

### 5.7.1 Mobile System Condition

The MBS model is assumed to be a MAC-PHY split (opt.  $D$ ). The mobile data traffic is generated by an LTE module [73] of a network simulator-3 (ns-3) [74]. The MBS model is implemented as an evolved node B (eNB) to the LTE module. The eNB controls all layer processing with one unit. Thus, the MFH stream is not defined in the LTE module. Thus, we refer the value of the fronthaul stream  $S_{FH}$  to 2.1. The MFH stream  $S_{FH}$  is divided and encapsulated in an Ethernet frame in accordance with the parameters in Table 5.1. For the distribution of the generated Ethernet-based MFH stream, the DUs randomly upload data from the UE. That is, the UE sends UDP flows to each DU as intermittent traffic. The intervals and durations of the bursts were exponentially distributed random variables. The average burst duration and interval were 1.0 and 5.0 sec, respectively. The data rates of the bursts were 2.0 Mbps. The packet lengths were 1024 bytes. The secondary stream was generated in a similar way to the MFH generation process. We assumed that the data generation interval was the same for the all DUs and secondary BSs (SBSs).

### 5.7.2 TSN Condition

The network topology is shown in Fig. 5.11. The four bridged nodes are connected in series. The 2 DUs and the 2 SBSs are accommodated in the same bridged node 0. The 2 SBSs are connected to nodes 1 and 2, respectively. The GS-frame is used the small data

Table 5.2 Simulation parameters.

Item	Value
Number of UE/DU	50 UE/DU
Carrier frequency	2 GHz
System bandwidth	20 MHz/carrier
Carrier aggregation	5 carriers
Number of MIMO layers	2 layers
Wireless transmission cycle	1 ms
Simulation time	20 s
Number of bridged nodes	4 nodes
Number of queue class	2
Forwarding delay	5 $\mu$ s/km
Wire rate	10 Gbps
Inter frame gap	12 bytes
Ethernet header	26 bytes
Maximum Ethernet payload size	1500 bytes
GS-frame size	46 bytes

size as shown in Table 5.2. This is because the TAS node counts the GS-frame when the TAS gate is open. When the number of counted GS-frames equals the number of MFH streams that arrive, the TAS gate is closed. Note that it is assumed that the number of MFH streams passing through each node is known. For the above reason, the information in the GS-frame has no meaning. The GS-frame size is allowed to have a small value. The frame scheduling scheme is strict priority (SP) and the frame forwarding scheme is a cut-through mode. The queue size is infinite. This is because we aim at a basal latency evaluation of the proposed scheme. Thus, we assume the frame loss of the propagation channel and the bridged node to be zero. For the time scheduler of TAS, a time slot of 160  $\mu$ s is reserved from the beginning of the transmission cycle. The reason for setting to 160- $\mu$ s window length is that the length of the MFH streams is about 160  $\mu$ s when the two DUs send the MFH streams with the maximum burst data size. When the DU is operating normally, the reservation time can be set at the number of DUs  $\times$  the maximum burst size of the MFH stream. When the DU operation is faulty, it is necessary to completely cover the latency requirement for safe operation. The transmission cycle is 1 ms. In the  $n$ -th connected node from the DUs, the reservation start time  $T_{rsvd,n}$  is set as below,

$$T_{rsvd,n} = T_{rsvd,n-1} + f_l. \quad (5.6)$$

It is the value obtained by adding the forwarding delay to the reservation time of the previous connected node.

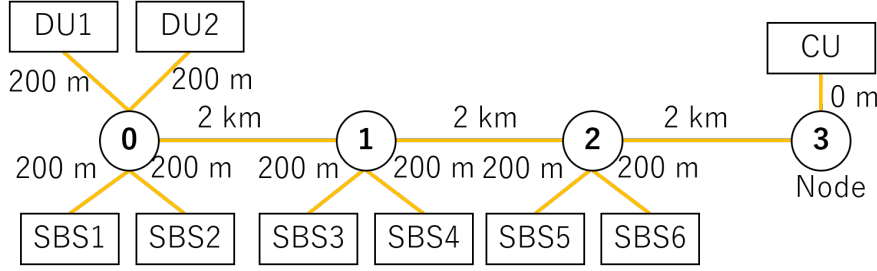


Fig. 5.11 Radio protocol stack in user-plane.

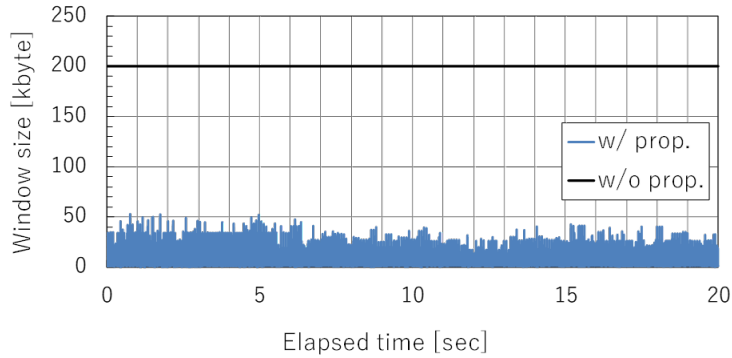


Fig. 5.12 Variable window size in node 0.

### 5.7.3 Results

#### Bandwidth Usage Efficiency of Bridge Nodes

Figure 5.12 shows the time variation of the window size  $w_{n,c,x}(v)$  of a gate connected to a priority queue at node 0. The window size can be greatly reduced. To easily understand the effectiveness of the proposed technique, we show a histogram with  $10\text{-}\mu\text{s}$  resolution in Fig. 5.13 that we obtained using the result in Fig. 5.12. The window size  $w_{n,c,x}(v)$  can be shrunk by more than 150 kbytes. The width of the shrunk window depends on the number of the MFH streams; even so, since the statistical multiplexing effect occurs, the window-shrunk effect can be obtained even if more than two MFH streams are multiplexed. The unusable bandwidth can also be greatly reduced. Note that, in accordance with our assumed numerical simulation parameters, one DU accommodates 50 UEs. The number of these UEs will be enormous in the 5G era. Even when this parameter is much larger than the expected value, a network with our proposed TAS can obtain a gate window size reduction.

#### Cumulative Distribution Function of Latency

We simulate the cumulative distribution function (CDF) of the latency performance for each DU and S-BS. The CDF is calculated with a  $1\text{-}\mu\text{s}$  resolution.

Figures 5.14 (a)–(e) show the CDF results of the latency performance. For two DUs, the CDFs in Fig. 5.14 (a) and (b) indicate that there is no latency difference with and

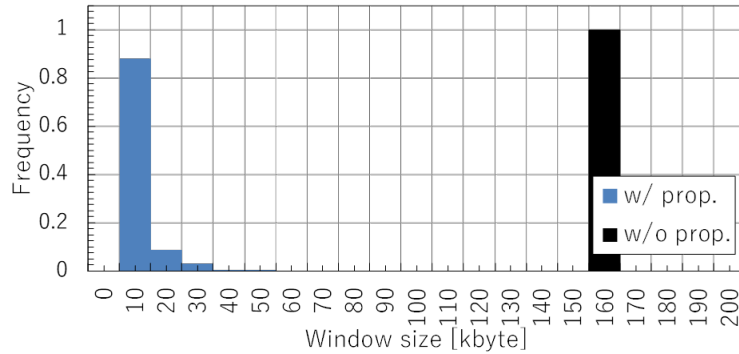


Fig. 5.13 Histogram depending on window size.

without the proposed GS-frame at  $CDF = 0.997$ . For node 0, the CDFs of the secondary streams with and without the GS-frame are shown in Fig. 5.14 (c). With  $CDF = 0.997$ , the latencies are reduced from 237 and 260  $\mu s$  to 105 and 118  $\mu s$ , respectively. The average reduction rate between the S-BSs is 55.2%.

For nodes 1 and 2, the CDFs of the secondary streams with and without the GS-frame are shown in Fig. 5.14 (d) and (f), respectively. The latency of all the streams can be improved as in the case of node 0. The latency performance is better than the other streams accommodated in node 0 in either case with or without the proposed scheme. This is because the time scheduling in accordance with 5.6 operates even though the data transmission interval is the same.

## 5.8 Conclusion

This chapter described a TAS technique, which is one of the component technologies of a TSN standard. As an issue, we reported that BUE is decreased by fixed TAS gate opening. To overcome this issue, we proposed a node architecture where a GS-frame is added at the end of the MFH signal. The gate in the node adjusts the gate opening and closing schedule. In this paper, we evaluate the latency performance of 2 MFH and 6 SBS signals with a series connected network topology by using a simulation. When  $CDF = 99.7\%$ , the latency reduction rate for the SBS signal is 55.2%. In addition, the MFH signals are not affected by adding the GS-frame. As further studies, we plan to evaluate the feasibility when network topology is more complex and the number of the accommodated DUs and SBSs are varied, and consider the scheduling of the gate open and close. Moreover, a method that does not require time synchronization is necessary due to construct the simple L2SW architecture.

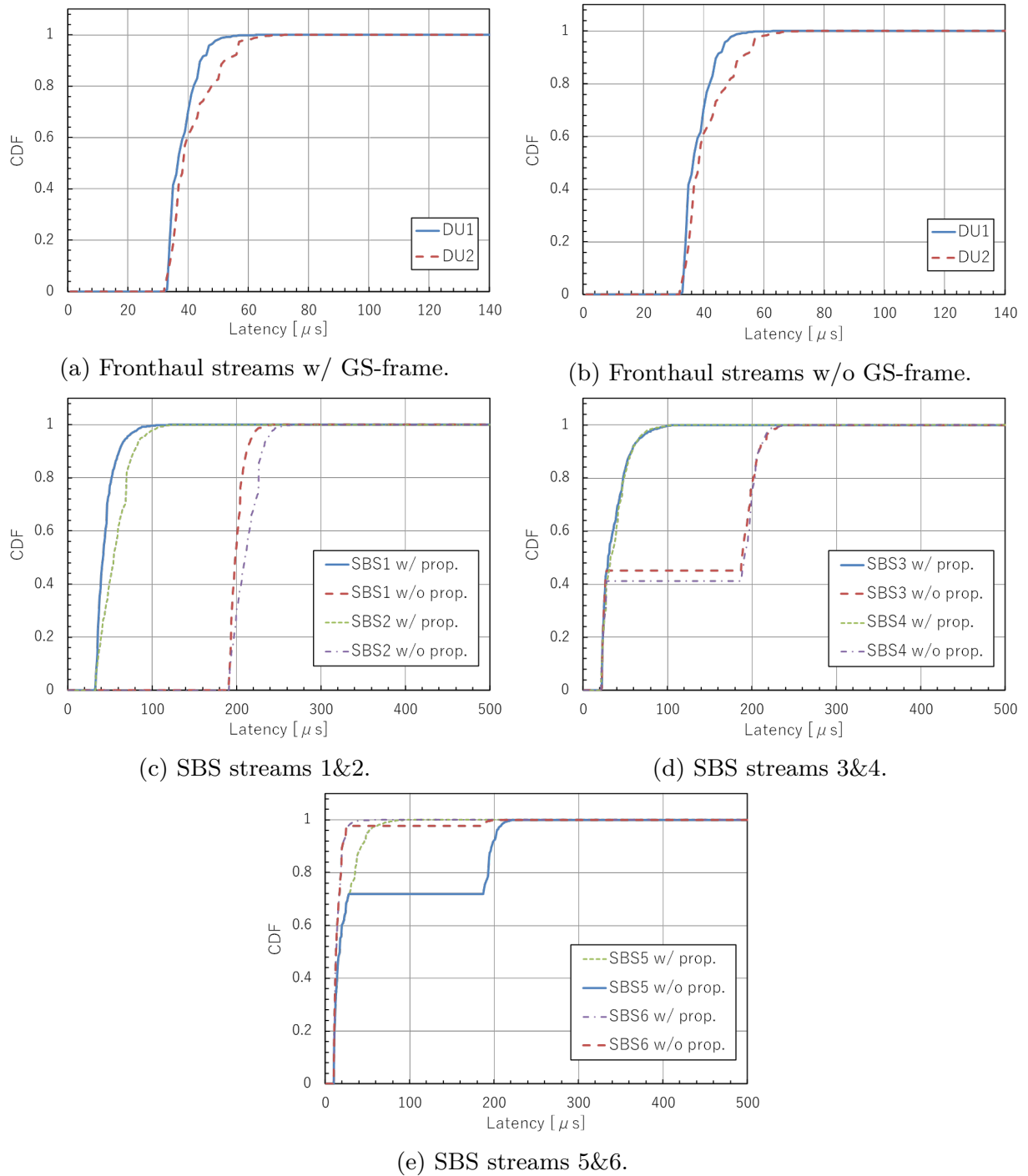


Fig. 5.14 CDF vs. latency.

## Chapter 6

# Conclusion

This thesis established bandwidth allocation schemes for accommodating mobile fronthaul (MFH) links and secondary services in a time sensitive network (TSN).

It needs to limit the number of mobile base stations (MBSs) that are accommodated in a TSN when the TSN supports only the service of forwarding MFH signals. Distributed units (DUs) deployed in antenna sites generate the burst MFH signals at the same time and forward the signals to the network node in the TSN. The network node buffers the burst MFH signal until it completes forwarding other burst MFH signal. This waiting time causes a huge latency. Therefore, we studied the TSN that accommodates the MFH link as the highest priority service and a public wireless local area network (LAN), a mobile backhaul (MBH), and a fiber-to-the-home (FTTH) as the lower priority services. By multiple service accommodations, it is expected to increase the number of user terminals in the TSN and construct more cost-effective TSN.

This thesis clarified that the TSN employing a time division multiplexing passive optical network (TDM-PON) and a layer-2 bridged network with a time aware shaper (TAS) is the best solution in terms of the cost effectiveness. In this thesis, we focused on the following technical issues:

1. Decrease in bandwidth usage efficiency (BUE) in the TSN
2. Decrease in throughput of secondary systems in the TSN

We have proposed bandwidth allocation schemes to overcome those technical issues. The details of the proposed bandwidth allocation schemes were described in Chapter 3, 4, and 5. Here, we summarize the main results obtained in this thesis.

Chapter 3 dealt with a bandwidth allocation scheme for the uplink transmission in a TDM-PON in which the MBS employed a time division duplex (TDD) scheme. The TDM-PON employs a wavelength division multiplexing (WDM) scheme to transmit the both signals of the uplink and downlink. In this case, there are periodical unallocated intervals in the optical link.

For the proposed bandwidth allocation scheme, the optical line terminal (OLT) captures the MFH signals using an uplink traffic monitor. Then the OLT estimates the head of burst MFH signals and the timing of periodical unallocated intervals of the MFH link. After performing the estimation, the OLT allocates the bandwidth to the secondary systems in the unallocated interval. It can increase the throughput of the secondary services while

forwarding the MFH signals with low latency.

We showed the feasibility of the proposed scheme with the numerical simulation, experiments, and theoretical evaluations. We experimentally confirmed the improvement of the throughput of the secondary services. The measured throughput of the secondary service was improved nine-fold with TDD index 2. The performance of the MFH link was not affected by the secondary systems. Moreover, we confirmed with the theoretical evaluations that the throughputs of the secondary services were improved up to 17.3 times with index 5 and at least 5.0 times with index 0.

Next, we confirmed with a numerical simulation that the OLT could activate the optical network units (ONUs) during the unallocated intervals of the MFH link.

Moreover, the maximum number of the ONUs was also confirmed. The OLT could accommodate up to 4 ONUs connected to the DUs when the MFH link of 1 Gbps was required. An OLT could accommodate up to 4 ONUs connected to the secondary systems with the throughput of 300 Mbps per one ONU when 4 DUs were accommodated.

Chapter 4 described a technique that is an automatic recovery scheme from an estimation error in the proposed TDM-PON described in Chapter 3. The OLT distinguishes the unallocated interval from the uplink interval of the MFH link and it allocates the bandwidth to the secondary system in the unallocated interval. However, in the proposed TDM-PON, the OLT cannot correct the estimated information for the unallocated interval when failing the estimation of the unallocated interval. This error is called a TDD pattern estimation error. We have proposed an automatic recovery scheme when the OLT detects the TDD pattern estimation error. When the TDD pattern estimation error occurs, the OLT resets the bandwidth allocation to the initial state and re-estimates unallocated interval.

We showed the feasibility of the estimation method by numerical simulation. The estimation success rate reached 99.7% when the OLT captured the uplink signal for 15 s and the number of user equipment (UE) was 5. We confirmed experimentally that the automatic recovery was executed within approximately 14 ms after detecting the TDD pattern estimation error.

Chapter 5 dealt with a bridged network employing a TAS. The TAS scheme minimizes a queueing latency and a time jitter in an MFH link. However, employing the TAS causes a decrease in the BUE and the throughput of the secondary services because the TAS scheme reserves a fixed time slot for the flow of the MFH link. We have proposed a gate shrunk TAS (GS-TAS) to achieve high BUE using the MFH characteristics.

The performance of the proposed scheme was evaluated by numerical simulation. The latency performance of 2 MFH and 6 secondary base station (SBS) signals in a series connected network topology, was evaluated. We confirmed that the latency reduction rate for the SBS signal was 55.2% when  $CDF = 99.7\%$ . In addition, the latencies of the MFH signals were not affected by adding the GS-frame.

In accordance with gained results, we summarize the following main points as effective means to overcome the technical issues:

1. For the TDM-PON, we established a bandwidth allocation scheme to forward uplink

Table 6.1 Comparison of study target and achievement of bandwidth allocation scheme in TDM-PON.

	Study goal	Achievement
Bandwidth usage efficiency	High	High (more improvement is possible)
Latency	Low	Low
Throughput of secondary system	High	High (more improvement is possible)
Hardware remodeling	Only OLT	Only OLT

signal for MFH link and secondary services. The throughput of the secondary services could be improved while maintaining the low-latency forwarding for the MFH signals. In addition, the OLT could perform an automatic recovery scheme. An advantage of the proposed architecture is no need of remodeling the mobile system. An uplink traffic monitor in the OLT is only an additional hardware to implement the scheme. So, the proposed scheme can be implemented in existing TDM-PON system quickly.

2. For the layer-2 bridged network, we proposed a basic principle of the GS-TAS. By adding the GS-frame at end of the MFH burst signal, the reserved time slot can be released according to the amount of the MFH signal. The normal TAS has not been commercially introduced yet. When the normal TAS is to be developed, it is easy to install GS-TAS as one of the initial functions of L2SW.

Further studies are described below. For the TSN employed the TDM-PON, the achievements are shown in Table 6.1. The throughput of the secondary services was drastically improved. However, the OLT allocates all the bandwidth to the ONUs connected to the DUs regardless of the actual required bandwidth when the MFH link is in an uplink state. There is still a margin for improvement in the BUE. Therefore, further improvement of BUE is an open to discussion. Assuming no remodeling of the mobile system, a statistical bandwidth allocation scheme tracking the MFH traffic is conceivable.

Meanwhile, for the TSN employed the layer-2 bridged network, the achievements are shown in Table 6.2. The BUE can be improved when the proposed GS-TAS is employed. In addition, the throughput of the secondary systems can be also increased. As further issues, the proposed GS-TAS requires the function of time synchronization. The cost to time synchronize is greatly increased since a global positioning system (GPS) or another wired line is required. For this reason, a scheme for time-synchronizing on the same line as the MFH signal and other signals is required.

In order to introduce a TSN for a radio access network (RAN), a network design considering the specificity of MFH signal will be needed from now on. In particular, conventional optical access network and TSN have not been considered to construct with the MFH link

Table 6.2 Comparison of study target and achievement in layer-2 bridged network.

	Study goal	Achievement
Bandwidth usage efficiency	High	High
Latency	Low	Low
Throughput of secondary system	High	High
Time synchronization	Unnecessary	<u>Necessary</u>
Hardware remodeling	Partial L2SWs	Partial L2SWs

that has the characteristic of simultaneous burst arrival. We expect that bandwidth allocation schemes of this thesis which makes MFH link coexist with secondary services will be a fundamental technology for realizing time sensitive network.

# Bibliography

- [1] Ministry of Internal Affairs and Communications, “2017 WHITE PAPER Information and Communications in Japan,” 2017.  
available: <http://www.soumu.go.jp/johotsusintokei/whitepaper/eng/WP2017/2017-index.html> (accessed 30 Jun. 2018)
- [2] E. Yamazaki, S. Yamanaka, Y. Kisaka, T. Nakagawa, K. Murata, E. Yoshida, T. Sakano, M. Tomizawa, Y. Miyamoto, S. Matsuoka, J. Matsui, A. Shibayama, J. Abe, Y. Nakamura, H. Noguchi, K. Fukuchi, H. Onaka, K. Fukumitsu, K. Komaki, O. Takeuchi, Y. Sakamoto, H. Nakashima, T. Mizuochi, K. Kubo, Y. Miyata, H. Nishimoto, S. Hirano, and K. Onohara, “Fast optical channel recovery in field demonstration of 100-Gbit/s Ethernet over OTN using real-time DSP,” *OSA Opt. Express*, vol. 19, no. 14, pp. 13179–13184, Jun. 2011.
- [3] Fujitsu limited, “Fujitsu Makes 100 Gbps DWDM Transmission Using Commercial Fiber Optic Line on Backbone Network Connecting Tokyo and Osaka,” Press releases, Jun. 2012.  
available: <http://www.fujitsu.com/global/about/resources/news/press-releases/2012/0621-01.html> (accessed 30 Jun. 2018)
- [4] S. Tsukamoto, D. S. Ly-Gagnon, K. Katoh, and K. Kikuchi, “Coherent demodulation of 40-Gbit/s polarization-multiplexed QPSK signals with 16-GHz spacing after 200-km transmission,” in *Proc. of Optical Fiber Communication Conference (OFC)*, PDP29, Mar. 2005.
- [5] H. Maeda, T. Kotanigawa, K. Saito, M. Yokota, S. Yamamoto, M. Suzuki, and T. Seki, “Field trial of simultaneous 100-Gbps and 400-Gbps transmission using advanced digital coherent technologies,” in *Proc. of Optical Fiber Communications Conference (OFC)*, W1K.4, Mar. 2016.
- [6] S. Inao, T. Sato, S. Sentsui, T. Kuroha, and Y. Nishimura, “Multicore optical fiber,” in *Proc. of Optical Fiber Communication Conference (OFC)*, WB1, Mar. 1979.
- [7] S. Berdagué and P. Facq, “Mode division multiplexing in optical fibers,” *Appl. Opt.*, vol. 21, no. 11, pp. 1950–1955, Jun. 1982.
- [8] K. Shibahara, T. Mizuno, L. Doowhan, Y. Miyamoto, H. Ono, K. Nakajima, S. Saitoh, K. Takenaga, and K. Saitoh, “DMD-Unmanaged Long-Haul SDM Transmission Over 2500-km 12-core  $\times$  3-mode MC-FMF and 6300-km 3-mode FMF Employing Intermodal Interference Cancelling Technique,” in *Proc. of Optical Fiber Communication Conference (OFC)*, Th4C.6, Mar. 2018.
- [9] *Time-Sensitive Networking Task Group*,  
available: <http://www.ieee802.org/1/pages/tsn.html>. (accessed 30 Jun. 2018)
- [10] *Audio Video Bridging Task Group*,  
available: <http://www.ieee802.org/1/pages/avbridges.html> (accessed 30 Jun. 2018)

- [11] P. Varis and T. Leyrer, “Time-sensitive networking for industrial automation,” *Texas Instruments*, Jan. 2018.  
available: <http://www.ti.com/lit/wp/spry316/spry316.pdf> (accessed 30 Jun. 2018)
- [12] *Time-Sensitive Networking for Fronthaul*, IEEE Standard 802.1CM (Draft 2.2), Mar. 2018.
- [13] NTT DOCOMO, “DOCOMO 5G White Paper, 5G Radio Access: Requirements, Concept and Technologies,” *White Paper*, Jul. 2014.
- [14] 総務省統計局, “平成 27 年国勢調査結果.”  
available: <http://www.stat.go.jp/data/kokusei/2015/kekka/kihon3/pdf/gaiyou.pdf> (accessed 9 May 2018)
- [15] Apple Inc., “iPhone5-Technical Specifications,”  
available: [https://support.apple.com/kb/SP655?viewlocale=en\\_US&locale=ja\\_JP](https://support.apple.com/kb/SP655?viewlocale=en_US&locale=ja_JP) (accessed 30 Jun. 2018)
- [16] Cisco Systems, Inc., “Cisco Visual Networking Index: Global Mobile Data Traffic Forecast Update, 2016–2021 White Paper,” Mar. 2017.  
available: <https://www.cisco.com/c/en/us/solutions/collateral/service-provider/visual-networking-index-vni/mobile-white-paper-c11-520862.html> (accessed 30 Jun. 2018)
- [17] J. Stern, J. Balance, D. Faulkner, S. Hornung, D. Payne, and K. Oakley, “Passive Optical Local Networks for Telephony Applications and Beyond,” *IEE Electron. Lett.*, vol. 23, no. 4, pp. 1255–1257, 1987.
- [18] S. S. Wagner, H. Kobrinski, H. Lemberg, and L. Smoot, “Experimental Demonstration of a Passive Optical Subscriber Loop Architecture,” *IEE Electron. Lett.*, vol. 24, no. 6, pp. 344–346, Mar. 1988.
- [19] IEEE 802.3, “IEEE Standard for Ethernet,” Dec. 2012.
- [20] ITU-T G.989, “40-Gigabit-capable passive optical networks (NG-PON2): Definitions, abbreviations and acronyms,” Oct. 2015.
- [21] IEEE P802.3ca 100G-EPON Task Force, “Physical Layer Specifications and Management Parameters for 25 Gb/s, 50 Gb/s, and 100 Gb/s Passive Optical Networks,”  
available: <http://ieee802.org/3/ca>. (accessed 30 Jun. 2018)
- [22] R. Koma, J. Kani, K. Asaka, and K. Suzuki, “Standardization Trends for Future High-speed Passive Optical Networks,” *NTT Technical Review*, vol. 15, no. 10, Oct. 2017.
- [23] Full service access network, “FSAN Roadmap,”  
available: <https://www.fsan.org/roadmap/> (accessed 30 Jun. 2018)
- [24] 総務省, “情報通信統計データベース, 我が国の移動通信トラヒックの現状.”  
available: <http://www.soumu.go.jp/johotsusintokei/field/data/gt010602.pdf> (accessed 30 Jun. 2018)
- [25] S. Suyama, T. Okuyama, Y. Inoue, and Y. Kishiyama, “5G Multi-antenna Technology,” *NTT DOCOMO Technical Journal*, vol. 17, no. 4, pp. 29–39, Jan. 2016.
- [26] S. Yoshioka, S. Suyama, T. Okuyama, J. Mashino, and Y. Okumura, “Digital Beamforming Algorithm for 5G Low-SHF-band Massive MIMO with Intersite Coordination,” in *Proc. of International Symposium on Wireless Personal Multimedia Communications* (WPMC), pp. 470–475, Dec. 2017.
- [27] H. Ishii, Y. Kishiyama, and H. Takahashi, “A novel architecture for LTE-B: C-plane/U-plane split and phantom cell concept,” in *Proc. of Globecom Workshops*,

- pp. 624–630, Dec. 2012.
- [28] 3GPP, TR 36.819 v11.2.0, “Coordinated Multi-Point Operation for LTE Physical Layer Aspects (Release 11),” Sep. 2013.
- [29] NTT DOCOMO, “Annual Report 2017,” Mar. 2017.  
available: <https://www.nttdocomo.co.jp/english/corporate/ir/library/annual/>  
(accessed 30 Jun. 2018)
- [30] *Enhancements for Scheduled Traffic*, IEEE Standard 802.1Qbv (Draft 3.1), Sep. 2015.
- [31] P. Chanclou, L. Anet Neto, K. Grzybowski, Z. Tayq, F. Saliou, and N. Genay, “Mobile Fronthaul Architecture and Technologies: A RAN Equipment Assessment [Invited],” *IEEE/OSA J. Opt. Commun. Netw.*, vol. 10, no. 1, pp. A1–A7, Jan. 2018.
- [32] CPRI, “CPRI Specification V7.0,” Oct. 2015.
- [33] OBSAI, “OBSAI System Spec V2.0,” Apr. 2006.
- [34] K. Tanaka and A. Agata, “Next-generation optical access networks for C-RAN,” in *Proc. of Optical Fiber Communications Conference (OFC)*, Tu2E.1, Mar. 2015
- [35] U. D’otsch, M. Doll, H.-P. Mayer, F. Schaich, J. Segel, and P. Sehier, “Quantitative Analysis of Split Base Station Processing and Determination of Advantageous Architectures for LTE,” *Bell Labs Technical Journal*, vol. 18, no. 1, pp. 105–128, Jun. 2013.
- [36] A. Maeder, M. Lalam, A. De Domenico, E. Pateromichelakis, D. W’ubben, J. Bartelt, R. Fritzsche, and P. Rost, “Towards a Flexible Functional Split for Cloud-RAN Networks,” in *Proc. of European Conference on Networks and Communications (EuCNC)*, pp. 1–5, Jun. 2014.
- [37] China Mobile Research Institute, “White Paper of Next Generation Fronthaul Interface,” White Paper v1.0, Jun. 2015.
- [38] T. Pfeiffer, “Next Generation Mobile Fronthaul and Midhaul Architectures [Invited],” *IEEE/OSA J. Opt. Commun. and Netw.*, vol. 7, no. 11, pp. B38–B45, Nov. 2015.
- [39] NGMN, “Future Study on Critical C-RAN Technologies,” The Next Generation Mobile Networks (NGMN) Alliance, Mar. 2015.
- [40] K. Miyamoto, S. Kuwano, J. Terada, and A. Otaka, “Analysis of Mobile Fronthaul Bandwidth and Wireless Transmission Performance in Split-PHY Processing Architecture,” *OSA Optics Express*, vol. 24, no. 2, pp. 1261–1268, Jan. 2016.
- [41] K. Miyamoto, S. Kuwano, T. Shimizu, J. Terada, and A. Otaka, “Performance Evaluation of Ethernet-Based Mobile Fronthaul and Wireless Performance in Split-PHY Processing,” *IEEE/OSA J. Opt. Commun. and Netw.*, vol. 9, no. 1, pp. A46–A54, Jan. 2017.
- [42] 3GPP, TR 38.801, v1.0.0, “Study on New Radio Access Technology; Radio Access Architecture and Interfaces (Release 14),” Dec. 2016.
- [43] eCPRI, “eCPRI Specification V1.0,” Aug. 2017.
- [44] 3GPP, TR 36.912, v14.0.0, “Feasibility study for Further Advancements for E-UTRA (LTE-Advanced) (Release 14),” Mar. 2017.
- [45] N. Shibata, T. Tashiro, S. Kuwano, N. Yuki, Y. Fukada, J. Terada, and A. Otaka, “Performance Evaluation of Mobile Fronthaul Employing Ethernet-based TDM-PON with IQ Data Compression,” *IEEE/OSA J. Opt. Commun. Netw.*, vol. 7, no. 11, pp. B16–B22, Nov. 2015.
- [46] P. Chanclou, H. Suzuki, J. Wang, Y. Ma, M. R. Boldi, K. Tanaka, S. Hong, C.

- Rodrigues, L. A. Neto, and J. Ming, "How Does Passive Optical Network Tackle Radio Access Network Evolution?," *IEEE/OSA J. Opt. Commun. Netw.*, vol. 9, no. 11, pp. 1030–1040, Nov. 2017.
- [47] M. Fujiwara, J. Kani, H. Suzuki, and K. Iwatsuki, "Impact of backreflection on upstream transmission in WDM single-fiber loopback access networks," *IEEE J. Lightw. Technol.*, vol. 24, no. 2, pp. 740–746, 2006.
- [48] T. Tashiro, S. Kuwano, J. Terada, T. Kawamura, N. Tanaka, S. Shigematsu, and N. Yoshimoto, "A Novel DBA Scheme for TDM-PON based Mobile Fronthaul," in *Proc. of Optical Fiber Communications Conference (OFC)*, Tu3F–3, Mar. 2014.
- [49] H. Ou, T. Kobayashi, T. Shimada, D. Hisano, J. Terada, and A. Otaka, "Passive Optical Network Range Applicable to Cost-effective Mobile Fronthaul," in *Proc. of IEEE International Conference on Communications (ICC)*, SAC/ASN1.5, May 2016.
- [50] H. Nomura, H. Ou, T. Shimada, T. Kobayashi, D. Hisano, H. Uzawa, J. Terada, and A. Otaka, "First Demonstration of Optical-Mobile Cooperation Interface for Mobile Fronthaul with TDM-PON," *IEICE Communications Express*, vol. 6, no. 6, pp. 375–380, Jun. 2017.
- [51] H. Uzawa, H. Nomura, T. Shimada, D. Hisano, K. Miyamoto, Y. Nakayama, K. Takahashi, J. Terada, and A. Otaka, "Practical Mobile-DBA Scheme Considering Data Arrival Period for 5G Mobile Fronthaul with TDM-PON," in *Proc. of European Conference on Optical Communication (ECOC)*, M.1.B.2, Sep. 2017.
- [52] Y. Nakayama, K. Maruta, T. Shimada, T. Yoshida, J. Terada, and A. Otaka, "Utilization Comparison of Small-Cell Accommodation With PON-Based Mobile Fronthaul," *IEEE/OSA J. Opt. Commun. Netw.*, vol. 8, no. 12, pp. 919–927, Dec. 2016.
- [53] S. Zhou, X. Liu, F. Effenberger, and Jonathan Chao, "Low-Latency High-Efficiency Mobile Fronthaul With TDM-PON (Mobile-PON)," *IEEE/OSA J. Opt. Commun. Netw.*, vol. 10, no. 1, pp. A20–A26, Jan. 2018.
- [54] T. Kobayashi, H. Ou, D. Hisano, T. Shimada, J. Terada, and A. Otaka, "Bandwidth Allocation Scheme based on Simple Statistical Traffic Analysis for TDM-PON based Mobile Fronthaul," in *Proc. of Optical Fiber Communications Conference (OFC)*, W3C.7, Mar. 2016.
- [55] M. Fiorani, S. Tombaz, J. Mårtensson, B. Skubic, L. Wosinska, and P. Monti, "Energy performance of C-RAN with 5G-NX radio networks and optical transport," in *Proc. of IEEE International Conference on Communications (ICC)*, pp. 1–6, May 2016.
- [56] X. Zhou and N. Deng, "A 25-Gb/s 20-km wavelength reused WDM system for mobile fronthaul applications," *European Conference on Optical Communication (ECOC)*, pp. 1–3, Sep. 2015.
- [57] E. Wong, E. Grigoreva, L. Wosinska, and C. M. Machuca, "Enhancing the survivability and power savings of 5G transport networks based on DWDM rings," *IEEE/OSA J. Opt. Comm. Netw.*, vol. 9, no. 9, pp. D74–D85, Sep. 2017.
- [58] A. Nakao, P. Du, Y. Kiriha, F. Granelli, A. A. Gebremariam, T. Taleb, and M. Bagaa, "End-to-end Network Slicing for 5G Mobile Networks," *IPSN J. Information Processing*, vol. 25, pp. 153–163, Feb. 2017.
- [59] A. Nagasawa, K. Nakura, T. Suehiro, Y. Hirano, S. Kozaki, and K. Ishida, "A method for resource allocation for creating slices," *IEICE Gen. Conf. '18*, B–8–51, Mar. 2018.
- [60] 総務省 総合通信基盤局, "信頼性・品質の確保 (技術基準) について," 23 Sep. 2016. available: [http://www.soumu.go.jp/main\\_content/000441100.pdf](http://www.soumu.go.jp/main_content/000441100.pdf) (accessed 30 Jun.

- 2018)
- [61] 3GPP TR 36.932 V12.1.0, “Scenarios and requirements for small cell enhancements for E-UTRA and E-UTRAN (Release 12)”, Mar. 2013.
  - [62] G. Kramer, B. Mukherjee, and G. Pesavento, “IPACT a dynamic protocol for an Ethernet PON (EPON),” *IEEE Communications Magazine*, vol. 40, no. 2, pp. 74–80, Feb. 2002.
  - [63] T. Tatsuta, N. Oota, N. Miki, and K. Kumozaki, “Design Philosophy and Performance of a GE-PON System for Mass Deployment,” *OSA J. Opt. Netw.*, vol. 6, no. 6, pp.689–700, Jun. 2007.
  - [64] H. Bang, S. Kim, D-. S. Lee, and C-. S. Park, “Dynamic Bandwidth Allocation Method for High Link Utilization to support NSR ONUs in GPON,” in *Proc. of International Conference on Advanced Communication Technology (ICACT)*, pp. 884–889, Feb. 2010.
  - [65] A. Walid and A. Chen, “Efficient and Dynamic Bandwidth Allocation for Non-Status Reporting Gigabit Passive Optical Networks (GPON),” in *Proc. of IEEE International Conference on Communications (ICC)*, pp. 1000–1005, May 2015.
  - [66] *Timing and Synchronization for Time-Sensitive Applications*, IEEE Standard 802.1AS–rev (Draft 7.0), Mar. 2015.
  - [67] *Path Control and Reservation*, IEEE Standard 802.1Qca (Draft 2.1), Jun. 2015.
  - [68] *Frame Preemption*, IEEE Standard 802.1Qbu (Draft 3.0), Sep. 2015.
  - [69] *Interspersing Express Traffic*, IEEE Standard 802.3br (Draft 2.3), Oct. 2015.
  - [70] T. Wan and P. Ashwood-Smith, “A Performance Study of CPRI over Ethernet with IEEE 802.1Qbu and 802.1Qbv Enhancements,” in *Proc. of IEEE Global Communications Conference (GLOBECOM)*, pp. 1–6, Dec. 2015.
  - [71] D. Thiele, R. Ernst, and J. Diemer, “Formal Worst-case Timing Analysis of Ethernet TSN’s Time-aware and Peristaltic Shapers,” in *Proc. of IEEE Vehicular Networking Conference (VNC)*, pp. 251–258, Dec. 2015.
  - [72] 3GPP, TS 36.300, v12.4.0, “Evolved Universal Terrestrial Radio Access (E-UTRA) and Evolved Universal Terrestrial Radio Access Network (EUTRAN); Overall description; Stage 2,” Dec. 2014.
  - [73] G. Piro, N. Baldo, and M. Miozzo, “An LTE Module for the ns-3 Network Simulator,” in *Proc. of the 4th International ICST Conference on Simulation Tools and Techniques. ICST (Institute for Computer Sciences, Social-Informatics and Telecommunications Engineering)*, pp. 415–422, Mar. 2011.
  - [74] ns-3, available: <http://www.nsnam.org/> (accessed 30 Jun. 2018)
  - [75] H. Ou, T. Kobayashi, T. Shimada, D. Hisano, J. Terada, and A. Otaka, “Passive Optical Network Range Applicable to Cost-effective Mobile Fronthaul,” in *Proc. of IEEE International Conference on Communications (ICC)*, SAC/ASN1.5, May 2016.
  - [76] H. Ou, Y. Sakai, H. Ujikawa, T. Tsutsumi, T. Fujiwara, Y. Kimura, T. Sakamoto, H. Suzuki, J. Terada, and A. Otaka, “Integrated Dynamic Bandwidth Allocation for Low Buffer Aggregated Passive Optical Network Systems,” *IEEE/OSA J. Opt. Commun. Netw.*, vol. 7, no. 8, pp. 814–824, Aug. 2015.
  - [77] D. Hisano, T. Kobayashi, H. Ou, T. Shimada, H. Uzawa, J. Terada, and A. Otaka, “TDM-PON for Accommodating TDD-based Fronthaul and Secondary Services,” *IEEE/OSA J. Lightw. Technol*, vol. 35, no. 14, pp. 2788–2796, Jul. 2017.
  - [78] D. Hisano, T. Shimada, H. Ou, T. Kobayashi, Y. Nakayama, H. Uzawa, J. Terada,

and A. Otaka, "Effective Utilization of Unallocated Interval in TDD-based Fronthaul Employing TDM-PON," *IEEE/OSA J. Opt. Comm. Netw.*, vol. 9, no. 9, pp. D1–D9, Jun. 2017.

# List of Publications

## A. Peer-reviewed Journals

1. D. Hisano, A. Maruta, and K. Kitayama, "Synchronization Detection Using XGM in SOA for All-Optical Preprocessing," *IEEE Photon. Technol. Lett.*, vol.26, no.10, pp.1015–1018, May 2014.
2. D. Hisano, T. Shimada, H. Ou, T. Kobayashi, Y. Nakayama, J. Terada, and A. Otaka, "Numerical Analysis on Accommodation of TDD-based Fronthaul and Secondary Services in a TDM-PON," *IEICE Commun. Exp.*, vol. 6, no. 1, pp. 46–52, Jan. 2017.
3. D. Hisano, T. Shimada, H. Ou, T. Kobayashi, Y. Nakayama, H. Uzawa, J. Terada, and A. Otaka, "Effective Utilization of Unallocated Interval in TDD-based Fronthaul Employing TDM-PON," *IEEE/OSA J. Opt. Comm. and Netw.*, vol. 9, no. 9, pp. D1–D9, Jun. 2017.
4. D. Hisano, T. Kobayashi, H. Ou, T. Shimada, H. Uzawa, J. Terada, and A. Otaka, "TDM-PON for Accommodating TDD-based Fronthaul and Secondary Services," *IEEE/OSA J. Lightw. Technol.*, vol. 35, no. 14, pp. 2788–2796, Jul. 2017.
5. D. Hisano, H. Uzawa, Y. Nakayama, T. Shimada, J. Terada, and A. Otaka, "TDD Pattern Estimation and Auto-Recovery from Estimation Error for Accommodations of Fronthaul and Secondary Services in TDM-PON," *IEEE/OSA J. Opt. Comm. and Netw.*, vol. 10, no. 2, pp. 104–113, Feb. 2018.
6. D. Hisano, H. Uzawa, Y. Nakayama, K. Miyamoto, J. Terada, and A. Otaka, "Clarification of Accommodatable Number of Functional Split Base Stations in TDM-PON Fronthaul," *IEICE Commun. Exp.*, vol. 7, no. 5, pp. 160–166, May 2018.

## B. Peer-reviewed International conferences

1. D. Hisano, T. Kono, A. Maruta, N. Ohata, H. Aruga, E. Ishimura, A. Sugitatsu, and K. Kitayama, "Wavelength Multicasting Accompanied with All-optical Modulation Format Conversion from NRZ-OOK to RZ-BPSK Using SOA-MZI Wavelength Converter," in *Proc. of Optoelectronics and Communications Conference (OECC)*, 6F1–4, Jul. 2012.
2. D. Hisano, A. Maruta, and K. Kitayama, "All-Optical Modulation Format Conversion from 4-channels NRZ-OOK to RZ-16QAM using SOA-MZI Wavelength Converters," in *Proc. of IEEE Photonics Conference (IPC)*, MM3, Sep. 2012.
3. D. Hisano, A. Maruta, and K. Kitayama, "Demonstration of All-Optical Network Coding by using SOA-MZI based XOR Gates," in *Proc. of Optical Fiber Commu-*

- nication Conference and Exposition and the National Fiber Optic Engineers Conference (OFC/NFOEC)*, JW2A.58, Mar. 2013.
4. D. Hisano, A. Maruta, and K. Kitayama, “Timing Detector using Cross Gain Modulation in Semiconductor Optical Amplifier for Adaptive All-Optical Signal Processing,” in *Proc. of JSAP Micro-Optics Conference (MOC)*, G-5, Oct. 2013.
  5. D. Hisano, A. Maruta, and K. Kitayama, “Mitigation of Pattern Effect in Semiconductor Optical Amplifier by Feed-forward Gain Clamped Current Injection,” in *Proc. of Optoelectronics and Communication Conference and the Australian Conference on Optical Fiber Technology (OECC/ACOF)*, WE9D2, Jul. 2014.
  6. D. Hisano, T. Shimada, H. Ou, T. Kobayashi, S. Kuwano, J. Terada, and A. Otaka, “Efficient Accommodation of Mobile Fronthaul and Secondary Services in a TDM-PON System with Wireless TDD Frame Monitor,” in *Proc. of IEEE International Conference on Communications (ICC)*, ONS 1. 1, May 2016.
  7. D. Hisano, T. Kobayashi, H. Ou, T. Shimada, J. Terada, and A. Otaka, “Experimental Demonstration of Accommodation of TDD-based Mobile Fronthaul and Secondary Services in a TDM-PON,” in *Proc. of IEEE/OSA European Conference on Optical Communication (ECOC)*, pp. 998–1000, Sep. 2016.
  8. D. Hisano, H. Uzawa, Y. Nakayama, T. Shimada, J. Terada, A. Otaka, “Automatic Recovery from Estimation Error for Accommodation of TDD-based Fronthaul and Secondary Service in a TDM-PON,” in *Proc. of IEEE/OSA European Conference on Optical Communication (ECOC)*, W.3.D.4, Sep. 2017.
  9. D. Hisano, Y. Nakayama, T. Kubo, T. Shimizu, H. Nakamura, J. Terada, and A. Otaka, “Gate-Shrunk Time Aware Shaper: Low-Latency Converged Network for 5G Fronthaul and M2M Services,” in *Proc. of IEEE Global Communications Conference (GLOBECOM)*, IPS.12.6, Dec. 2017.
  10. D. Hisano, K. Nishimura, Y. Nakayama, T. Kubo, M. Hirota, Y. Fukada, J. Terada, and A. Otaka, “Gate Shrunk Time Aware Shaper: Dynamic Shaping Control on White Box Switch,” in *Proc. of Optoelectronics and Communications Conference (OECC)*, P1-06, Jul. 2018.

### C. Domestic Conferences

1. 久野大介, 河野智徳, 丸田章博, 北山研一, “SOA-MZI 型波長変換器を用いた波長マルチキャスト対応全光 NRZ-OOK/RZ-BPSK 変換,” 2011 年信学ソ大, B-10-45, 2011 年 9 月.
2. 久野大介, 丸田章博, 大畠伸夫, 有賀博, 石村栄太郎, 杉立厚志, 北山研一, “SOA-MZI 型波長変換器を用いた全光ネットワークコーディングの実験的検討,” 信学技報, vol. 113, no. 156, OCS2013-19, pp. 1-5, 2013 年 7 月.
3. 久野大介, 丸田章博, 北山研一, “半導体光増幅器中の相互利得変調を用いたタイミング抽出器,” 2013 年信学ソ大, B-10-99, 2013 年 9 月.
4. 久野大介, 丸田章博, 北山研一, “半導体光増幅器におけるゲインクランプ電流のフィードフォワードによるパターン効果の抑圧,” 信学技報, vol. 113, no. 446, OCS2013-116, pp. 87-91, 2014 年 2 月.
5. 久野大介, 柴田直剛, 桑野 茂, 寺田 純, 大高明浩, “5G に向けた WDM オーバレイによるモバイルバックホール収容時の光伝送方式に関する一検討,” 2015 年信学総

- 大, B-8-14, 2015年3月.
6. 久野大介, 柴田直剛, 桑野 茂, 寺田 純, 大高明浩, “モバイル TDD フレーム推定を用いたモバイルシステムと他システムの同一 PON 収容の一検討,” 2015年信学ソ大, B-8-10, 2015年9月.
  7. 久野大介, 島田達也, 王 寛, 小林孝行, 桑野 茂, 寺田 純, 大高明浩, “モバイル/他システム同一 PON 収容における帯域利用効率の評価,” 2016年信学総大, B-8-29, 2016年3月.
  8. 久野大介, 島田達也, 王 寛, 小林孝行, 中山 悠, 寺田 純, 大高明浩, “TDD-based Mobile Fronthaul と他サービスの同一 TDM-PON 収容の提案と評価,” 信学技報, vol. 116, no. 401, CS2016-66, pp. 13-18, 2017年1月.
  9. 久野大介, 小林孝行, 王 寛, 島田達也, 鵜澤寛之, 寺田 純, 大高明浩, “TDD-based Fronthaul と他サービスの同一 TDM-PON 収容の実験評価,” 2017年信学総大, B-8-41, 2017年3月.
  10. 久野大介, 鵜澤寛之, 中山 悠, 島田達也, 寺田 純, 大高明浩, “[招待講演]TDD-based Mobile Fronthaul と他サービスの同一 TDM-PON 収容実現へ向けた実験評価,” 信学技報, vol. 117, no. 156, CS2017-25, pp. 59-64, 2017年7月.
  11. 久野大介, 中山 悠, 久保尊広, 清水達也, 中村浩崇, 寺田 純, 大高明浩, “レイヤ 2NW によるモバイル/IoT サービス収容を想定したゲート縮退型 Time Aware Shaper の提案,” 2017年信学ソ大, B-8-23, 2017年9月.
  12. 久野大介, 中山 悠, 丸田一輝, 丸田章博, “光ファイバ数削減に向けたモバイルフロントホールの無線リンク収容,” 信学技報, vol. 117, no. 504, CS2017-89, pp. 13-17, 2018年3月.
  13. 久野大介, 中山 悠, 丸田一輝, 丸田章博, “モバイルフロントホールの無線リンク収容に関する一検討,” 2018年信学総大, B-8-52, 2018年3月.